

DESIGN, REALIZATION, AND IMPLEMENTATION OF
2-D CIRCULARLY SYMMETRIC PSEUDO-ROTATED DIGITAL FILTERS

Gelson Vieira Mendonça

A Thesis
in
The Department
of
Electrical Engineering

Presented in Partial Fulfilment of the Requirements
for the degree of Doctor of Philosophy at
Concordia University
Montréal, Québec, Canada

October 1984

© Gelson Vieira Mendonça, 1984

ABSTRACT

Design, Realization, and Implementation of
2-D Circularly Symmetric Pseudo-Rotated Digital Filters

Gelson Vieira Mendonça, Ph.D.

Concordia University, 1984

The design, realization, and implementation of 2-D circularly symmetric digital filters are investigated.

A transformation that performs pseudo-rotation of the s_1 and s_2 axes is obtained by combining two known transformations, and is then used in the design of 2-D digital filters. This transformation leads to stable filters which are free of non-essential singularities of the second kind.

Two methods for the design of "pseudo-rotated" lowpass filters are described. In the first method the design starts from a 1-D analog filter or a 1-D infinite-impulse-response digital filter, and in the second method the design starts from a 1-D finite-impulse-response filter. The first method leads to lower-order filters for given specifications, and the need for guard filters is eliminated. The second on the other hand leads to fewer data manipulations of the input data but guard filters are necessary.

A new configuration is proposed which can be used for the design of 2-D circularly symmetric highpass digital filters. Either rotated or pseudo-rotated filter sections can be used in the design. In addition, the design of 2-D circularly symmetric bandpass and bandstop filters is considered.

Methods and procedures for the design of 2-D circularly symmetric filters satisfying prescribed specifications are described, and are then applied for the design of a diverse range of lowpass, highpass, bandpass, bandstop, Butterworth, Chebyshev, and elliptic filters. The results show that prescribed band edges, maximum passband ripple, minimum stopband loss, and degree of circularity can easily be achieved.

An attempt is made to check if improvements can be brought about in pseudo-rotated designs through the use of an optimization method. The improvements sought are reduced filter order and passband ripple, and increased stopband loss and degree of circularity. The results show that the degree of circularity is usually improved but the remaining specifications are degraded.

The realization of pseudo-rotated filters in terms of direct and wave structures is examined. In the direct realization, the transfer function is realized by connecting in cascade first- and second-order filter sections with real multiplier constants. In the wave realization, on the other hand, the 2-D digital structure is deduced from a

v

corresponding 1-D analog structure by applying impedance transformations. The two types of realizations are compared to some extent, and the effect of coefficient quantization is considered.

Finally, several issues pertaining to the software implementation of pseudo-rotated filters are studied to some extent.

ACKNOWLEDGEMENTS

I wish to acknowledge the supervision of Dr. A. Antoniou and his extremely careful and thorough review of my thesis. I thank Dr. V. Ramachandran for his helpful comments on my thesis and Eliana for immense encouragement provided by her during my stay in Canada. I also thank my friend Francira for her enormous help during my leave from the Federal University of Rio de Janeiro. I gratefully acknowledge the fellowship awarded by 'Coordenação de Aperfeiçoamento de Pessoal de Nível Superior' (CAPES) and the leave of absence granted by 'Universidade Federal do Rio de Janeiro' (UFRJ) which enabled me to study at Concordia University.

DEDICATION

With affection and appreciation, this thesis is dedicated to my mother Dna. Iracema; to my sister Marisa and to my brother Marcio; to my children Flavio, Renata and Patricia, and to Alda Regina for their patience, tolerance and understanding, and in memory of my father Sr. Jefferson, to my beloved brother Mendonçinha and my grandmother Dna. Maria.

TABLE OF CONTENTS

	Page
LIST OF TABLES	xi
LIST OF FIGURES	xiii
LIST OF IMPORTANT ABBREVIATIONS AND SYMBOLS	xvi
1. INTRODUCTION ,	1
1.1 General	1
1.2 Problems Encountered in the Design	3
1.3 Different Methods of Designing 2-D IIR Filters	6
1.4 1-D to 2-D Reactance Transformation	12
1.5 Scope of the Thesis	14
2. DESIGN OF PSEUDO-ROTATED DIGITAL FILTERS	18
2.1 Introduction	18
2.2 Design of 2-D Rotated Lowpass Filters	19
2.2.1 Design Starting from a 1-D Analog Filter	19
2.2.2 Design Starting from a 1-D digital Filter	21
2.3 Proposed Transformation	23
2.3.1 The Transformation	23
2.3.2 Stability of the Designed Filters	24
2.3.3 Type Preservation	25
2.4 New Design Procedure Based on a 1-D Analog Filter	28
2.5 New Design Procedure Based on 1-D Digital Filter	32
2.6 Design of Circularly Symmetric Zero-Phase Lowpass Filters	36

2.7	New Design Procedure Based on 1-D FIR Filters	47
2.8	Design of 2-D Highpass Filters	52
2.9	Design of 2-D Bandpass Pseudo-Rotated Filters	65
2.10	Design of 2-D Bandstop Pseudo-Rotated Filters	72
2.11	Conclusions	75
3.	DESIGN OF PSEUDO-ROTATED FILTERS SATISFYING PRESCRIBED SPECIFICATIONS	77
3.1	Introduction	77
3.2	Typical Characteristics of 2-D Filters	78
3.3	Prediction of the Minimum Number of Pseudo-Rotated Filters Required	86
3.4	Prediction of 1-D Lowpass Digital Filter Specifications	94
3.4.1	Prediction of the Minimum Stopband Attenuation	95
3.4.2	Prediction of the Maximum Passband ripple	97
3.5	Design of 1-D Analog Filter	101
3.6	Design Procedure	101
3.7	Design of Highpass Filters	104
3.8	Design of Bandpass and Bandstop Filters	116
3.9	Conclusions	126
4.	OPTIMIZATION OF PSEUDO-ROTATED FILTERS	131
4.1	Introduction	131
4.2	The Design Problem	132
4.2.1	The Objective Function	134
4.2.2	The Optimization method	135

4.2.3	Derivatives of the Objective Function	136
4.3	Design of Lowpass Filters	139
4.3.1	Design Examples and Results	141
4.4	Conclusions	157
5.	REALIZATION AND IMPLEMENTATION OF PSEUDO-ROTATED FILTERS	159
5.1	Introduction	159
5.2	Direct Realization	160
5.2.1	Rearrangement of the Transfer Function Coefficients	160
5.2.2	Digital Structures	166
5.3	Wave Realization of Pseudo-Rotated Filters	168
5.3.1	Impedance Transformation	171
5.4	Comparison between Direct and Wave Realizations	175
5.4.1	Direct Realization	180
5.4.2	Wave Realization	180
5.4.3	Comparison of Direct and Wave Realizations	185
5.5	Software Implementation of Pseudo-Rotated Filters	190
5.5.1	Implementation of Lowpass Filters	192
5.5.2	Implementation of Highpass Filters	195
5.6	Conclusions	196
6.	SUMMARY AND CONCLUSIONS	199
6.1	Conclusions	199
6.2	Scope for Further Work	203
	REFERENCES	206

LIST OF TABLES

Table 2.1	Specifications for the 2-D Digital Filters
Table 2.2	Actual Characteristics Obtained for the Lowpass Filters
Table 2.3	Design Specifications for the FIR and Guard Filters
Table 2.4	Specifications for the 2-D Digital Highpass Filters
Table 2.5	Actual Characteristics Obtained for the Highpass Filters
Table 2.6	Specifications for the Bandpass Filter and for the Corresponding Lowpass (LP) and Highpass (HP) Filters
Table 2.7	Specifications for the Bandstop Filter and for the Corresponding Lowpass (LP) and Highpass (HP) Filters
Table 3.1	Coefficients of the Variance (Lowpass Filters)
Table 3.2	Coefficients of the Variance (Highpass Filters)
Table 3.3	Value of N for Minimum Variance in 2-D Lowpass Filters
Table 3.4	Value of N for Minimum Variance in 2-D Highpass Filters
Table 3.5	2-D Lowpass-Filter Specifications
Table 3.6	1-D Digital-Filter Specifications (Butterworth Filters)
Table 3.7	1-D Digital-Filter Specifications (Chebyshev, Filters)
Table 3.8	1-D Digital-Filter Specifications (Elliptic Filters)
Table 3.9	Results Obtained for Butterworth Filters
Table 3.10	Results Obtained for Chebyshev Filters
Table 3.11	Results Obtained for Elliptic Filters
Table 3.12	2-D Highpass-Filter Specifications

Table 3.13	1-D Digital-Filter Specifications (Butterworth Filters)
Table 3.14	1-D Digital-Filter Specifications (Chebyshev Filters)
Table 3.15	1-D Digital-Filter Specifications (Elliptic Filters)
Table 3.16	Results Obtained for Butterworth Filters
Table 3.17	Results Obtained for Chebyshev Filters
Table 3.18	Results Obtained for Elliptic Filters
Table 3.19	2-D Bandpass- and Bandstop-Filter Specifications
Table 3.20	1-D Digital-Filter Specifications (Bandpass and Bandstop Filters)
Table 3.21	Results Obtained for Bandpass and Bandstop Filters
Table 4.1	Design Specifications for the 2-D Digital Filters
Table 4.2	Actual Losses and Variance at the Passband Edge (Pseudo-Rotated and Optimized Designs of Example 1)
Table 4.3	Actual Losses and Variance at the Passband Edge (Pseudo-Rotated and Optimized Designs of Example 2)
Table 4.4	Actual Losses and Variance at the Passband Edge (Pseudo-Rotated and Optimized Designs of Example 3)
Table 4.5	Actual Losses and Variance at the Passband Edge (Pseudo-Rotated and Optimized Designs of Example 4)
Table 4.6	Actual Losses and Variance at the Passband Edge (pseudo-Rotated and Optimized Designs of Example 5)
Table 4.7	Actual Losses and Variance at the Passband Edge (Pseudo-Rotated and Optimized Designs of Example 6)
Table 5.1	Actual Maximum Passband Ripple and Minimum Stopband Attenuation for Direct and Wave Realizations

LIST OF FIGURES

- Fig. 2.1 2-D Butterworth Lowpass Filter, (a) 3-D Plot, (b) Contour Plots for Attenuations of 0.2 dB, 1.0 dB, and 40.0 dB
- Fig. 2.2 2-D Chebyshev Lowpass Filter, (a) 3-D Plot, (b) Contour Plots for Attenuations of 0.2 dB, 1.0 dB, and 40.0 dB
- Fig. 2.3 2-D Elliptic Lowpass Filter, (a) 3-D Plot, (b) Contour Plots for Attenuations of 0.2 dB, 1.0 dB, and 40.0 dB
- Fig. 2.4 3-D plot of 2-D Lowpass Filter without Guard Filter
- Fig. 2.5 2-D Lowpass Filter with Guard Filter, (a) 3-D Plot, (b) Contour Plots for Attenuations of 0.5 dB, 1.0 dB, and 40.0 dB
- Fig. 2.6 (a) Rotation by θ , (b) Rotation by $-\theta$, (c) Series Interconnection, (d) Parallel Interconnection, (e) Rotated Highpass Filter
- Fig. 2.7 Block Diagram of the Proposed 2-D Circularly Symmetric Highpass Filter
- Fig. 2.8 Block Diagram of the Proposed 2-D Highpass Filter Recursing in the (+,+) Direction
- Fig. 2.9 2-D Butterworth Highpass Filter, (a) 3-D Plot (b) Contour Plots for Attenuations of 1.2 dB, 3.0 dB, and 40.0 dB
- Fig. 2.10 2-D Chebyshev Highpass Filter, (a) 3-D Plot, (b) Contour Plots for Attenuations of 0.5 dB, 1.0 dB, and 40.0 dB
- Fig. 2.11 2-D Elliptic Highpass Filter, (a) 3-D Plot, (b) Contour Plots for Attenuations of 0.5 dB, 1.0 dB, and 40.0 dB
- Fig. 2.12 2-D Butterworth Bandpass Filter, (a) 3-D Plot, (b) Contour Plots for Attenuations of 1.0 dB, 3.0 dB, and 40.0 dB
- Fig. 2.13 2-D Elliptic Bandstop Filter, (a) 3-D Plot, (b) Contour Plots for Attenuations of 1.0 dB, 3.0 dB, and 40.0 dB

- Fig. 3.1 Passband and Stopband Boundaries of 2-D Circularly Symmetric Lowpass Filter
- Fig. 3.2 Passband and Stopband Boundaries of 2-D Circularly Symmetric Highpass Filter
- Fig. 3.3 Passband and Stopband Boundaries of 2-D Circularly Symmetric Bandpass Filter
- Fig. 3.4 Passband and Stopband Boundaries of 2-D Circularly Symmetric Bandstop Filter
- Fig. 3.5 Actual and Ideal Passband Boundaries
- Fig. 3.6 Radius of Actual Passband Boundary Versus Angle
- Fig. 4.1 (a) 3-D Plot (Example 1, Pseudo-Rotated Design), (b) Corresponding Contour Plots for Attenuations of 0.5 dB and 40.0 dB
- Fig. 4.2 (a) 3-D Plot (Example 1, Configuration I), (b) Corresponding Contour Plots for Attenuations of 0.5 dB and 40.0 dB
- Fig. 4.3 (a) 3-D Plot (Example 1, Configuration II), (b) Corresponding Contour Plots for Attenuations of 0.5 dB and 40.0 dB
- Fig. 4.4 (a) 3-D Plot (Example 1, Configuration III), (b) Corresponding Contour Plots for Attenuations of 0.5 dB and 40.0 dB
- Fig. 4.5 (a) 3-D Plot (Example 1, Configuration IV), (b) Corresponding Contour Plots for Attenuations of 0.5 dB and 40.0 dB
- Fig. 4.6 (a) 3-D Plot (Example 1, Configuration V), (b) Corresponding Contour Plots for Attenuations of 0.5 dB and 40.0 dB
- Fig. 5.1 Scanning the Input Data Column by Column
- Fig. 5.2 (a) Flowgraph Representation of a Second-Order Section for Scanning the Input Data Row by Row, (b) The Transpose Flowgraph
- Fig. 5.3 (a) Flowgraph Representation of a First-Order Section for Scanning the Input Data Row by Row, (b) The Transpose Flowgraph

- Fig. 5.4 Impedance Transformations, (a) Capacitor,
(b) Inductor
- Fig. 5.5 Digital Realizations of Capacitors and Inductors
- Fig. 5.6 Equally-Terminated LC Elliptic Filter
- Fig. 5.7 Direct Realization of Pseudo-Rotated Filter
($L = \infty$), (a) 3-D Plot, (b) Contour Plot for
Attenuation of 0.4 dB
- Fig. 5.8 Direct Realization of Pseudo-Rotated Filter
($L = 10$), (a) 3-D Plot, (b) Contour Plot for
Attenuation of 0.4 dB
- Fig. 5.9 Direct Realization of Pseudo-Rotated Filter
($L = 8$), (a) 3-D Plot, (b) Contour Plot for
Attenuation of 0.4 dB
- Fig. 5.10 2-D Wave Realization Derived from Fig. 5.6
- Fig. 5.11 Wave Realization of Pseudo-Rotated Filter
($L = \infty$), (a) 3-D Plot, (b) Contour Plot for
Attenuation of 0.4 dB
- Fig. 5.12 Wave Realization of Pseudo-Rotated Filter
($L = 10$), (a) 3-D Plot, (b) Contour Plot for
Attenuation of 0.4 dB
- Fig. 5.13 Wave Realization of Pseudo-Rotated Filter
($L = 8$), (a) 3-D Plot, (b) Contour Plot for
Attenuation of 0.4 dB
- Fig. 5.14 Filtering Process and Operations Involved in
Software Implementation
- Fig. 5.15 Data Transformations for Different Recursion
Directions
- Fig. 5.16 Block Diagram for Implementing Pseudo-Rotated
Filters
- Fig. 5.17 Recursion in Different Directions
- Fig. 5.18 Implementation of Pseudo-Rotated Filters Using
Different Recursion Directions

LIST OF IMPORTANT ABBREVIATIONS
AND SYMBOLS

A_p	Maximum passband ripple in dB
A_a	Minimum stopband loss in dB
FIR	Finite impulse response
$H(z_1, z_2)$	Two-variable digital transfer function
IIR	Infinite impulse response
MPRF	Multivariable positive real function
N	Number of rotated filters in the (+,+) direction
SHF	Strictly Hurwitz polynomial
s_1, s_2	Complex frequency variables in the analog domain
T_1, T_2	Sampling periods in two-dimensions
VSHP	Very strictly Hurwitz polynomial
w_1, w_2	Analog domain frequencies in two-dimensions
w_a	Stopband edge in rad/s
w_{a1}	Lower stopband edge in rad/s
w_{a2}	Upper stopband edge in rad/s
w_p	Passband edge in rad/s
w_{p1}	Lower passband edge in rad/s
w_{p2}	Upper passband edge in rad/s
w_s	Sampling frequency in rad/s
z_1, z_2	Complex frequency variables in the digital domain
α, β	Rotation angles
σ^2	Variance of the passband boundary

CHAPTER 1

INTRODUCTION

1.1 General

Two-dimensional (2-D) digital filters have been used extensively in recent years for the processing, enhancement, and restoration of images. Their application encompasses many fields and includes tomography, seismic record processing, geophysical exploration, oil prospecting, radar, and radio astronomy, to name just a few [1]-[5]. Two-dimensional processing of an image is accomplished by scanning the image and then digitizing it by means of an analog-to-digital converter. The discrete data generated are then stored in the memory of a computer and, subsequently, they are processed by using a 2-D digital filter. It is possible to process such signals by means of 1-D techniques such as Fast Fourier Transforms or 1-D digital filters. However, it is preferable to use 2-D techniques, because of some important inherent advantages in these techniques. On the one hand, computation time can be reduced and on the other 2-D systems have many more degrees of freedom which give a system designer a flexibility not encountered in one-dimensional techniques [6]-[8]. In addition, in 2-D techniques the rate at which a bandlimited

signal is sampled can be adjusted and also the scanning of an image can be performed in several directions, whereas in 1-D techniques only the sampling rate can be adjusted.

Two classes of digital filters can be identified depending on the nature of their impulse response, namely, infinite-impulse-response (IIR) and finite-impulse-response (FIR) filters. IIR filters are, in general, implemented recursively while FIR filters are, in general, implemented nonrecursively.

FIR filters are always stable and can easily be designed to have constant group delay. However, in order to obtain high selectivity, the order of an FIR filter has to be much larger relative to that of an IIR filter having similar characteristics.

IIR filters, on the other hand, cannot be designed to have constant group delay and, consequently, their design entails the solution of a difficult approximation problem whereby amplitude and group-delay specifications must be satisfied simultaneously. A solution of this problem is to equalize the phase by using an allpass filter in cascade with a filter which has the desired amplitude response. A second problem associated with IIR filters is that their stability is not always assured as in the case of FIR filters and hence their design must often incorporate stability tests in order to ensure that the filters obtained

in the solution of the approximation problem are stable.

Much more attention has been devoted to IIR digital filters than to FIR filters due to their potential advantages and efficiency in processing large amounts of data. However, several problems remain unsolved and are currently under investigation. Before proceeding further, we shall discuss some of the outstanding problems encountered in the design of 2-D filters.

1.2 Problems encountered in the design

In 2-D digital filters, the first problem we face is the absence of the fundamental theorem of algebra [9]. That is, polynomials in two variables are not, in general, factorizable into products of polynomial factors of first degree. More general, a polynomial of any degree whose coefficients lie in a domain of rationality R is not always reducible to a product of two nontrivial polynomials whose coefficients also lie in this domain. In view of the above, parallel or cascade realization of a given 2-D filter is not always possible [10]. Nevertheless, these realizations have been explored in the past [11]. The approach used is to apply transformations to an analog-filter structure in order to obtain a corresponding 2-D digital-filter structure.

A problem encountered in the design is that some two-variable transfer functions possessing denominators which are strictly Hurwitz polynomials [12] in the analog domain, upon application of the double bilinear transformation result in discrete transfer functions possessing non-essential singularities of the second kind on the distinguished boundary[†] in the unit bidisc of the z_1 and z_2 complex planes [13]. These singularities are characterized by the fact that in the analog domain, the even and odd parts of the numerator and denominator of transfer functions can individually and simultaneously become zero at a set of points (w_{10}, w_{20}) of the frequency plane. Such singularities would in theory render a 2-D digital filter unstable.

The approximation problem in 2-D digital filters has received considerable attention in recent years and several solutions have been proposed [14] - [21]. Most of these methods are based on optimization techniques and are almost always focussed towards the solution of the approximation problem for lowpass filters. The solution of the approximation problem for the case where prescribed circularly-symmetric filter specifications are required has not been solved, although it is sometimes possible to obtain a solution through extensive trial and error.

[†]The distinguished boundary of the unit bidisc is defined as $T^2 = \{ (z_1, z_2) : |z_1| = 1, |z_2| = 1 \}$.

In the past, difficulties with polynomial factorization and stability checking in 2-D digital filters led to design methods whereby the 2-D filter is designed in separable form [14] or in terms of 1-D digital filters [15]. Filters designed by these methods have the following disadvantages :

- 1) Filters in separable form cannot achieve circularly symmetric amplitude response
- 2) The approximation problem in terms of 1-D IIR filters is a very difficult task.

Once a suitable approximation is obtained, the realization of the 2-D transfer function may be required. This is the process of converting the transfer function into a digital-filter network. The realization has been considered by several authors [11], [16]-[17].

The implementation of 2-D digital filters which is the embodiment of the digital-filter network by means of software or hardware has been considered in [1] - [6], [15]. Most of the time the complete set of data to be processed is available and, consequently, the processing can be carried out off-line by means of a software implementation. Occasionally, however, real-time processing is required in which case a hardware implementation would be preferable.

Like 1-D digital filters, 2-D digital filters are implemented by using finite arithmetic. Consequently, the effects of quantizing coefficients and products must be considered. The quantization of coefficients tends to change the frequency response and sometimes may render a filter unstable. On the other hand, the quantization of products causes roundoff noise to appear at the output of the filter, and it may sometimes cause granularity and overflow oscillations.

1.3 Different methods of designing 2-D IIR filters

Basically there are three general approaches for the solution of the approximation problem in 2-D IIR digital filters, as follows :

- 1) By applying transformations to analog or digital 1-D filters
- 2) By applying optimization methods
- 3) By applying transformations to analog or digital filters in conjunction with optimization methods.

The first approach makes use of spectral transformations which are also widely used in the design of

1-D digital filters. Shanks et al [18] introduced the technique of rotated filters which entails the transformation of variable s into variables s_1 and s_2 . This transformation is used to rotate the frequency response of a 1-D analog filter and results in a 2-D analog filter. After the transformation is applied, it is necessary to transform the 2-D analog filter into a 2-D digital filter, by making use of the double bilinear transformation. Filters so obtained are said to be rotated filters. Costa and Venetsanopoulos [19] have used this design method to obtain good approximations for circularly symmetric filters. The disadvantages of the method are that extensive trial and error is needed to achieve the desired cutoff frequency of the filter and, in addition, singularities of the second kind can appear in the transfer function. Chang and Aggarwal [20] proposed a method for rotating filters in the 2-D digital domain rather than the analog domain. Rotation in the z -plane is not generally possible because the resulting transfer functions may turn out to be irrational, and the frequency response may not have periodicity with respect to the Nyquist frequency in both w_1 and w_2 frequency axes. Chang and Aggarwal were able to design only lowpass, highpass, and bandpass filters and their method requires interpolation of the input signal. Ahmadi et al [21] have employed a 2-D reactance function as a spectral transformation from the 1-D to the 2-D domain in conjunction with the bilinear transformation. Their transformation is

such that it is necessary to use a guard filter in order to avoid spikes in the stopband region. The technique is applicable to the design of 2-D lowpass filters. Pendergrass et al [22] developed a procedure through which a given stable 2-D filter can be transformed into 2-D filters with many other amplitude response shapes. In their procedure, it is necessary to find an appropriate transformation in the form of a 2-D stable allpass function that maps the frequency response of a prototype filter into that of a desired filter. The approach of using a transformation from the 2-D to the 2-D domain is a very useful one. Techniques developed so far in this direction, however, lack the generality that would allow the design of 2-D filters satisfying desired specifications. Chakrabarti et al [23], [24] have shown that there are two strategies based on spectral transformation, namely, transformation from a 1-D to a 2-D transfer function and transformation from a 2-D to another 2-D transfer function. These two strategies have their advantages and limitations and are discussed in [23]-[24]. In the approach of applying a transformation to the transfer function of an analog filter, only the direct form realization can be guaranteed, if the realization is needed.

The second approach to the design of 2-D IIR filters corresponds to the direct approximation of amplitude or

phase shift characteristics by a ratio of polynomials. This technique was first used by Maria and Fahmy [25]. It involves defining an error function which is, in general, a sum of differences between the desired and the actual values of the amplitude or phase response raised to an even power and taken on a dense grid of points in the 2-D frequency plane. This error function is minimized by using the well-known least-squares technique. Sometimes minimum error is obtained by means of optimization algorithms which incorporate stability constraints. In order to make easier the stability checking at each iteration in the minimization process, the filter is designed with low-order sections which are cascaded in order to form the overall amplitude or phase response characteristics. Karivaratharajan and Swamy [26], [27] have proposed techniques which simplify the design when the goal is quadrantal symmetric filters. In their work, the denominator of the transfer function is a separable function of z_1 and z_2 . Stability checking is avoided except at the end when the minimum is reached.

Charalambous [28] proposed an alternative design method in which the desired amplitude response is obtained by using a minimax technique rather than the least-squares technique. Although the minimax technique leads to smaller error, more points are required in the sampling grid, in order to reduce the chances of large errors appearing between the grid points [29].

The realization of transfer functions obtained by optimization methods is achieved by using the direct form as a single section or as a cascade arrangement of direct-form sections.

The third approach for the design of 2-D IIR filters involves transformation of a 2-D analog transfer function into a 2-D discrete transfer function by using the double bilinear transformation. Then an optimization technique is used. Ramamoorthy and Bruton [30] have shown how a 2-D stable analog filter can be designed by using the properties of an immittance function of a lossless frequency-independent N-port network. However, their approach does not eliminate non-essential singularities of the second kind which could result in an unstable filter. Ahmadi and Ramachandran [31] have modified the technique in [30] so as to obtain a denominator which is a very-strictly-Hurwitz polynomial (VSHP) [32] in order to avoid non-essential singularities. This is done by using constrained optimization. The method was improved later by the same authors [33] by generating denominators which are VSHP without using constraints in the minimization process. In this approach, the generation of the 2-D analog denominator polynomial for the general case is complicated since no closed-form solution is available. The transfer function can be realized by using the direct form.

It is not always possible to obtain a 2-D analog structure from a given 2-D transfer function since no general method exists for the synthesis of multivariable positive real functions (MPRF's). So, one way to overcome this difficulty is to generate an analog 2-D transfer function from a given structure. The parameters of the structure are then obtained by an optimization method such that the amplitude response of the filter meets desired specifications. However, some methods for synthesis of certain classes of MPRF have been developed by several authors, e.g., Raman [11], Ramachandran and Rao [16], Ahmad et al [17], [35] and Kamp [34]. With the parameters of the analog structure known, the digital realization can be obtained by using the direct form or by using the methodology of wave digital filters. Different wave digital-filter realizations can be used. A wave digital filter approach due to Fettweis is an extension of the well-known 1-D approach [36]. Two others due to Constantinides are known as the invariant-voltage-ratio and the modified-transfer-admittance methods [2]. Another one, which permits certain alternative realizations, is due to Swamy, Thyagarajan and Ramachadran [37], [38].

1.4 1-D to 2-D reactance transformation

A traditional problem in the design of 2-D digital filters has been the generation of stable 2-D digital transfer functions whose amplitude and phase responses satisfy desired requirements. A method frequently used for generating such a transfer function is to apply the double bilinear transformation to a 2-D analog transfer function which is stable. However, in some cases this can cause singularities of the second kind as it has been shown by Goodman [16].

It has been shown by Karivaratharajan et al [32] that in order to obtain a 2-D transfer function which is free of such singularities, the denominator $D(s_1, s_2)$ of the analog transfer function has to be a very-strictly-Hurwitz (VSH) polynomial in s_1 and s_2 , that is, $D(s_1, s_2)$ should not possess singularities in the region

$$\{ (s_1, s_2) \mid \operatorname{Re}(s_1) \geq 0, \operatorname{Re}(s_2) \geq 0, |s_1| \leq \infty, |s_2| \leq \infty \}$$

A natural approach for obtaining a 2-D analog transfer function is to apply a spectral transformation to a 1-D analog filter whose amplitude and phase characteristics are known. The effect of such a transformation is to convert a stable 1-D analog transfer function into a 2-D analog transfer function exhibiting similar characteristics.

In order to avoid singularities of the second kind in the (z_1, z_2) plane, the spectral transformation itself has to be free of such singularities as has been shown by Karivaratharajan et al. In other words, the sum of the numerator and denominator of the spectral transformation, has to be a VSH polynomial. For example, the spectral transformation due to Shanks et al [18] given by

$$s = -s_1 \sin(\beta) + s_2 \cos(\beta) \quad (1.1)$$

which represents s -plane rotation, introduces such singularities as has been noted by Goodman [39]. On the other hand, the spectral transformation used by Ahmadi et al [21] given by

$$s = (a s_1 + b s_2) / (1 + c s_1 s_2) \quad (1.2)$$

does not cause such singularities. However, the transformation causes another problem. Spurious spikes are introduced in the amplitude response at the points $(W_{s1}/2, W_{s2}/2)$, where W_{s1} and W_{s2} are the sampling frequencies [24].

1.5 Scope of the thesis

In Chapter 2, a combination of the two spectral transformations in Eqns. 1.1 and 1.2 is used for the design of 2-D stable filters. This transformation leads to pseudo-rotation of the s_1 and s_2 axes, but under certain circumstances, the results achieved are very close to those obtained by using true rotation of the axes. The approach eliminates non-essential singularities of the second kind. In addition, spikes in the amplitude response at the Nyquist points $(\pm W_{s1}/2, \pm W_{s2}/2)$ can usually be eliminated. The approach is first applied to the design of lowpass filters. The design can start from a 1-D analog or 1-D IIR filter and equations for obtaining the filter coefficients are derived for both cases. The filters obtained will be referred to as 'pseudo-rotated' filters.

Conditions are derived which lead to a pseudo-rotated filter with circularly symmetric amplitude response. Based on these conditions, the required direction of recursion is deduced in order to obtain a stable filter.

In order to reduce the number of data transformations, a design method is proposed whereby 2-D circularly symmetric filters are obtained by starting from 1-D FIR filters. In these filters, the use of guard filters is needed to eliminate spikes in the amplitude response at the Nyquist points.

The design of pseudo-rotated filters is extended to include the design of highpass 2-D digital filters. In this case, a combination of series and parallel highpass filters is used which implements highpass filtering. Transmission zeros appear at ($z_1 = \pm 1$, $z_2 = \pm 1$) and could be a problem in certain applications.

By using combinations of highpass and lowpass 2-D digital filters in cascade or in parallel, the design method is extended to the case of bandpass and bandstop 2-D circularly symmetric filters. Examples are given for a diverse range of filters which illustrate the effectiveness of the proposed design method.

In Chapter 3, methods are considered for the solution of the approximation problem for the case where circularly symmetric 2-D filters satisfying prescribed specifications are required. The specifications of interest include the passband and stopband edges, the maximum passband ripple, and the minimum stopband attenuation. In addition, specifications may also be prescribed for the degree of circularity. The techniques considered are based on the method of 2-D pseudo-rotated filters described in Chapter 2, and can be used to design lowpass, highpass, bandpass and bandstop filters. These techniques are based on empirical prediction formulas which can be used to deduce the necessary specifications for the 1-D prototype filter so as

to satisfy the required 2-D specifications. This chapter also deals with techniques by which the minimum order for the 1-D prototype filter can be determined. In addition, consideration is given to the minimum number of rotations that is necessary in order to achieve a specified degree of circularity. The reliability of the design methods is illustrated by several examples.

In Chapter 4, an optimization method is used in conjunction with the method of pseudo-rotated filters for the design of 2-D circularly symmetric filters meeting desired specifications. This is done in order to check if improvements can be brought about in pseudo-rotated filters by using optimization techniques. The improvements of interest are reduction in the number of cascade first-order sections, reduction in the maximum passband ripple, increase in the minimum stopband loss, and increase in the degree of circularity of the filter.

The optimization method used is based on a sequential minimization technique. A least-squares error function is used which is defined in terms of the difference between the actual and the required response. The starting values for the variables of the optimization problem are assumed to be the coefficients of the 2-D pseudo-rotated filter as designed by the method of Chapter 3. This approach is applied to elliptic lowpass filters. In order to check if it is possible to decrease the order of the overall cascade

filter without violating the required specifications, optimizations are carried out with one or more of the filter sections removed.

In Chapter 5, the realization of 2-D pseudo-rotated filters is discussed. Direct and wave digital realizations are considered. In direct realizations, the transfer function is realized by connecting in cascade or in parallel first- and second-order filter sections. In wave realizations, a 2-D structure is deduced from a corresponding 1-D analog filter by using impedance transformations. Then by applying the wave characterization the 2-D wave digital filter can be obtained. This chapter concludes with an example which illustrates the realization procedure. This example provides also some idea about the performance of the two types of realization when coefficient quantization is applied.

Finally, the software implementation of pseudo-rotated lowpass and highpass filters is considered and several features of the implementation are studied.

CHAPTER 2DESIGN OF PSEUDO-ROTATED DIGITAL FILTERS2.1 Introduction

In this chapter a transformation is proposed which combines the transformations in Eqns. 1.1 and 1.2. This transformation like that in Eqn. 1.2 is in terms of a reactance function, and it can perform pseudo-rotation in the s -plane.

By using the proposed transformation, procedures are developed for the design of 2-D circularly symmetric lowpass filters. These procedures lead to IIR filters which are free of non-essential singularities of the second kind, and some of them render the use of guard filters unnecessary. A new approach is then developed for the design of 2-D circularly symmetric highpass filters. Subsequently, the design of 2-D circularly symmetric bandpass and bandstop filters by means of corresponding lowpass and highpass filters is considered.

2.2 Design of 2-D rotated lowpass filters

The problem we wish to address here is the following. Given a 1-D filter with some frequency response characteristics, we need to obtain a corresponding 2-D digital filter that exhibits similar frequency response characteristics. The starting 1-D filter can be analog or digital.

2.2.1 Design starting from a 1-D analog filter

The design technique described by Costa and Venetsanopoulos in [19] consists of the following steps :

- 1) Consider a stable 1-D analog filter whose transfer function is given by

$$H_{al}(s) = \frac{N_{al}(s)}{D_{al}(s)} \quad (2.1)$$

where $N_{al}(s)$ and $D_{al}(s)$ are mutually prime polynomials in s with $D_{al}(s) \neq 0$ in the closed right-half s -plane.

- 2) Apply the transformation

$$s = -s_1 \cos(\theta) + s_2 \sin(\theta) \quad (2.2)$$

to $H_{al}(s)$ in Eqn. 2.1 to obtain the 2-D continuous

transfer function

$$H_{a2}(s_1, s_2) = H_{a1}(-s_1 \sin(\beta) + s_2 \cos(\beta)) \quad (2.3)$$

3) Apply the double bilinear transformation

$$s_1 = \frac{2}{T_1} \frac{z_1 - 1}{z_1 + 1}, \quad s_2 = \frac{2}{T_2} \frac{z_2 - 1}{z_2 + 1} \quad (2.4)$$

to $H_{a2}(s_1, s_2)$ in Eqn. 2.3 to obtain the 2-D discrete transfer function

$$H_{d2}(z_1, z_2) = H_{a1}\left(\frac{2}{T_1} \frac{z_1 - 1}{z_1 + 1} \sin(\beta) + \frac{2}{T_2} \frac{z_2 - 1}{z_2 + 1} \cos(\beta)\right) \quad (2.5)$$

(T_1 and T_2 are the sampling intervals).

4) Cascade several rotated filters with different values of β to obtain a 2-D circularly symmetric discrete transfer function.

5) Calculate the actual cutoff frequency and if it is not in the desired range, replace s by s/α_k in Eqn. 2.1 and continue until the required cutoff frequency is achieved.

2.2.2 Design starting from a 1-D digital filter

The previous section has shown how a rotated filter can be obtained from a 1-D analog filter. In this section a procedure due to Goodman [39] is described whereby a 2-D rotated digital filter can be obtained from a 1-D digital filter. The design steps involved are as follows :

- 1) Consider a 1-D digital filter whose transfer function is given by

$$H_{d1}(z) = \frac{N_{d1}(z)}{D_{d1}(z)} \quad (2.6)$$

- 2) Apply the transformation

$$z = \frac{c+bz_1+az_2+z_1z_2}{1+az_1+bz_2+cz_1z_2} \quad (2.7)$$

to the transfer function in Eqn. 2.6 to obtain a 2-D discrete transfer function

$$H'_{d2}(z_1, z_2) = H_{d1} \left(\frac{c + bz_1 + az_2 + z_1 z_2}{1 + az_1 + bz_2 + cz_1 z_2} \right)$$

If

$$H'_{d2}(z_1, z_2) = H_{d2}(z_1, z_2)$$

where $H_{d2}(z_1, z_2)$ is given by Eqn. 2.5, then coefficients a , b , and c in Eqn. 2.7 can be expressed in terms of $\sin(\beta)$, $\cos(\beta)$, and α_k .

- 3) Cascade distinct rotated filters corresponding to different values of β , to obtain a 2-D circularly symmetric digital filter.
- 4) Compute the actual cutoff frequency and if it is not as required, use an optimization technique to adjust the transfer function coefficients.

As can be seen in the above procedures, trial and error is needed in the first method to obtain the desired specifications, while an optimization technique is necessary in the second approach to achieve the desired cutoff frequency. In addition, the 2-D transfer function can possess pole and zero cancellations on the distinguished boundary of the unit bidisc of the z_1 and z_2 complex plane. This might render the 2-D digital filter unstable due to rounding of the filter coefficients.

2.3 Proposed transformation

In this section an alternative transformation is proposed which combines the transformations due to Shanks et al [18], and Ahmadi et al [21] given in Eqns. 1.1 and 1.2. This will be used in Sec. 2.4 to develop a procedure for the design of 2-D lowpass filters.

2.3.1 The transformation

The proposed transformation is given by

$$s = g(s_1, s_2) = \frac{s_1 \cos(\beta) + s_2 \sin(\beta)}{1 + c s_1 s_2} \quad (2.8)$$

and like the transformation of Eqn. 1.2 it is a reactance function. We shall refer to this transformation as pseudo-rotation of the s_1 and s_2 axes by analogy with the true rotation of the axes when $c = 0$. 2-D filters designed through this transformation will be referred to as pseudo-rotated filters.

2.3.2 Stability of the designed filters

The filters designed using the spectral transformation in Eqn. 2.8 will be stable if the transformation itself is free of any singularity [32].

The necessary condition for $g(s_1, s_2)$ to transform a 1-D stable analog filter into a 2-D stable analog filter is that $g(s_1, s_2)$ be a strictly-Hurwitz polynomial (SHP). Since $q(s_1, s_2)$ is a 2-D reactance function, it is necessary that

$$\cos(\beta) > 0, \sin(\beta) > 0, c > 0$$

or, alternatively

$$0 < \beta < \frac{\pi}{2} \quad (2.9)$$

$$c > 0 \quad (2.10)$$

The necessary and sufficient conditions to ensure that the filter is free from any non-essential singularity of second kind is that $g(s_1, s_2)$ be a very-strictly-Hurwitz polynomial (VSHP). Sufficiency can be tested by applying the relations [32]

- a) $D(\infty, s_2) \neq \frac{0}{0}$ for $\operatorname{Re}(s_2) = 0, |s_2| < \infty$
- b) $D(s_1, \infty) \neq \frac{0}{0}$ for $\operatorname{Re}(s_1) = 0, |s_1| < \infty$
- c) $D(\infty, \infty) \neq \frac{0}{0}$

where $D(s_1, s_2)$ is equal to the sum of the numerator and denominator of $g(s_1, s_2)$.

We can see that these conditions hold if

$$\cos(\beta) \neq 0, \sin(\beta) \neq 0, c \neq 0$$

and since the constraints in Eqns. 2.9 and 2.10 are a subset of the above conditions, we conclude that if the conditions in Eqns. 2.9 and 2.10 hold, then the resulting transfer function will be free of any singularities, and the designed filter will thus be stable.

2.3.3 Type preservation

We shall now determine conditions under which the spectral transformation in Eqn. 2.8 will convert a 1-D

analog filter into a 2-D analog filter such that the amplitude response is preserved, and that the inequalities in Eqs. 2.9 and 2.10 hold in order to ensure a stable 2-D analog filter. That is, we wish to determine the mapping properties of the transformation.

It has been shown in [23] that if $H(s)$ represents a particular filter type over $[0, w_0)$, $w_0 > 0$, then $H(g(s_1, s_2))$ represents a filter of the same type (local type preservation) over a region Ω_I , which is a subset of

$$\Omega = \{ (w_1, w_2) \mid w_1 \geq 0, w_2 \geq 0 \}$$

if and only if

- a) $\Gamma(\Omega)$ is continuous in Ω_I
- b) $\Gamma(0,0) = 0$ and $[0, w_0) \subseteq \Gamma(\Omega_I)$
- c) $\Gamma(\Omega)$ is positive monotonically increasing function in each variable in Ω_I

where

$$\Gamma(w_1, w_2) = \frac{g(jw_1, jw_2)}{j} = \frac{w_1 \cos(\beta) + w_2 \sin(\beta)}{1 - cw_1 w_2} \quad (2.11)$$

$$\Gamma(\Omega_I) = \{ (w_1, w_2) \mid (w_1, w_2) \in \Omega_I \}$$

In effect, the transformation in Eqn. 2.8 will lead to local type preservation in the region

$$\Omega_I = \{ (w_1, w_2) \mid w_1 w_2 < \frac{1}{c}, w_1 \geq 0, w_2 \geq 0 \} \quad (2.12)$$

In order to understand the behaviour of $g(s_1, s_2)$, we note that $\Gamma(\Omega_I)$ has a discontinuity at $cw_1w_2 = 1$ which defines a hyperbolic function. We can see that for a fixed value of $w_2 = w_{20}$ (or equivalently for $w_1 = w_{10}$), $\Gamma(w_1, w_2)$ is a piecewise increasing function in the interval $[0, w_{10}^-) \cup (w_{10}^+, +\infty)$ where $w_{10} = 1/cw_{20}$ and the superscripts $(-)$ and $(+)$ of w_{10} , indicate immediately to the left and to the right, respectively.

Consequently, we have to choose the value of c small in order to ensure type preservation in the filter. Since we are interested in designing 2-D circularly symmetric lowpass filters with stopband edge W_a , we should have

$$c \ll \frac{W_s}{2\pi W_a} \quad (2.13)$$

This condition ensures type preservation over a large fraction of the Nyquist frequency.

2.4 New design procedure based on a 1-D analog filter

Consider the 1-D continuous transfer function

$$H_{a1}(s) = \frac{N(s)}{D(s)}$$

$$= K \frac{\prod_{i=1}^{M_N} (s - z_{ai})}{\prod_{i=1}^{M_D} (s - p_{ai})} \quad (2.14)$$

where z_{ai} and p_{ai} , $i=1,2,\dots$ are the zeros and poles of the analog filter and K is a constant representing the gain factor of the filter. To ensure stability, the poles are assumed to lie in the open left-half s -plane.

Applying the transformation in Eqn. 2.8 to the transfer function in Eqn. 2.14, we get a 2-D analog transfer function

$$H_{d1}(s_1, s_2) = K T_{s_1 s_2} \frac{\prod_{i=1}^{M_N} [s_1 \cos(\beta) + s_2 \sin(\beta) - z_{ai}(1 + c s_1 s_2)]}{\prod_{i=1}^{M_D} [s_1 \cos(\beta) + s_2 \sin(\beta) - p_{ai}(1 + c s_1 s_2)]} \quad (2.15)$$

where

$$T_{s_1 s_2} = (1 + c s_1 s_2)^{M_D - M_N} \quad (2.16)$$

The digital filter is obtained by using the double bilinear transformation

$$s_1 = \frac{2}{T_1} \frac{z_1 - 1}{z_1 + 1}, \quad s_2 = \frac{2}{T_2} \frac{z_2 - 1}{z_2 + 1} \quad (2.17)$$

If $T_1 = T_2 = T$, the 2-D transfer function of the digital filter is obtained from Eqns. 2.15 and 2.17 as

$$H_{d2}(z_1, z_2) = K_1 T_{z_1 z_2} \frac{\prod_{i=1}^{M_N} (a_{11i} + a_{21i} z_1 + a_{12i} z_2 + a_{22i} z_1 z_2)}{\prod_{i=1}^{M_D} (b_{11i} + b_{21i} z_1 + b_{12i} z_2 + b_{22i} z_1 z_2)} \quad (2.18)$$

where

$$K_1 = K \left(\frac{T}{2} \right)^{M_D - M_N} \quad (2.19)$$

$$T_{z_1 z_2} = \left(\left(1 + \frac{4c}{T^2}\right) + \left(1 - \frac{4c}{T^2}\right) z_1 + \left(1 - \frac{4c}{T^2}\right) z_2 + \left(1 + \frac{4c}{T^2}\right) z_1 z_2 \right)^{M_D - M_N} \quad (2.20)$$

and

$$a_{11i} = -\cos(\beta) - \sin(\beta) - z_{ai} \left(\frac{T}{2} + \frac{2c}{T} \right) \dots$$

$$\begin{aligned}
a_{21i} &= \cos(\beta) - \sin(\beta) - z_{ai} \left(\frac{T}{2} - \frac{2C}{T} \right) \\
a_{12i} &= -\cos(\beta) + \sin(\beta) - z_{ai} \left(\frac{T}{2} - \frac{2C}{T} \right) \\
a_{22i} &= \cos(\beta) + \sin(\beta) - z_{ai} \left(\frac{T}{2} + \frac{2C}{T} \right) \\
b_{11i} &= -\cos(\beta) - \sin(\beta) - p_{ai} \left(\frac{T}{2} + \frac{2C}{T} \right) \\
b_{21i} &= \cos(\beta) - \sin(\beta) - p_{ai} \left(\frac{T}{2} - \frac{2C}{T} \right) \\
b_{12i} &= -\cos(\beta) + \sin(\beta) - p_{ai} \left(\frac{T}{2} - \frac{2C}{T} \right) \\
b_{22i} &= \cos(\beta) + \sin(\beta) - p_{ai} \left(\frac{T}{2} + \frac{2C}{T} \right)
\end{aligned} \tag{2.21}$$

The behaviour of the transfer function in Eqn. 2.18 at some specific points of the (z_1, z_2) plane is of interest. Let us consider the points $z_1 = \pm 1$, $z_2 = \pm 1$.

a) At $z_1 = 1$, $z_2 = 1$

$$H_{d2}(1,1) = (-1)^{M_N - M_D} K \frac{\prod_{i=1}^{M_N} z_{ai}}{\prod_{i=1}^{M_D} p_{ai}}$$

b) At $z_1 = 1$, $z_2 = -1$

$$H_{d2}(1,-1) = \begin{cases} 0 & \text{for } M_D > M_N \\ K & \text{for } M_D = M_N \end{cases}$$

c) At $z_1 = -1$, $z_2 = 1$

$$H_{d2}(-1, 1) = \begin{cases} 0 & \text{for } M_D > M_N \\ K & \text{for } M_D = M_N \end{cases}$$

d) At $z_1 = -1$, $z_2 = -1$

$$H_{d2}(-1, -1) = \left(-\frac{2}{T^2}\right)^{M_D - M_N} K \frac{\prod_{i=1}^{M_N} z_{di}}{\prod_{i=1}^{M_D} p_{ai}}$$

As can be seen, no singularities exist in the transfer function and, in addition, there is no dependency on c at these points. In effect, c can be decreased as much as desired provided that c remains machine representable. Evidently, a very small value of c can be rounded to zero when the transfer function coefficients are calculated and then a non-essential singularity of the second kind would occur at $z_1 = z_2 = -1$, which would cause the filter to be unstable.

An observation is worthwhile at this point. The transformation in Eqn. 2.8 tends to shift the poles and zeros by a small amount relative to the position of the poles and zeros for true rotation (i.e. $c = 0$). This eliminates non-essential singularities of the second kind

but at the same time global type preservation is lost.

2.5 New design procedure based on 1-D digital filter

The design of pseudo-rotated filters can also start from a 1-D digital filter. This approach provides the flexibility whereby 2-D pseudo-rotated digital filters can be obtained either from 1-D IIR or FIR filters.

Let us consider the analog transfer function given by Eqn. 2.14. On applying the bilinear transformation to this transfer function, we obtain the 1-D discrete transfer function

$$H_{d1}(z) = K_1 T_z \frac{\prod_{i=1}^{M_N} \left(z \left(1 - \frac{T}{2} z_{ai} \right) - \left(1 + \frac{T}{2} z_{ai} \right) \right)}{\prod_{i=1}^{M_D} \left(z \left(1 - \frac{T}{2} p_{ai} \right) - \left(1 + \frac{T}{2} p_{ai} \right) \right)} \quad (2.22)$$

where

$$T_z = (z + 1)^{M_D - M_N}$$

Alternatively, we can write

$$H_{d1}(z) = K_1 T_z A \frac{\prod_{i=1}^{M_N} \left(z - \frac{1 + \frac{T}{2} z_{ai}}{1 - \frac{T}{2} z_{ai}} \right)}{\prod_{i=1}^{M_D} \left(z - \frac{1 + \frac{T}{2} p_{ai}}{1 - \frac{T}{2} p_{ai}} \right)}$$

$$= K_1 T_z A \frac{\prod_{i=1}^{M_N} (1 - z_{di})}{\prod_{i=1}^{M_D} (1 - p_{di})} \quad (2.23)$$

where

$$A = \frac{\prod_{i=1}^{M_N} (1 - \frac{T}{2} z_{ai})}{\prod_{i=1}^{M_D} (1 - \frac{T}{2} p_{ai})} \quad (2.24)$$

and z_{di} and p_{di} are zeros and poles of $H_{d1}(z)$ in the z -plane. These poles must be inside the unit circle in order that the filter be stable.

Let the transformation from the 1-D digital domain to the 2-D digital domain be the following allpass form

$$z = g(z_1, z_2) = \frac{g + fz_1 + ez_2 + dz_1z_2}{d + ez_1 + fz_2 + gz_1z_2} \quad (2.25)$$

where d , e , f and g are constants to be determined.

Applying the transformation in Eqn. 2.25 to the transfer function in Eqn. 2.23, we obtain the 2-D discrete transfer function

$$H_{d2}(z_1, z_2) = K_1 T_{z_1 z_2} \frac{\prod_{i=1}^{M_N} \left[(g - dz_{di}) + (f - ez_{di})z_1 + (e - fz_{di})z_2 + (d - gz_{di})z_1z_2 \right]}{\prod_{i=1}^{M_D} \left[(g - dp_{di}) + (f - ep_{di})z_1 + (e - fp_{di})z_2 + (d - gp_{di})z_1z_2 \right]} \quad (2.26)$$

where

$$K_1 = K \left(\frac{T}{2} \right)^{M_D - M_N} \quad (2.27)$$

$$T_{z_1 z_2} = ((d+g) + (e+f) z_1 + (e+f) z_2 + (d+g) z_1 z_2)^{M_D - M_N} \quad (2.28)$$

Now by equating corresponding coefficients in Eqns. 2.18 and 2.26, we obtain after some manipulation, the following relations

$$\left. \begin{aligned} d &= \frac{1 + \cos(\beta) + \sin(\beta) + \frac{4c}{T^2}}{2} \\ e &= \frac{1 - \cos(\beta) + \sin(\beta) - \frac{4c}{T^2}}{2} \\ f &= \frac{1 + \cos(\beta) - \sin(\beta) - \frac{4c}{T^2}}{2} \\ g &= \frac{1 - \cos(\beta) - \sin(\beta) + \frac{4c}{T^2}}{2} \end{aligned} \right\} \quad (2.29)$$

By using these relations, the design of a 2-D lowpass digital filter can be obtained from a corresponding 1-D digital filter.

The stability requirements follow from the actual procedure. It is known that if the transformation has no singularities on or inside the unit bidisc, then the 1-D stable filter will be transformed into a 2-D filter with any singularities [32], [40] on or inside the (z_1, z_2) unit bidisc.

The necessary and sufficient conditions for the transformation in Eqn. 2.25 to be stable are

$$\left. \begin{aligned} e + f - g &< d \\ e - f + g &< d \\ -e + f + g &< d \\ -e - f - g &< d \end{aligned} \right\} \quad (2.30)$$

If these inequalities are applied to the relations in Eqn. 2.29, we get

$$\cos(\beta) > 0, \quad \sin(\beta) > 0, \quad c > 0$$

These inequalities are the same as in Eqns. 2.9 and 2.10.

2.6 Design of circularly symmetric zero-phase lowpass filters

2-D transfer functions are often required with circular symmetry in the (w_1, w_2) plane. For example, in image processing where both of the frequency axes should receive the same treatment. Perfectly circularly symmetric filters are impossible to achieve in practice [6]. Nevertheless, it is possible to design 2-D digital filters that are approximately circularly symmetric. In this section, we use the techniques of Secs. 2.4 and 2.5 for the design of circularly symmetric 2-D digital filters.

As shown in Eqn. 2.9, β must be in the range $(0^\circ, 90^\circ)$ in order to ensure stability in the resulting filter. We can design a filter by pseudo-rotating the transfer function by several angles and then cascading the filters obtained. Eventually an overall transfer function is obtained which is a product of several transfer functions each of them rotated by a different value of β , that is,

$$H_{d2}(z_1, z_2) = \prod_{i=1}^M H_{d2i}(z_1, z_2) \quad (2.31)$$

where $H_{d2i}(z_1, z_2)$ is the transfer function obtained by

rotating the 1-D transfer function by an angle β_i . For the sake of simplicity $H_{d2}(z_1, z_2)$ and $H_{d2i}(z_1, z_2)$ will be represented by $H(z_1, z_2)$ and $H_i(z_1, z_2)$, respectively.

In order to have approximately circular symmetry, we need to design the filters such that

- i) the coefficients of z_1 and z_2 in Eqns. 2.18 and 2.26 interchange,
- ii) a rotation by an angle β , $0^\circ < \beta < 90^\circ$, must be accompanied by a rotation by an angle $-\beta$.

The first condition will ensure that the coefficients of z_1 and z_2 are symmetrical and that the variations in the amplitude response are the same in the w_1 and w_2 directions. The second condition is related with the characteristics of the transformation itself. When we apply the rotation of the transfer function, we get a 2-D digital filter with a lowpass amplitude response on line $w_1 = w_2$ and a allpass amplitude response on line $w_1 = -w_2$. Thus, if we cascade several filters that have been designed with angles in the range $0^\circ < \beta < 90^\circ$ and $270^\circ < \beta < 360^\circ$, we get an overall transfer function in which the amplitude response is circularly symmetric in the (w_1, w_2) plane.

Unfortunately, the use of rotation angles in the range $(270^\circ, 360^\circ)$ results in filters which are unstable when the recursion is carried out in the $(+, +)$ direction. However, according to Huang [12], if a 2-D digital filter is stable

when the recursion is performed in at least one of the $(+,+)$, $(+,-)$, $(-,+)$ and $(-,-)$ directions, then the filter can be made stable by properly transforming the input data before filtering. For example, let $H_1(z_1, z_2)$ be the transfer function of a filter designed with a rotation angle β , $0^\circ < \beta < 90^\circ$. Designing a filter with $-\beta$, will yield a transfer function $H_1(z_1, z_2)$ which is unstable in the $(+,+)$ direction. However, by performing the recursion in the $(+,-)$ direction, stability is achieved.

In image processing it is very important that the group delay of the filter be constant. Otherwise, the filtered image will be distorted. As is well known the double bilinear transformation does not preserve the phase linearity of a two-variable linear-phase analog transfer function. However, given a 2-D transfer function $H(z_1, z_2)$, a zero-phase filter can be obtained by forming the transfer function

$$G(z_1, z_2) = H(z_1, z_2) H(z_1^{-1}, z_2^{-1}) \quad (2.32)$$

Such a filter has an amplitude response

$$| G(e^{j\omega_1 T}, e^{j\omega_2 T}) | = | H(z_1, z_2) |^2 \quad (2.33)$$

For example, if two filters which are recursing in the $(+,+)$ and $(+,-)$ direction are to be cascaded to obtain a

quasi-circular symmetric amplitude response, in which case

$$H_2(z_1, z_2) = H_1(z_1, z_2) H_1(z_1, z_2^{-1}) \quad (2.34)$$

then a zero-phase filter, can be obtained by forming the product

$$\begin{aligned} H_3(z_1, z_2) &= H_2(z_1, z_2) H_2(z_1^{-1}, z_2^{-1}) \\ &= H_1(z_1, z_2) H_1(z_1, z_2^{-1}) H_1(z_1^{-1}, z_2) H_1(z_1^{-1}, z_2^{-1}) \end{aligned} \quad (2.35)$$

In this expression, transfer functions $H_1(z_1^{-1}, z_2)$ and $H_1(z_1^{-1}, z_2^{-1})$ represent stable filters in the $(-, +)$ and $(-, -)$ directions, respectively.

Finally, if we design a pseudo-rotated filter with $0^\circ < \beta_4 < 45^\circ$ with corresponding transfer function $H_4(z_1, z_2)$, then we have to design a pseudo-rotated filter with an angle $\beta_5 = 90^\circ - \beta_4$ with corresponding transfer function $H_5(z_1, z_2) = H_4(z_2, z_1)$ in order to have symmetry in the coefficients, as required by condition (i) above. Therefore, if the design requires two different first quadrant rotation angles, then an approximately circularly symmetric zero-phase filter, will be obtained by forming the transfer function

$$\begin{aligned}
 H(z_1, z_2) = & H_4(z_1, z_2) H_5(z_1, z_2) H_4(z_1, z_2^{-1}) H_5(z_1, z_2^{-1}) \\
 & H_4(z_1^{-1}, z_2) H_5(z_1^{-1}, z_2) H_4(z_1^{-1}, z_2^{-1}) H_5(z_1^{-1}, z_2^{-1})
 \end{aligned}
 \quad (2.36)$$

The direction of recursion can be changed by transforming the input data at each filtering stage. If the input array has many elements per row and/or column, considerable amount of data manipulation is required. This is one of the drawbacks of methods based on the use of rotated or pseudo-rotated filters.

Example 2.1

The method described in this section was used to design three lowpass zero-phase filters using a Butterworth, a Chebyshev, and an elliptic analog filter as prototype. The rotation angles were $\pm 30^\circ$, $\pm 60^\circ$, $180^\circ \pm 30^\circ$, $180^\circ \pm 60^\circ$. Design specifications for the passband edge (W_p), for the stopband edge (W_a), for the maximum passband ripple (A_p), and the minimum stopband attenuation (A_a) for the 2-D digital filters are summarized in Table 2.1. The sampling frequency used was 2π rad/s. A value for c in Eqn. 2.8 equal to 10^{-5} was used in all the examples. The specifications of the analog prototype filters were assumed to be the same as for the 2-D digital filters except that

Table 2.1 Specifications for the 2-D Digital Lowpass Filters

Prototype Filter	W_p (rad/s)	W_a (rad/s)	A_p (dB)	A_a (dB)	Rotation Angles
Butterworth	1.0	1.5	1.0	40.0	$\pm 30^\circ$, $180^\circ \pm 30^\circ$ $\pm 60^\circ$, $180^\circ \pm 60^\circ$
Chebyshev	1.5	2.0	0.1	40.0	$\pm 30^\circ$, $180^\circ \pm 30^\circ$ $\pm 60^\circ$, $180^\circ \pm 60^\circ$
elliptic	1.5	2.0	0.1	40.0	$\pm 30^\circ$, $180^\circ \pm 30^\circ$ $\pm 60^\circ$, $180^\circ \pm 60^\circ$

the warping effect was taken into account in the calculation of the edges of the analog filters.

The amplitude response of 2-D filters and the corresponding contour plots are shown in Figs. 2.1 to 2.3. In all examples, the computation time for the calculation of the filter coefficients was less than 8 seconds. It can be seen from the amplitude response of these filters, that no spikes appear at the Nyquist points and so no guard filters are necessary.

Table 2.2 shows the actual characteristics obtained for the 2-D filters. As can be seen from Table 2.2, the calculated passband and stopband attenuation differ from the corresponding specified values. However, this problem will be eliminated in Chapter 3 where a design procedure is described which yields filters satisfying prescribed amplitude specifications.

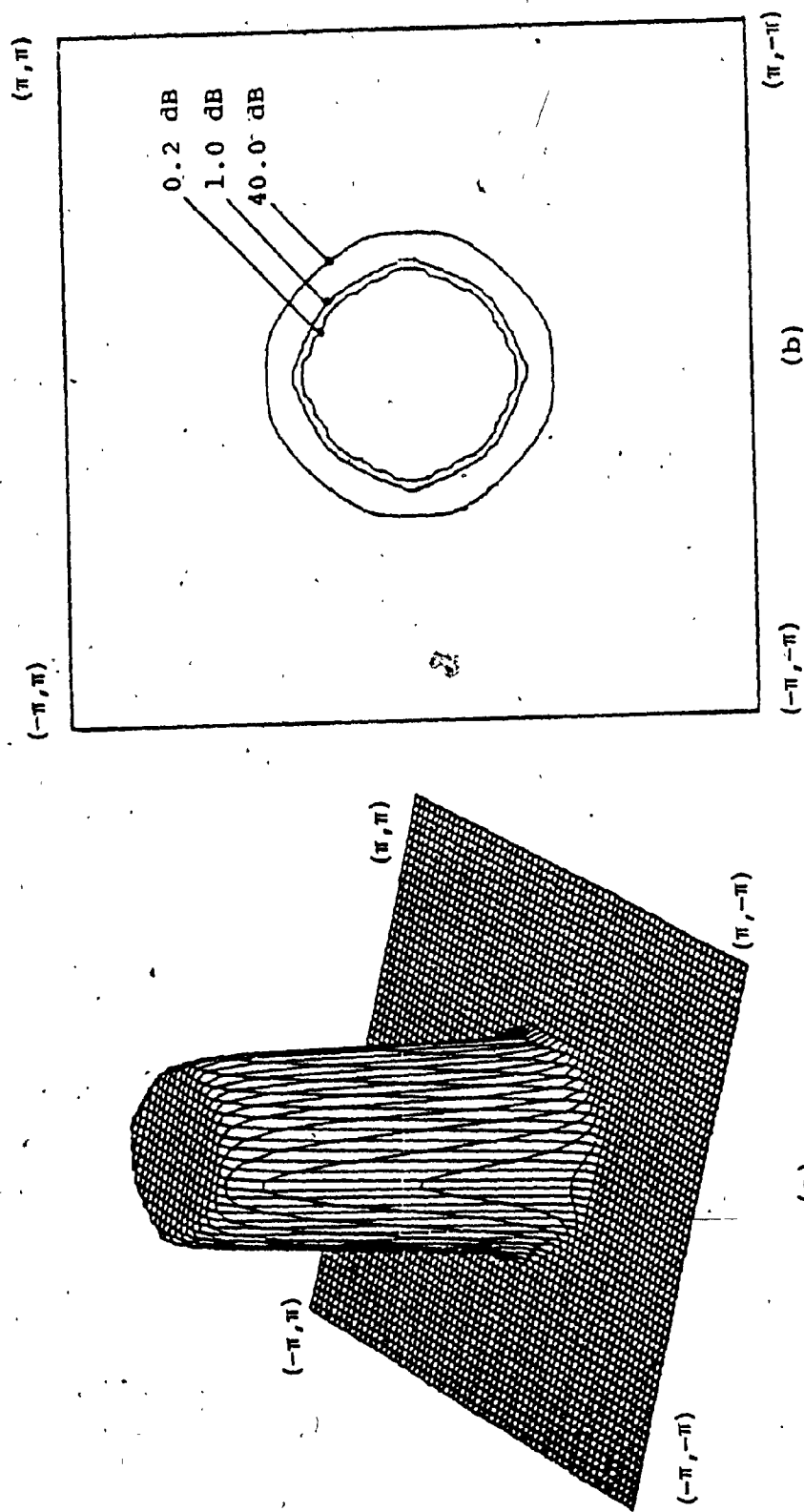


Figure 2.1 2-D Butterworth Lowpass Filter, (a) 3-D Plot, (b) Contour Plots for Attenuations of 0.2 dB, 1.0 dB, and 40.0 dB.

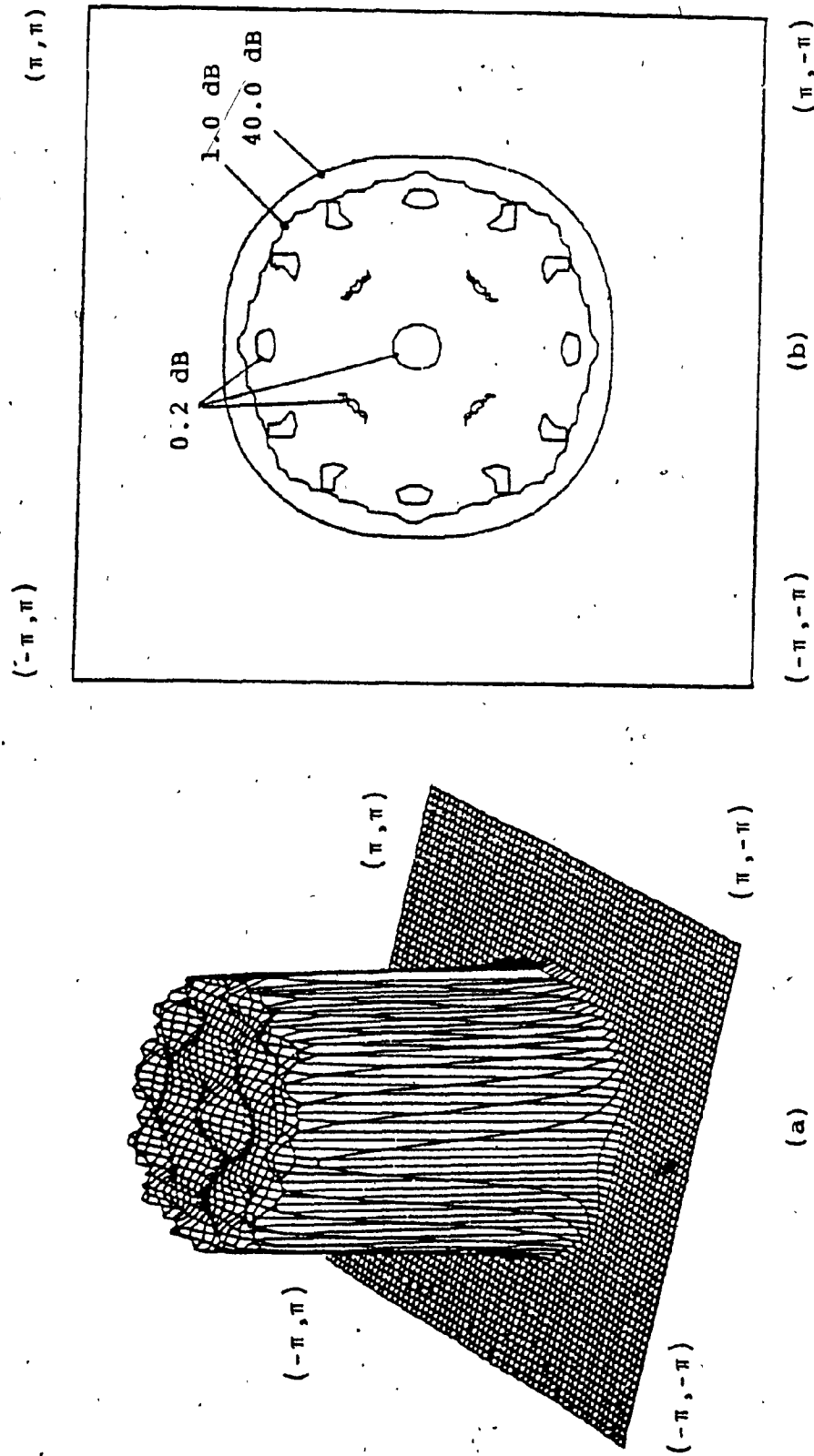


Figure 2.2 2-D Chebyshev Lowpass Filter, (a) 3-D Plot, (b) Contour Plots for Attenuations of 0.2 dB, 1.0 dB, and 40.0 dB.

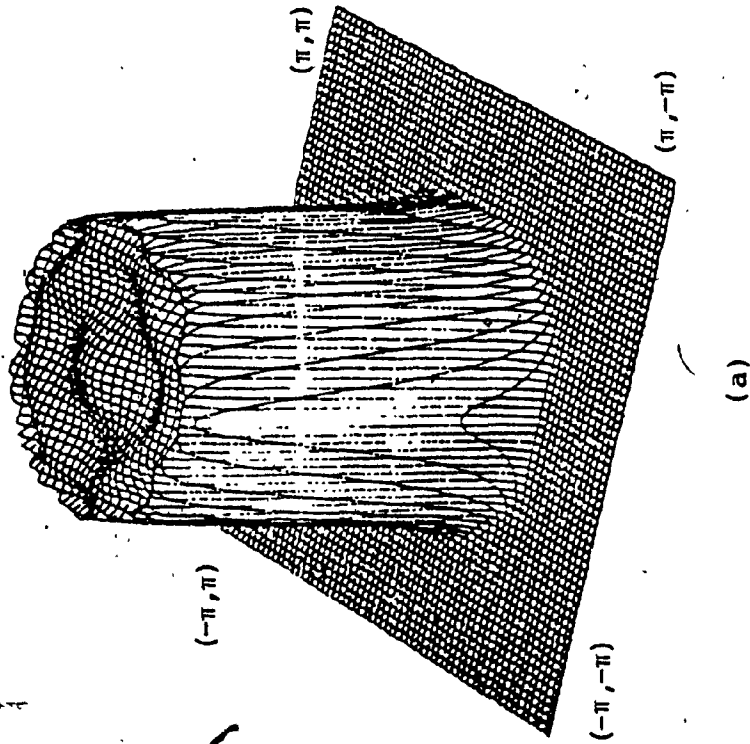
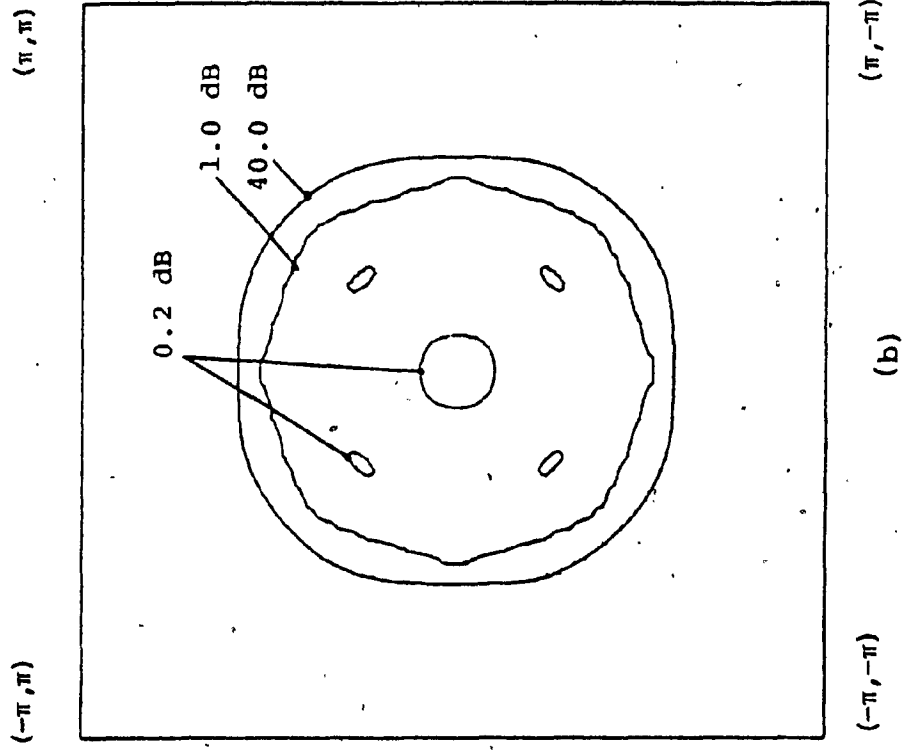


Figure 2.3 2-D Elliptic Lowpass Filter, (a) 3-D Plot, (b) Contour Plots for Attenuations of 0.2 dB, 1.0 dB, and 40.0 dB.

Table 2.2 Actual Characteristics Obtained for the Lowpass Filters

Prototype Filter	A_p (dB)	A_a (dB)
Butterworth	2.6973	97.72
Chebyshev	0.6585	77.09
elliptic	0.6597	58.20

2.7 New design procedure based on 1-D FIR filters

The problem we want to solve here is to design a 2-D IIR lowpass filter using a 1-D FIR filter such that the pseudo-rotated filter section is stable in the $(+,+)$ direction, when rotation angles outside the range $(0^\circ, 90^\circ)$ are used. If this can be achieved, the amount of data manipulations between sections can be reduced.

Suppose that we have designed a 1-D FIR filter [40] with a transfer function

$$H(z) = \sum_{n=0}^N h(n) z^n \quad (2.37)$$

where N is the filter order. By obtaining the zeros of $H(z)$ [41] we can write

$$H(z) = K \prod_{i=1}^N (z - z_{di}) \quad (2.38)$$

where K is the gain factor and z_{di} for $i=1, \dots, N$ are the zeros of $H(z)$.

Now on applying the transformation of Eqn. 2.25 to the transfer function in Eqn. 2.38, we get

$$H(z_1, z_2) = K \prod_{i=1}^N \frac{g_i - d_i z_{di} + (f_i - e_i z_{di}) z_1 + (e_i - f_i z_{di}) z_2 + (d_i - g_i z_{di}) z_1 z_2}{d_i + e_i z_1 + f_i z_2 + g_i z_1 z_2} \quad (2.39)$$

where d_i, e_i, f_i and g_i are given by Eqn. 2.29. We can see that Eqn. 2.39 has a denominator in which the variables z_1 and z_2 have constant coefficients.

Now we wish to find out relationships among the coefficients $\cos(\beta)$, $\sin(\beta)$ and c in Eqn. 2.29 in order to render the denominator in Eqn. 2.39 factorizable, i.e.,

$$\begin{aligned} D(z_1, z_2) &= d + e z_1 + f z_2 + g z_1 z_2 \\ &= F_1(z_1) F_2(z_2) \end{aligned} \quad (2.40)$$

If this is possible, $H(z_1, z_2)$ can be stabilized easily by inverting the poles of $F_1(z_1)$ and/or $F_2(z_2)$ that are outside the unit bidisc and then properly normalizing the transfer function.

From Eqn. 2.40 we note that factorization is possible if

$$e f = d g \quad (2.41)$$

that is

$$D(z_1, z_2) = d \left(1 + \frac{e}{d} z_1 \right) \left(1 + \frac{f}{d} z_2 \right) \quad (2.42)$$

Now by using the relations in Eqn. 2.29 for d , e , f and g , we have

$$d g = \frac{1 + \cos(\beta) + \sin(\beta) + C}{2} \quad \frac{1 - \cos(\beta) - \sin(\beta) + C}{2}$$

$$e f = \frac{1 - \cos(\beta) + \sin(\beta) - C}{2} \quad \frac{1 + \cos(\beta) - \sin(\beta) - C}{2}$$

where

$$C = \frac{4c}{T^2} \quad (2.43)$$

In effect, Eqn. 2.40 is satisfied

if

$$C = \cos(\beta) \sin(\beta) \quad (2.44)$$

Some implications of Eqn. 2.44 are as follows. As was pointed out in Sec. 2.3.3, we should have c , or equivalently C , small in order to have local type preservation of the filter after the application of the double bilinear transformation. Consequently, Eqn. 2.44 suggests that the product $\cos(\beta)\sin(\beta)$ or $\cos(\beta)$ and $\sin(\beta)$ should be scaled down. However, $\cos(\beta)$ and $\sin(\beta)$ can not be decreased separately by different quantities since

circularly symmetric filters would not be possible. It is thus necessary to scale down both $\cos(\beta)$ and $\sin(\beta)$ by the same amount. One way for scaling down these quantities is to divide both of them by a positive number greater than or equal to 1. If this is done, our 2-D digital filters will have their passbands expanded in both frequency axes. So, in designing the 1-D prototype filter we would have to compress the bandwidth by the same amount. In addition, we should take the warping effect into account. However, if we were to decrease $\cos(\beta)$ and $\sin(\beta)$ by a large amount a narrow-band FIR filter would be needed, which would necessitate a high-order transfer function. Consequently, the 2-D filter order would increase tremendously and this is not desirable.

The filter can also be designed without decreasing $\cos(\beta)$ and $\sin(\beta)$ in Eqn. 2.8. However, since the transformation does not present global type preservation, spikes will show up in the 2-D amplitude response at the Nyquist points. Nevertheless, this problem can be overcome by using a guard filter.

When we use rotation angles β , outside the range $(0^\circ, 90^\circ)$ we end up with an unstable filter in the $(+,+)$ direction. Stabilization can be achieved by performing the recursion in one of directions $(+,-)$, $(-,+)$, $(-,-)$. However, the denominator in Eqn. 2.42 is factorizable. Stabilization in the $(+,+)$ direction can be easily achieved

by replacing the poles outside of the unit bidisc by their inverses, which will be located inside the unit bidisc.

If a zero-phase filter is not required, the 1-D filter can be rotated by angles in the range $\beta \in (-90^\circ, 90^\circ)$. For each angle in the range $(0^\circ, 90^\circ)$, the 2-D filter is stable in the $(+, +)$ direction and for each angle in the range $(-90^\circ, 0^\circ)$ the 2-D filter can be stabilized in the $(+, +)$ direction as described above. Hence a cascade filter can be obtained which is stable in the $(+, +)$ direction.

If a zero-phase filter is required, the 1-D filter should be rotated using angles β in each quadrant, i.e., $\beta \in (0^\circ, 360^\circ)$. For each angle in the range $(-90^\circ, 90^\circ)$ the 2-D digital filter can be stabilized in the $(+, +)$ direction as in the previous case, and for each angle in the range $(90^\circ, 270^\circ)$ the 2-D digital filter can be stabilized in the $(-, -)$ direction by using the same technique. Hence a cascade filter can be obtained which would require just two data transformations.

The disadvantage of using an 1-D FIR filter as a prototype in the design is that the order of the resulting 2-D filter is much greater than the order of a corresponding 2-D filter designed using a 1-D analog filter or a 1-D IIR filter as a starting filter. However, an advantage is gained in that the amount of data manipulations can be reduced.

Example 2.2

The technique described in this section was used to design a lowpass nonzero-phase filter. The resulting 2-D filter is causal and stable in the $(+,+)$ direction. The design specifications of the FIR filter and the required guard filter are shown in Table 2.3. For the guard filter, a 2-D separable Butterworth transfer function was used. The rotation angles were $\pm 30^\circ$ and $\pm 60^\circ$. The amplitude response of the filter without guard filter is shown in Fig. 2.4. The amplitude response of the combined filter incorporating the guard filter is shown in Fig. 2.5(a). The corresponding contour plot is shown in Fig. 2.5(b).

2.8 Design of 2-D highpass filters

In this section a method is proposed for the design of 2-D circularly symmetric highpass filters.

Consider two rotated or pseudo-rotated filters which were obtained from an analog highpass filter using rotation angles β and $-\beta$, where $0^\circ < \beta < 90^\circ$. The idealized contour plots for the two filters are shown in Figs. 2.6(a) and

Table 2.3 Design Specifications for the FIR and Guard Filters

Prototype Filter	W_p (rad/s)	W_a (rad/s)	A_p (dB)	A_a (dB)	Rotation Angles
Chebyshev (FIR)	1.5	2.0	0.1	40.0	$\pm 30^\circ$, $\pm 60^\circ$
Butterworth (guard filter)	2.1	2.7	0.1	40.0	separable filters

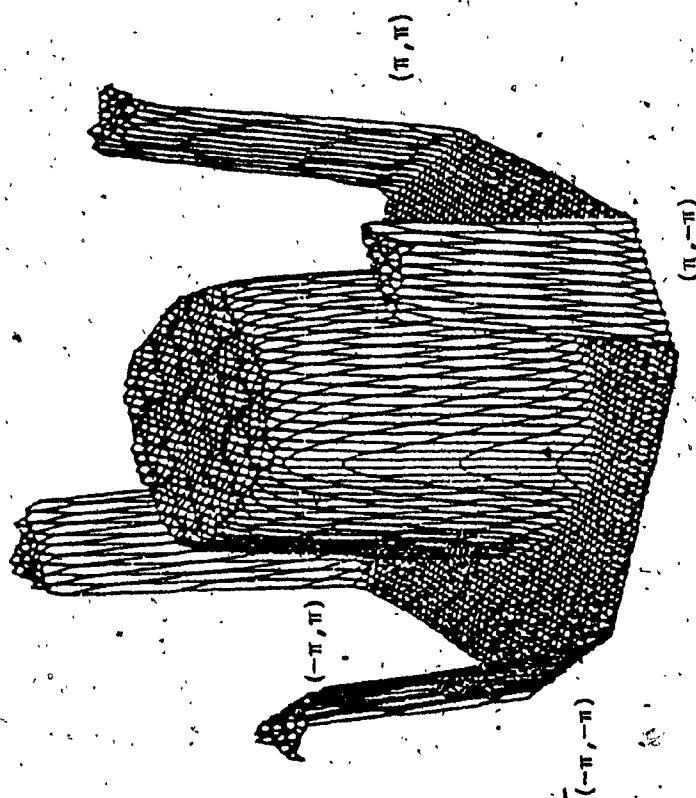


Figure 2.4. 3-D Plot of 2-D Lowpass Filter without Guard Filter

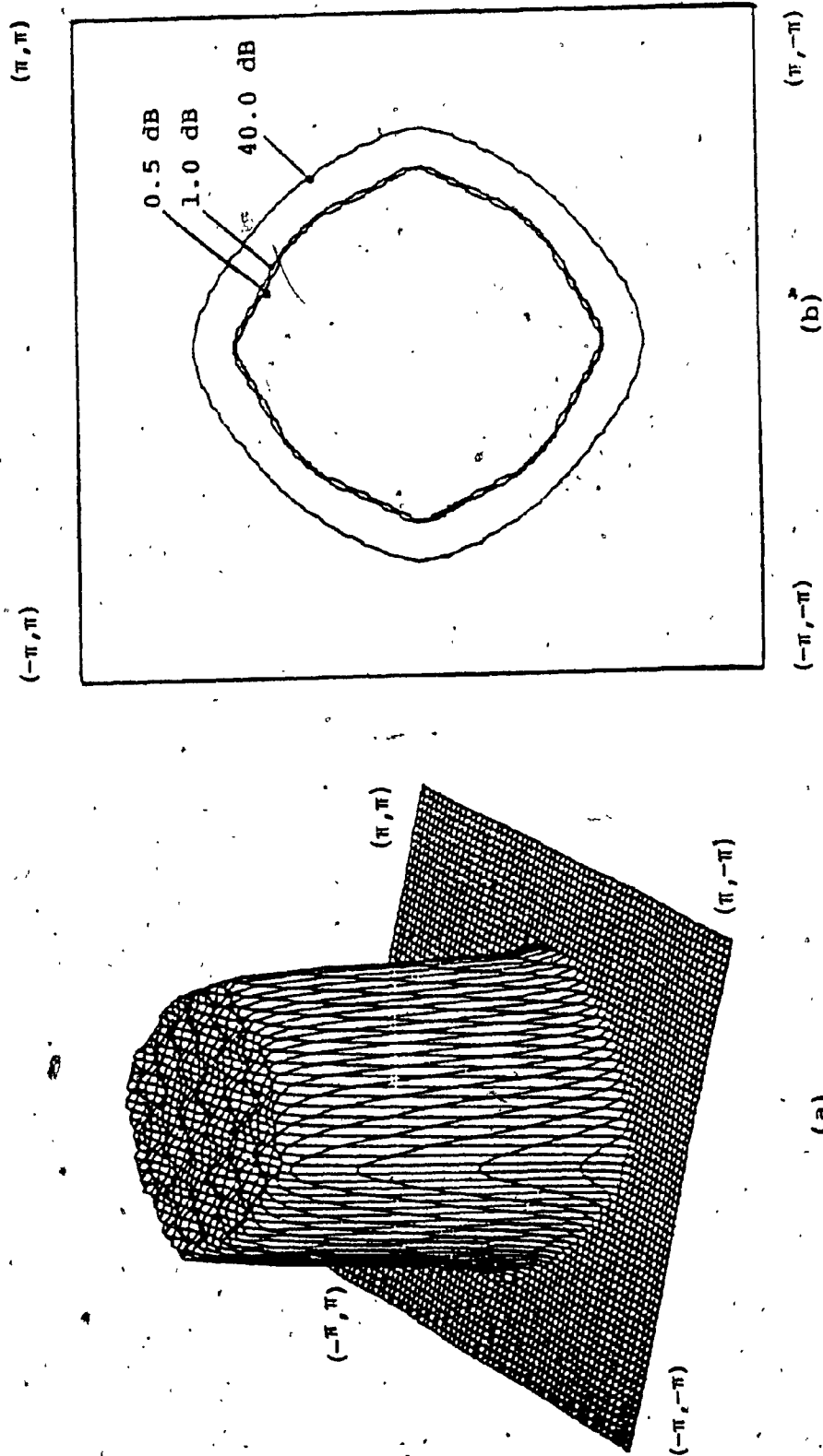


Figure 2.5 2-D Lowpass Filter with Guard Filter, (a) 3-D Plot, (b) Contour Plots for Attenuations of 0.5 dB, 1.0 dB, and 40.0 dB.

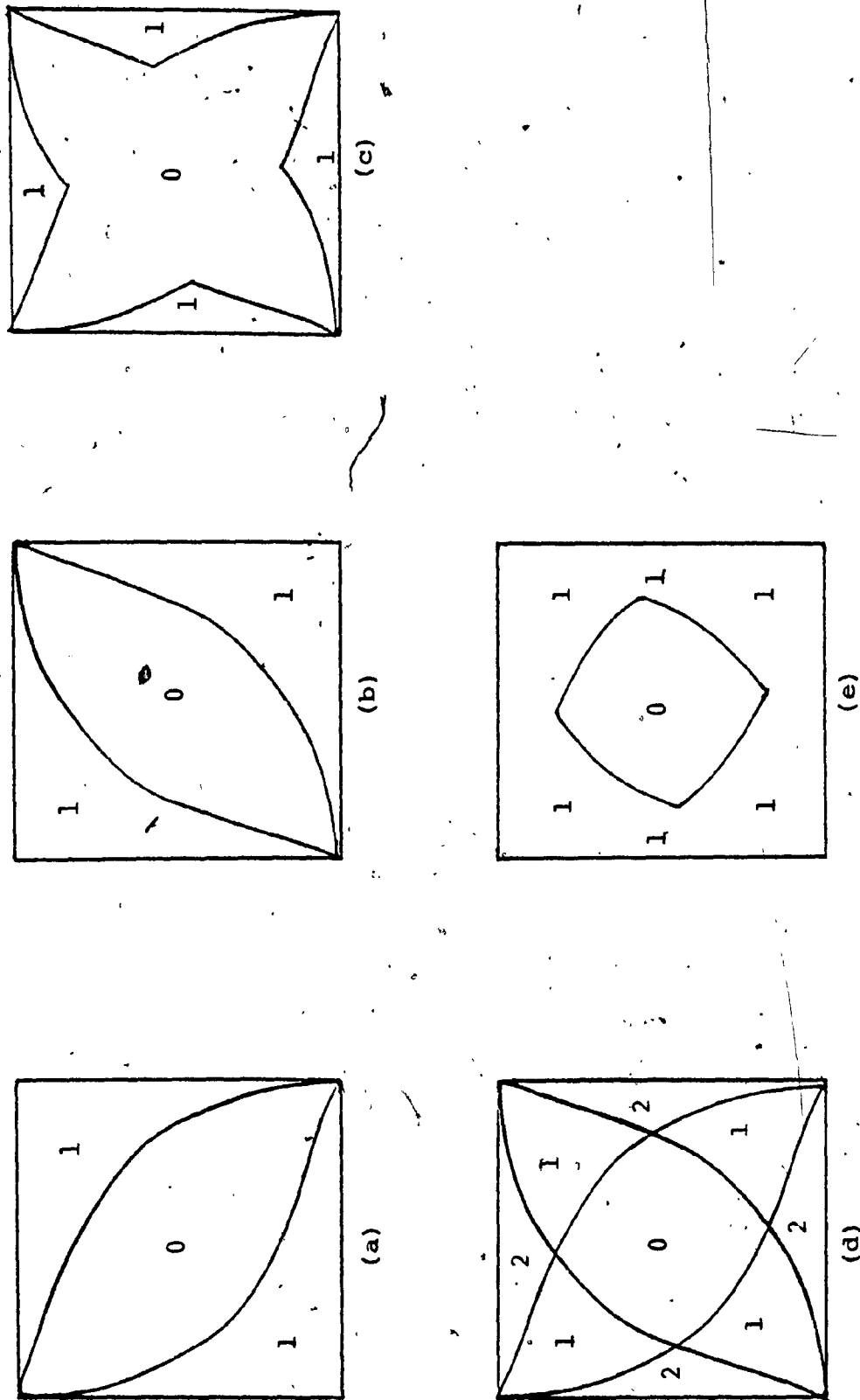


Figure 2.6 (a) Rotation by β , (b) Rotation by $-\beta$, (c) Series Interconnection, (d) Parallel Interconnection, (e) Rotated Highpass Filter.

2.6(b). If these two filters are cascaded, the amplitude response of the combination is obtained by multiplying the gains of the filters at corresponding points. The composite idealized contour plot is thus obtained as shown in Fig. 2.6(c). As can be seen, the contour plot does not represent a 2-D circularly symmetric highpass filter and, therefore, the design of these filters cannot be obtained by simply cascading pseudo-rotated filters as in the case of lowpass filters. Nevertheless, the design of such filters is possible through the use of a combination of cascade and parallel filters, as will be shown below.

If the above pseudo-rotated filters are connected in parallel, we obtain a composite filter whose contour plot is shown in Fig. 2.6(d). By subtracting the output of the cascade filter from the output of the parallel filter, we achieve an overall filter whose contour plot is shown in Fig. 2.6(e). Evidently, this plot resembles the idealized plot of a 2-D circularly symmetric highpass filter. In effect, a filter configuration is available for the design of these filters. Since each filter must have zero phase, it is necessary to use in cascade with each filter its counterpart filter whose recursion is taken in the opposite direction in both spacial dimensions. Therefore, a 2-D highpass filter can be designed by forming the transfer function

$$H_1^{\beta} = H^{++} H^{--} + H^{+-} H^{-+} - H^{++} H^{--} H^{+-} H^{-+} \quad (2.45)$$

For two different rotation angles, we apply the same basic block implementation, that is

$$H = H_1^{\beta_1} + H_2^{\beta_2} - H_1^{\beta_1} H_2^{\beta_2} \quad (2.46)$$

where H_2 is of the form given in Eqn. 2.45.

For three or more rotation angles we keep applying repetitively the basic block implementation and we obtain the block diagram of Fig. 2.7. It is worthwhile to point out here that the coefficients of each pseudo-rotated filter have to be such that the output of two cascaded section filters $H^{++} H^{--}$ and $H^{+-} H^{-+}$ have zero-phase shift, that is, the coefficients have to be properly adjusted after rounding or truncation is done. Also, since the number of data manipulations is higher relative to that in lowpass filters, it is desirable to keep the number of pseudo-rotated filters to a minimum.

A problem associated with the above method is that spurious transmission zeros occur in the resulting 2-D digital filter at points $(\pm 1, \pm 1)$ of the (z_1, z_2) plane. To illustrate this problem, consider the first-order transfer function

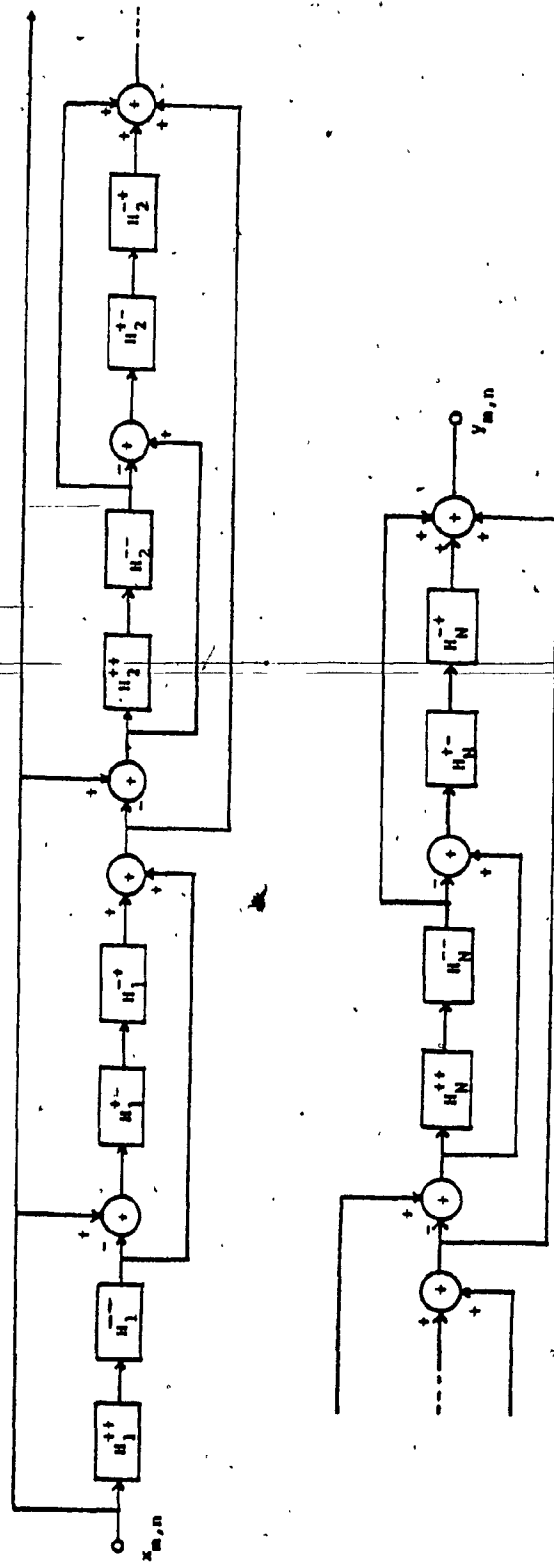


Figure 2.7 Block Diagram of the Proposed 2-D Circularly Symmetric Highpass Filter.

$$H(s) = \frac{s}{s + f} \quad (2.47)$$

where f is a constant.

On applying the transformation of Eqn. 2.8 to this transfer function, and after the double bilinear transformation, we obtain

$$H(z_1, z_2) = \frac{(z_1 - 1)(z_2 - 1)\cos(\beta) + (z_1 + 1)(z_2 - 1)\sin(\beta)}{(z_1 - 1)(z_2 + 1)\cos(\beta) + (z_1 + 1)(z_2 - 1)\sin(\beta)} + f \frac{T}{2} \left[(1 + z_1)(1 + z_2) + (z_1 - 1)(z_2 - 1) \frac{4c}{T^2} \right] \quad (2.48)$$

As can be seen, for any of the points $z_1 = \pm 1$ and $z_2 = \pm 1$, the amplitude response of the transfer function becomes zero.

On the other hand, if the analog transfer function is of the form

$$H(s) = \frac{s + g}{s + f} \quad (2.49)$$

where f and g are complex or real constants then

$$H(z_1, z_2) = \frac{(z_1 - 1)(z_2 + 1)\cos(\beta) + (z_1 + 1)(z_2 - 1)\sin(\beta) + g \frac{T}{2} \left[(1 + z_1)(1 + z_2) + (z_1 - 1)(z_2 - 1) \frac{4c}{T^2} \right]}{(z_1 - 1)(z_2 + 1)\cos(\beta) + (z_1 + 1)(z_2 - 1)\sin(\beta) + f \frac{T}{2} \left[(1 + z_1)(1 + z_2) + (z_1 - 1)(z_2 - 1) \frac{4c}{T^2} \right]} \quad (2.50)$$

Although transmission zeros at $z_1 = \pm 1$ and $z_2 = \pm 1$ tend to distort the amplitude response of the filter, they do not present serious difficulties if the frequency spectrum of the 2-D signal does not contain components at the Nyquist frequencies. In certain applications, however, these zeros might be objectionable.

The number of data manipulations for the proposed 2-D highpass filter structure is higher relative to that in a corresponding 2-D lowpass filter. It is possible to obtain a 2-D pseudo-rotated highpass filter with fewer manipulations by starting the design from FIR filters in conjunction with phase equalizers. In this case, we can have for a single angle β , $0^\circ < \beta < 90^\circ$, the following configuration

$$H(z_1, z_2) = H_1(z_1, z_2) E_1(z_1, z_2) + H_2(z_1, z_2) E_2(z_1, z_2) - H_1(z_1, z_2) H_2(z_1, z_2) E_3(z_1, z_2) \quad (2.51)$$

where H_1 and H_2 represent the transfer function of the filter rotated by angles β and $-\beta$, respectively. The filters whose transfer functions are $E_1(z_1, z_2)$ and $E_2(z_1, z_2)$ represent phase equalizers for the transfer functions H_1 and H_2 , respectively. Since the design starts from an FIR filter, the denominator of $H(z_1, z_2)$ can be factorized and hence by changing the poles outside of the unit bidisc by

their inverses the recursion can be performed in the $(+,+)$ direction. Phase equalizers characterized by E_1 and E_2 also should recurse in the $(+,+)$ direction only.

Now for different angles β_i , $0^\circ < \beta_i < 90^\circ$, $i=1,2, \dots$, we can apply the above procedure to obtain the configuration shown in Fig. 2.8. In this way a 2-D pseudo-rotated highpass filter is obtained which is recursing only in the $(+,+)$ direction.

Example 2.3

The 2-D highpass configuration of Fig. 2.7 was used to design 3 highpass filters, namely, a Butterworth, a Chebyshev and an elliptic filter. The design specifications for the passband edge (W_p), for the stopband edge (W_a), for the maximum passband ripple (A_p), and the minimum stopband attenuation (A_a) are shown in Table 2.4. The sampling frequency was 2π rad/s and the rotation angles were $\pm 30^\circ$, $\pm 60^\circ$, $180^\circ \pm 30^\circ$ and $180^\circ \pm 60^\circ$. The specifications of the analog prototype filters were assumed to be identical as for the 2-D digital filters except that the warping effect was taken into account in the calculation the passband and stopband edges of the analog filters.

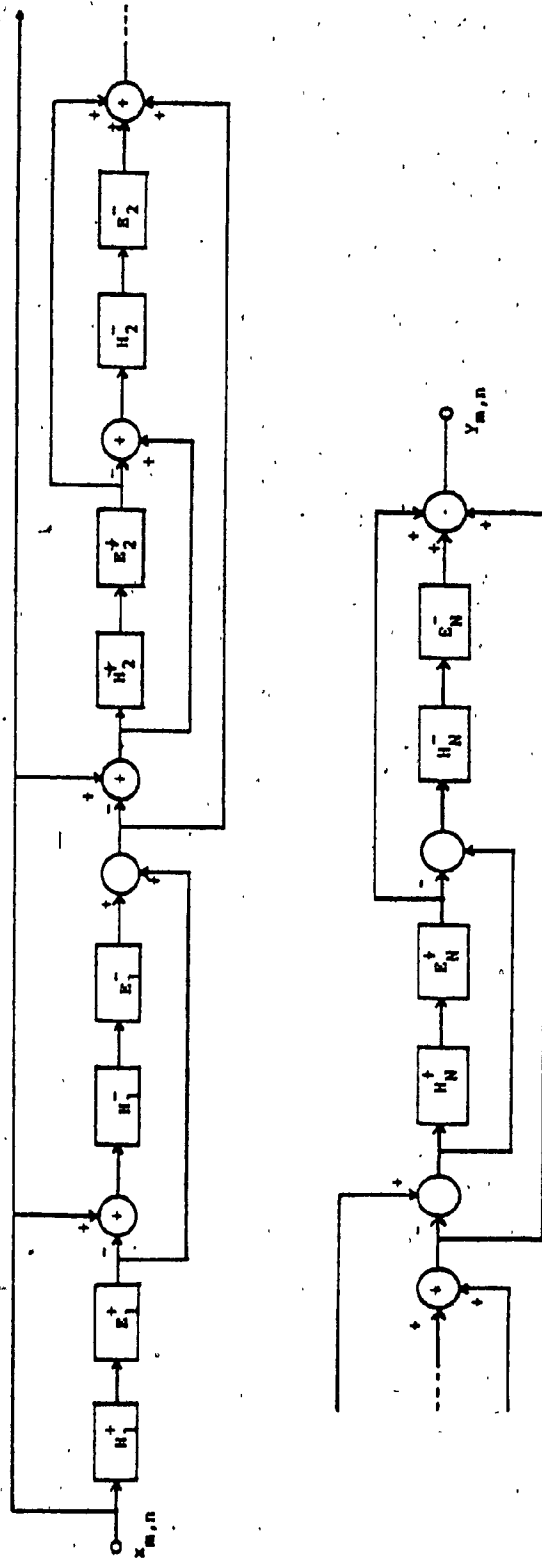


Figure 2.8 Block Diagram of the Proposed 2-D Highpass Filter Recursing in the $(+,+)$ Direction.

Table 2.4 Specifications for the 2-D Digital Highpass Filters

Prototype Filter	W_p (rad/s)	W_a (rad/s)	A_p (dB)	A_a (dB)	Rotation Angles
Butterworth	2.0	1.5	0.3	30.0	$\pm 30^\circ$, $180^\circ \pm 30^\circ$ $\pm 60^\circ$, $180^\circ \pm 60^\circ$
Chebyshev	2.0	1.5	0.3	30.0	$\pm 30^\circ$, $180^\circ \pm 30^\circ$ $\pm 60^\circ$, $180^\circ \pm 60^\circ$
elliptic	2.0	1.5	0.3	30.0	$\pm 30^\circ$, $180^\circ \pm 30^\circ$ $\pm 60^\circ$, $180^\circ \pm 60^\circ$

The amplitude responses and the corresponding contour plots of the filters obtained are shown in Figs. 2.9 to 2.11. Table 2.5 shows the actual values for A_p and A_a obtained for the designed filters. These values disagree with the corresponding specified values. However, improved results can be obtained by using the method of Chapter 3.

2.9 Design of 2-D bandpass pseudo-rotated filters

Circularly symmetric bandpass filters can be obtained by cascading lowpass and highpass filters having appropriate specifications. The design can be completed by designing the lowpass and highpass filters using the methods described so far.

Example 2.4

The above approach is illustrated by designing a 2-D circularly symmetric pseudo-rotated bandpass filter whose specifications are shown in Table 2.6. The rotation angles were $\pm 30^\circ$, $\pm 60^\circ$, $180^\circ \pm 30^\circ$ and $180^\circ \pm 60^\circ$. The amplitude response and the contour plots are shown in Figs. 2.12(a) and 2.12(b), respectively. The actual passband ripple and stopband attenuation of the 2-D filter are $A_p = 0.9125$ dB.

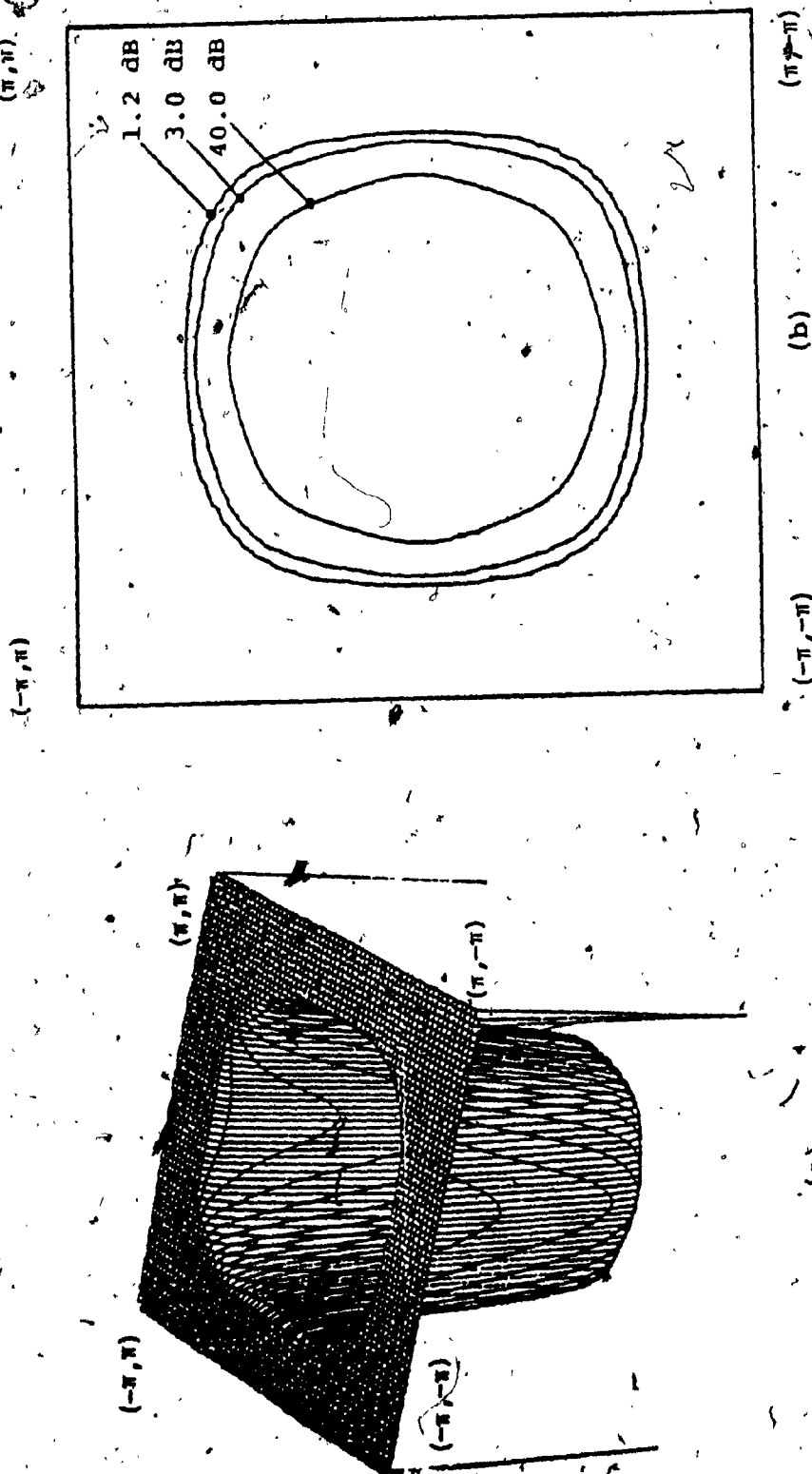


Figure 2.9 2-D Butterworth Highpass Filter, (a) 3-D Plot, (b) Contour Plots for Attenuations of 1.2 dB, 3.0 dB, and 40.0 dB.

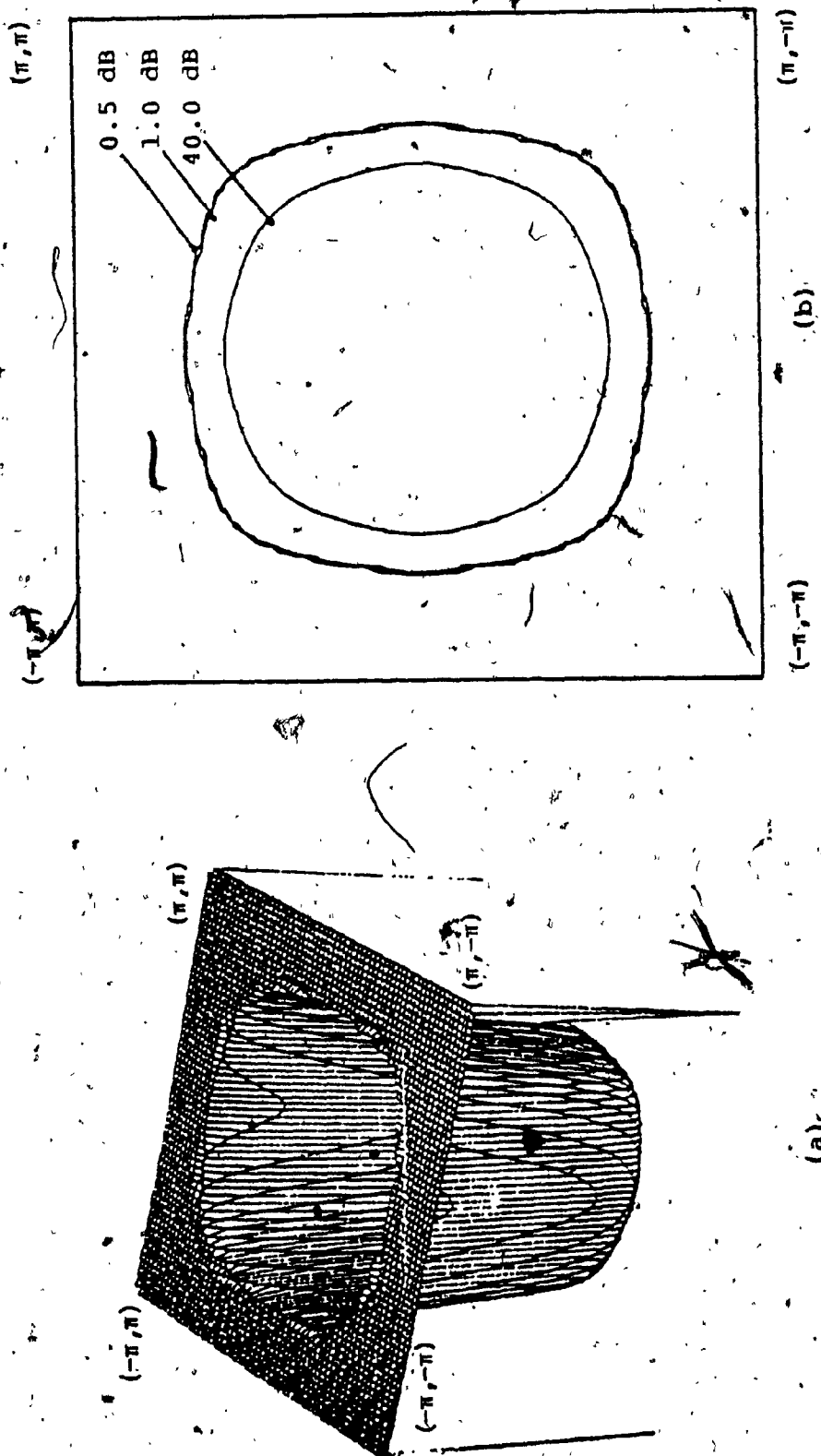


Figure 2.10 2-D Chebyshev Highpass Filter, (a) 3-D Plot, (b) Contour Plots for Attenuations of 0.5 dB, 1.0 dB, and 40.0 dB.

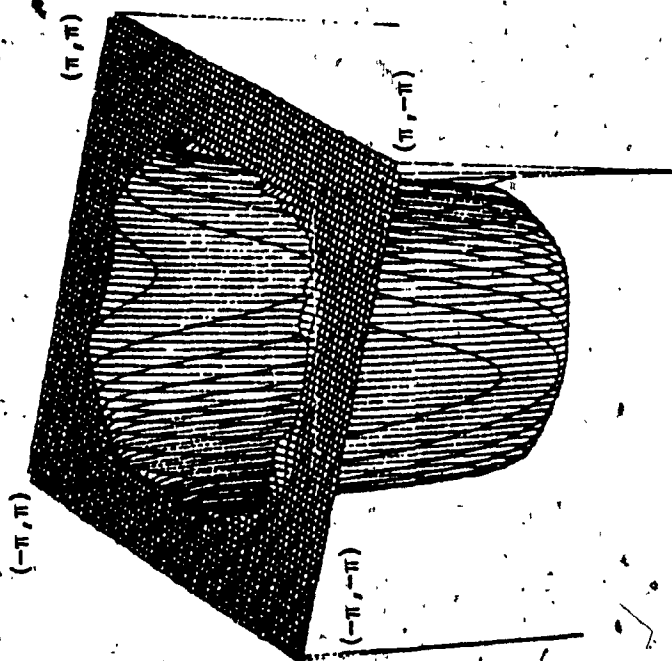
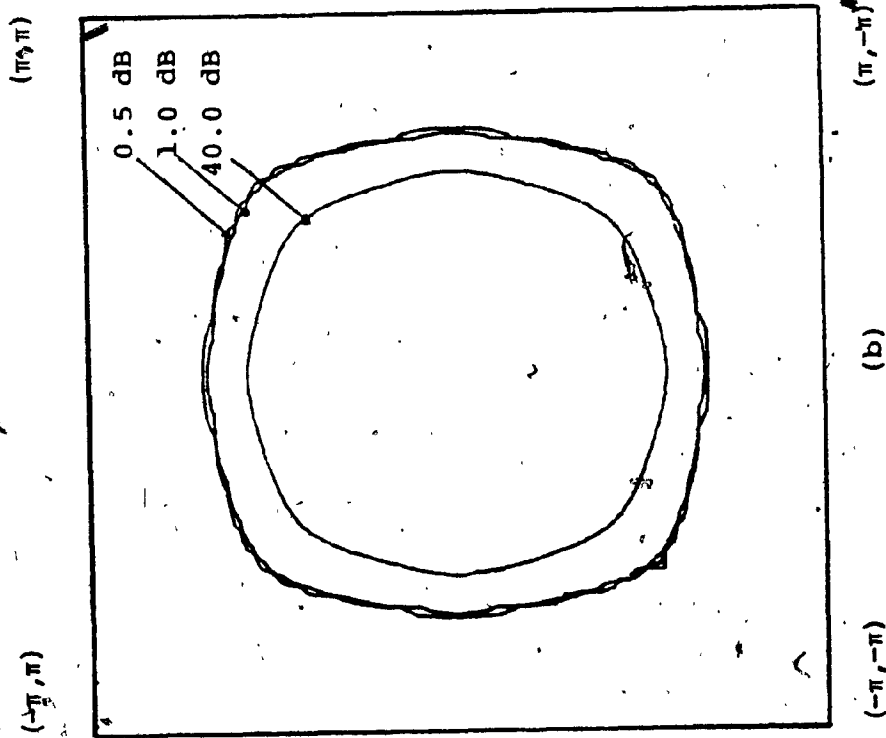


Figure 2.11 2-D Elliptic Highpass Filter, (a) 3-D Plot, (b) Contour Plots for Attenuations of 0.5 dB, 1.0 dB, and 40.0 dB

Table 2.5 Actual Characteristics Obtained for the Highpass Filters

Prototype Filter	A'_p (dB)	A'_a (dB)
Butterworth	1.04	78.00
Chebyshev	3.36	67.93
elliptic	2.54	69.29

Table 2.6 Specifications for the Bandpass Filter and for the Corresponding Lowpass (LP) and Highpass (HP) Filters

Prototype Filter	ω_{p1} (rad/s)	ω_{p2} (rad/s)	ω_{a1} (rad/s)	ω_{a2} (rad/s)	A_p (dB)	A_a (dB)	Rotation Angles
Butterworth LP	-	1.7	-	2.0	0.1	7.0	$\pm 30^\circ$, $180^\circ \pm 30^\circ$ $\pm 60^\circ$, $180^\circ \pm 60^\circ$
Butterworth HP	0.8	-	0.5	-	0.2	10.0	$\pm 30^\circ$, $180^\circ \pm 30^\circ$ $\pm 60^\circ$, $180^\circ \pm 60^\circ$

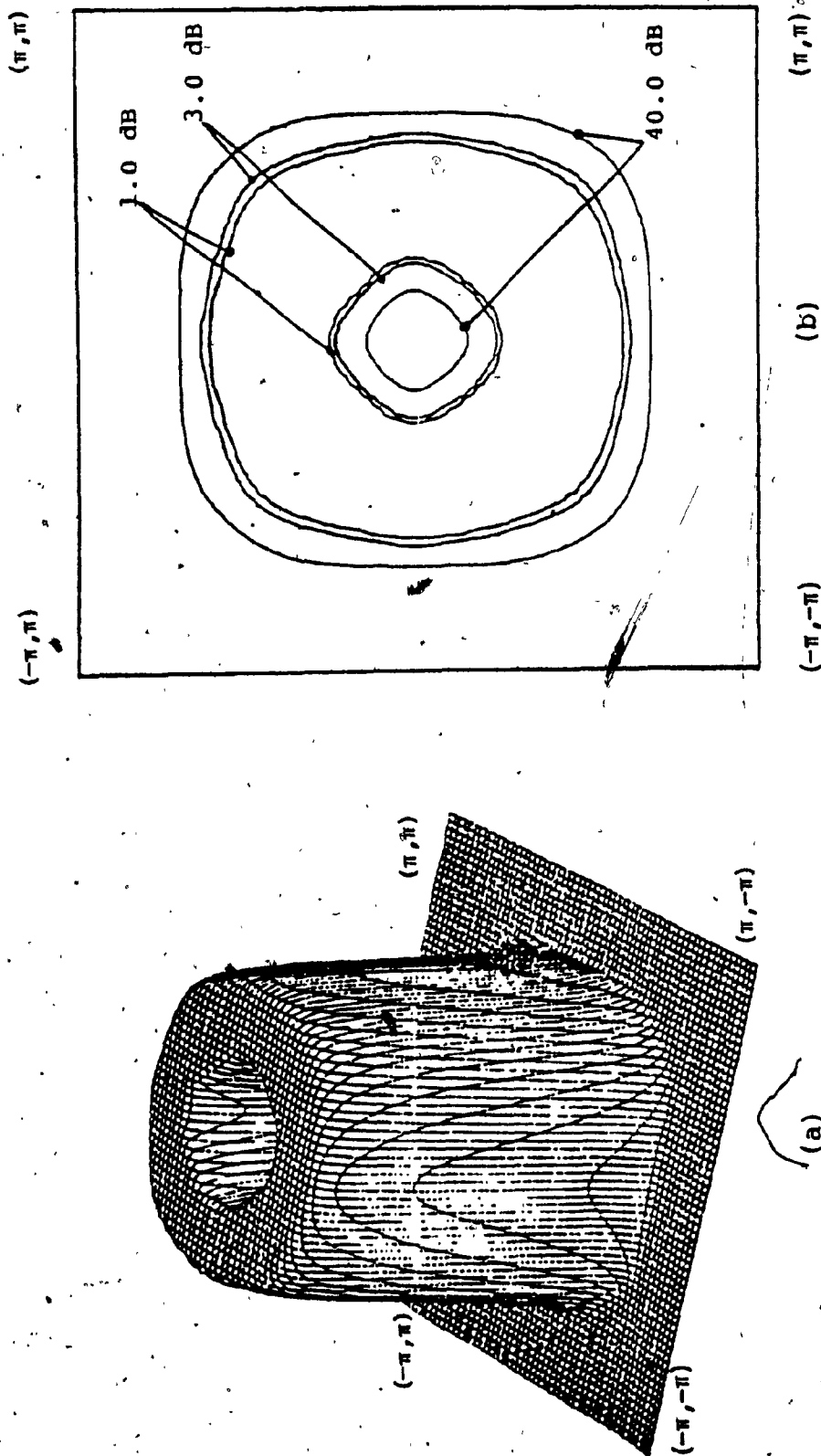


Figure 2.12 2-D Butterworth Bandpass Filter, (a) 3-D Plot, (b) Contour Plots for Attenuations of 1.0 dB, 3.0 dB, and 40.0 dB.

and $A_a = 8.76$ dB, respectively.

2.10 Design of 2-D bandstop pseudo-rotated filters

Bandstop filters can be obtained by connecting lowpass and highpass filters in parallel.

Example 2.5

The above approach is illustrated by designing a 2-D circularly symmetric bandstop filter having the specifications shown in Table 2.7. Using rotation angles of $\pm 30^\circ$, $\pm 60^\circ$, $180^\circ \pm 30^\circ$ and $180^\circ \pm 60^\circ$, we obtain the amplitude shown in Fig. 2.13(a). The corresponding contour plots are shown in Fig. 2.13(b). The actual maximum passband ripple and the minimum stopband attenuation are $A_p = 5.019$ dB and $A_a = 16.94$ dB, respectively.

Table 2.7 Specifications for the Bandstop Filter and for the Corresponding Lowpass (LP) and Highpass (HP) Filters

Prototype Filter	ω_{p1} (rad/s)	ω_{p2} (rad/s)	ω_{a1} (rad/s)	ω_{a2} (rad/s)	A_p (dB)	A_a (dB)	Rotation Angles
elliptic (LP)	1.0	-	1.3	-	0.1	5.0	$\pm 30^\circ$ $180^\circ \pm 30^\circ$ $\pm 60^\circ$ $180^\circ \pm 60^\circ$
elliptic (HP)	-	2.0	-	1.7	0.4	20.0	$\pm 30^\circ$ $180^\circ \pm 30^\circ$ $\pm 60^\circ$ $180^\circ \pm 60^\circ$

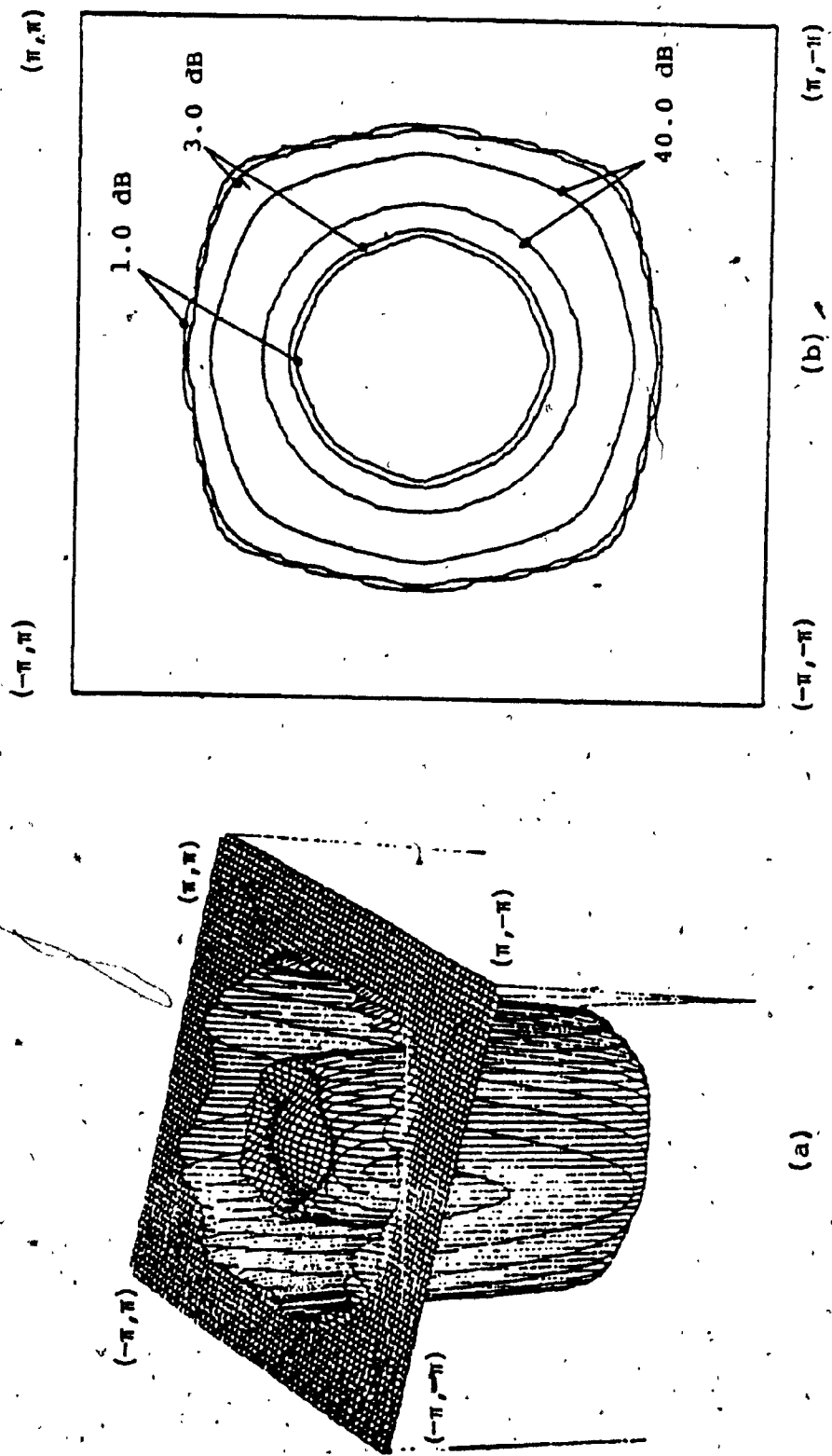


Figure 2.13 2-D Elliptic Bandstop Filter, (a) 3-D Plot, (b) Contour Plots for Attenuations of 1.0 dB, 3.0 dB, and 40.0 dB.

2.11 Conclusions

In this chapter a transformation has been obtained by combining two known transformations. The new transformation performs pseudo-rotation of the s_1 and s_2 axes which can be made to approach true rotation as closely as desired. The transformation leads to stable 2-D digital filters which are free of non-essential singularities of the second kind.

Two methods for the design of 2-D circularly symmetric pseudo-rotated lowpass filters have been described. In the first method the design starts with a 1-D analog or a 1-D IIR filter while in the second method the design starts with a 1-D FIR filter. In the first method, the pseudo-rotation of the axes is forced to approach true rotation closely and, consequently, the amplitude response of the prototype filter, is preserved in the 2-D digital filter. Therefore, no guard filters were found to be necessary. On the other hand, in the second method the pseudo-rotation is not allowed to approach true rotation too closely, and the transformation does not preserve the amplitude response of the prototype filter at points in the neighborhoods of the Nyquist points. Therefore, guard filters are necessary in this case. The first method leads to lower-order transfer functions but two additional manipulations of the input data

are necessary in the implementation.

A new configuration has been proposed for the design of 2-D circularly symmetric rotated or pseudo-rotated highpass filters. In the design four transmission zeros appear at $z_1 = \pm 1$ $z_2 = \pm 1$, which may cause difficulties in certain applications. A procedure for designing 2-D highpass filters which are recursing in just the $(+,+)$ direction has also been presented. This design starts with a 1-D FIR filter.

Finally, the design of 2-D bandpass and 2-D bandstop circularly symmetric filters was investigated and appropriate design methods were developed.

CHAPTER 3DESIGN OF PSEUDO-ROTATED FILTERSSATISFYING PRESCRIBED AMPLITUDE SPECIFICATIONS3.1 Introduction

The design of 2-D pseudo-rotated lowpass, highpass, etc., filters is accomplished in two steps. First, the analog transfer function is transformed many times by the method of pseudo-rotation in order to obtain a set of cascade pseudo-rotated filter sections. Then the double bilinear transformation is applied. The specifications achieved in the 2-D filter obtained, namely, the resulting maximum passband ripple, minimum stopband loss, and band edges differ significantly from those of the analog prototype. The maximum passband ripple and the minimum stopband loss depend not only on the corresponding parameters in the analog prototype but also on the number of rotations. On the other hand, the band edges depend not only on the band edges of the analog prototype but also on the sampling frequencies used owing to the warping effect. This chapter deals with the details that are inherent in the design of pseudo-rotated filters.

In the previous chapter, several methods for designing 2-D circularly symmetric pseudo-rotated filters have been studied. Though these methods lead to fast designs, extensive trial and error is necessary if prescribed amplitude specifications are to be achieved. It is thus of interest to develop straightforward design techniques which lead to filters satisfying desired specifications.

Initially typical characteristics for practical lowpass, highpass, bandpass and bandstop 2-D filters are described. Then circularity measures are defined which can be used in the design process. Subsequently, the design of Butterworth, Chebyshev and elliptic 2-D filters is considered in detail. The design method consists of a set of techniques which yield predictions for the required parameters of the analog prototype in order to meet the required amplitude response specifications in the 2-D digital filters.

3.2 Typical characteristics of 2-D filters

A 2-D circularly symmetric filter is characterized by the following parameters :

A_p^{2D} = maximum passband ripple in dB

A_a^{2D} = minimum stopband loss in dB

W_p^{2D} = passband edge in rad/s

W_a^{2D} = stopband edge in rad/s

W_{p1}^{2D} = lower passband edge in rad/s

W_{p2}^{2D} = upper passband edge in rad/s

W_{a1}^{2D} = lower stopband edge in rad/s

W_{a2}^{2D} = upper stopband edge in rad/s

where W_p^{2D} and W_a^{2D} apply to lowpass and highpass filters and W_{p1}^{2D} , W_{p2}^{2D} , W_{a1}^{2D} , and W_{a2}^{2D} apply to bandpass and bandstop filters. The sampling frequencies are assumed to be W_{s1} and W_{s2} in rad/s.

The transfer function of a 2-D digital filter is of the form

$$H(z_1, z_2) = \frac{\sum_{k=1}^M a_{k1} z_1^{1-k} z_2^{1-l}}{\sum_{i=1}^{M_b} \sum_{j=1}^{N_b} b_{ij} z_1^{1-i} z_2^{1-j}} \quad (3.1)$$

If $W_{s1} = W_{s2} = W_s$ where $W_s = 2\pi/T$ and T is the sampling interval, then the frequency response of the filter at frequencies w_1 and w_2 is given by Eqn. 3.1 as

$$H(e^{jw_1 T}, e^{jw_2 T}) = M(w_1, w_2) e^{j\theta(w_1, w_2)} \quad (3.2)$$

where $M(w_1, w_2)$ is the amplitude response and $\theta(w_1, w_2)$ is the phase response of the filter. In this and the following chapters T is assumed to be 1, i.e., $W_s = 2\pi$.

Assuming that the maximum of the amplitude response is equal to 1 in the passband region, the loss characteristic is obtained as

$$L(w_1, w_2) = -20 \log(M(w_1, w_2)) \quad (3.3)$$

Based on the parameters defined above, the loss characteristic of a practical 2-D circularly symmetric filter has to meet the following specifications :

i) Lowpass filters

$$L(w_1, w_2) = \begin{cases} \leq A_p^{2D} & \text{for } 0 \leq R \leq w_p^{2D} \\ \geq A_a^{2D} & \text{for } w_a^{2D} \leq R \leq \pi \end{cases} \quad (3.4)$$

$$\text{where } R = \sqrt{(w_1^2 + w_2^2)}$$

(see Fig. 3.1)

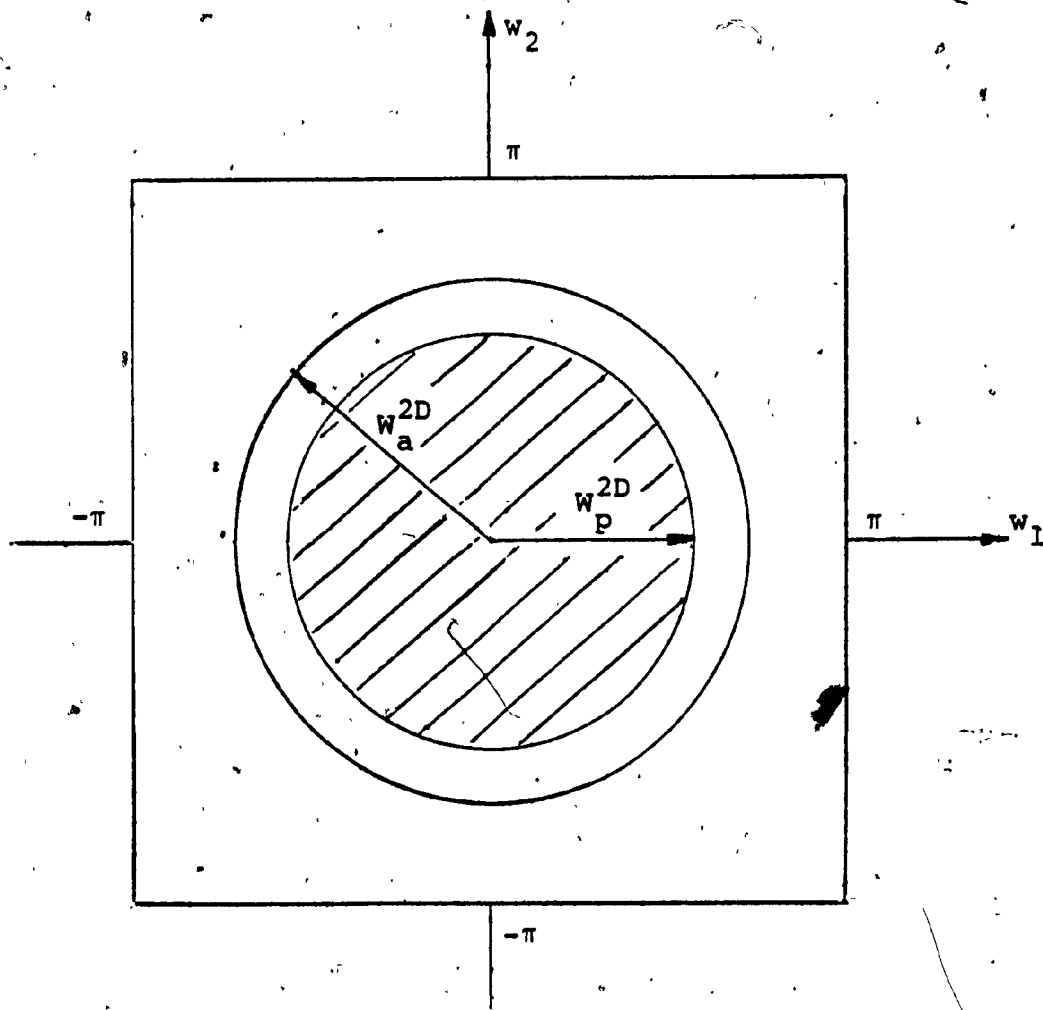


Figure 3.1 Passband and Stopband Boundaries of 2-D
Circularly Symmetric Lowpass Filter

ii) Highpass filters

$$L(w_1, w_2) = \begin{cases} \geq A_a^{2D} & \text{for } 0 \leq R \leq w_a^{2D} \\ \leq A_p^{2D} & \text{for } w_p^{2D} \leq R \leq \pi \end{cases} \quad (3.5)$$

(see Fig. 3.2)

iii) Bandpass filters

$$L(w_1, w_2) = \begin{cases} \leq A_p^{2D} & \text{for } w_{p1}^{2D} \leq R \leq w_{p2}^{2D} \\ \geq A_a^{2D} & \text{for } 0 \leq R \leq w_{a1}^{2D} \\ \geq A_a^{2D} & \text{for } w_{a2}^{2D} \leq R \leq \pi \end{cases} \quad (3.6)$$

(see Fig. 3.3)

iv) Bandstop filters

$$L(w_1, w_2) = \begin{cases} \leq A_p^{2D} & \text{for } 0 \leq R \leq w_{p1}^{2D} \\ \leq A_p^{2D} & \text{for } w_{p2}^{2D} \leq R \leq \pi \\ \geq A_a^{2D} & \text{for } w_{a1}^{2D} \leq R \leq w_{a2}^{2D} \end{cases} \quad (3.7)$$

(see Fig. 3.4)

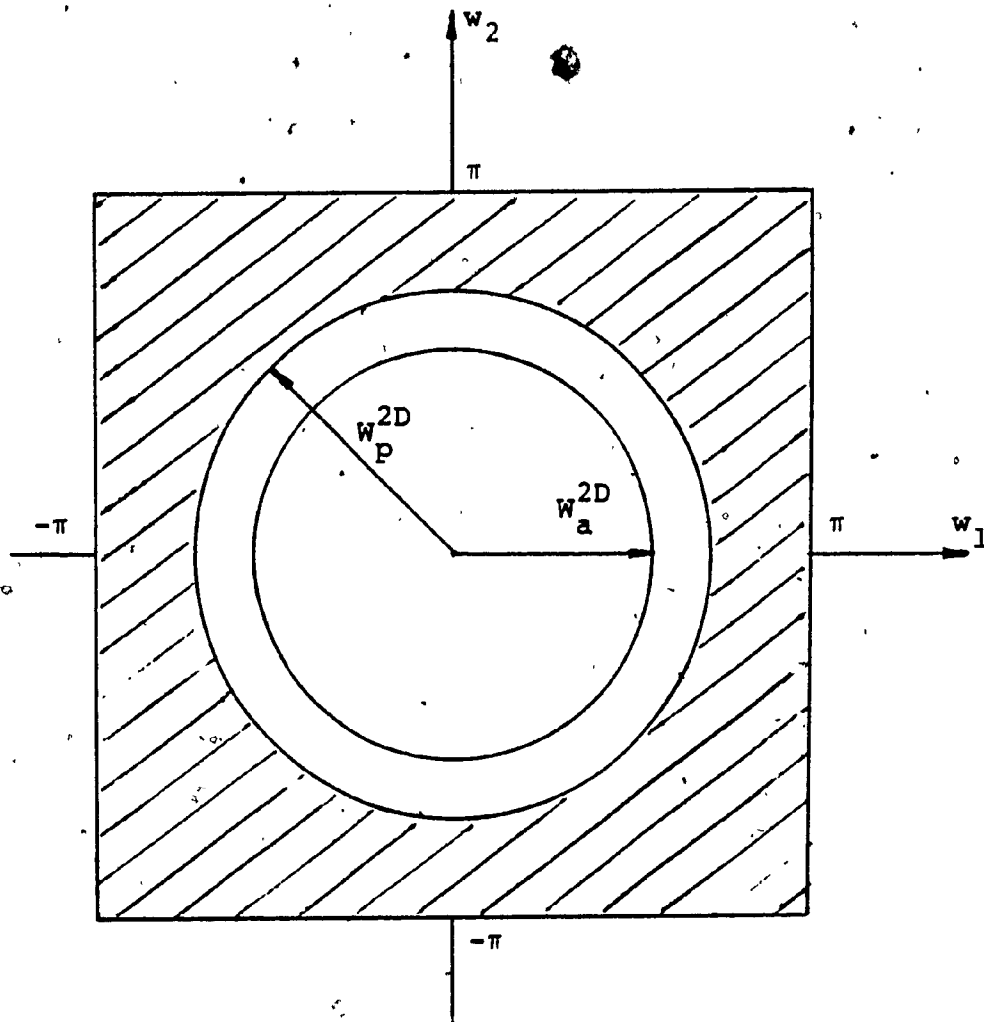


Figure 3.2 Passband and Stopband Boundaries of 2-D Circularly Symmetric Highpass Filter

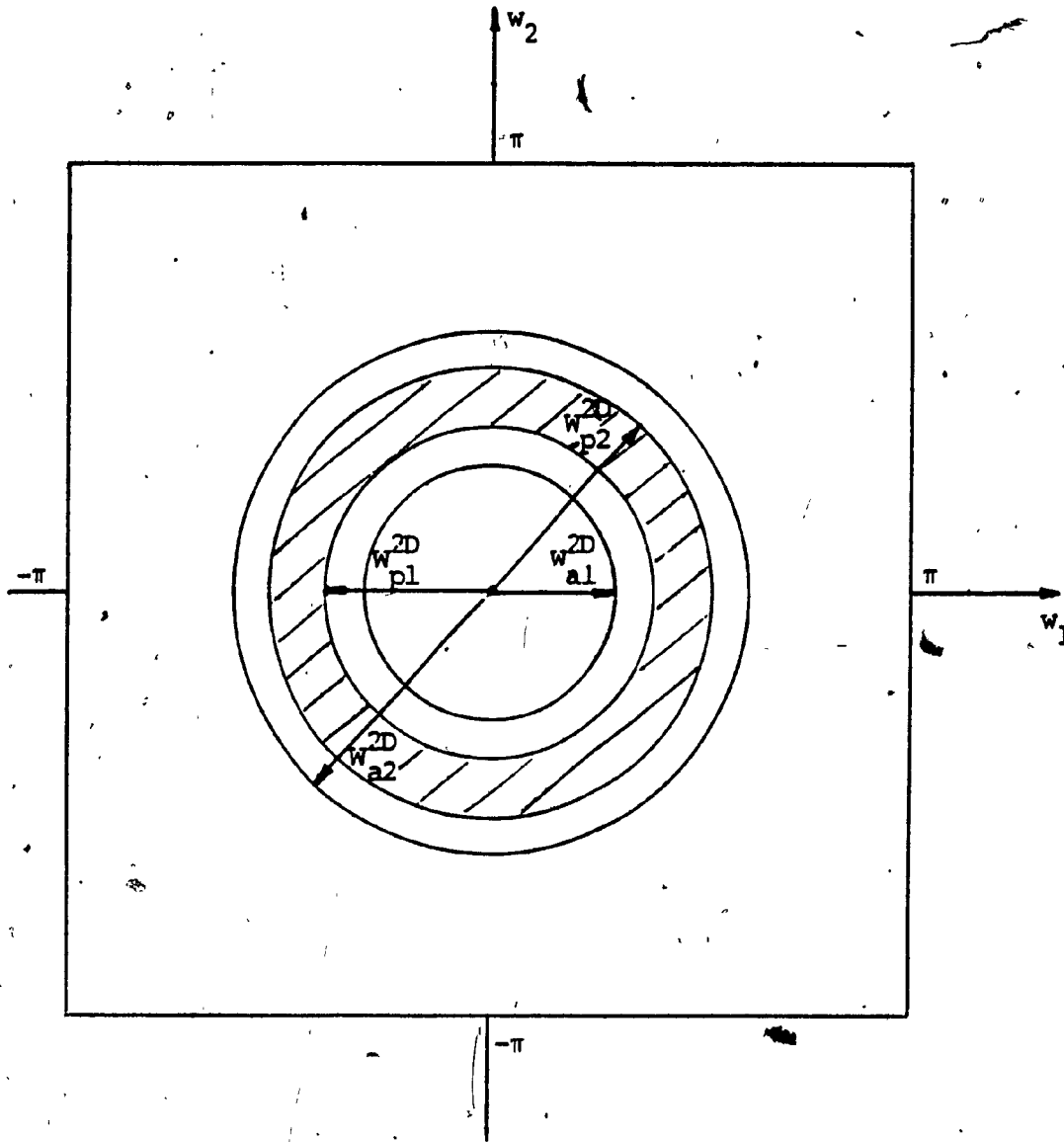


Figure 3.3 Passband and Stopband Boundaries of 2-D Circularly Symmetric Bandpass Filter

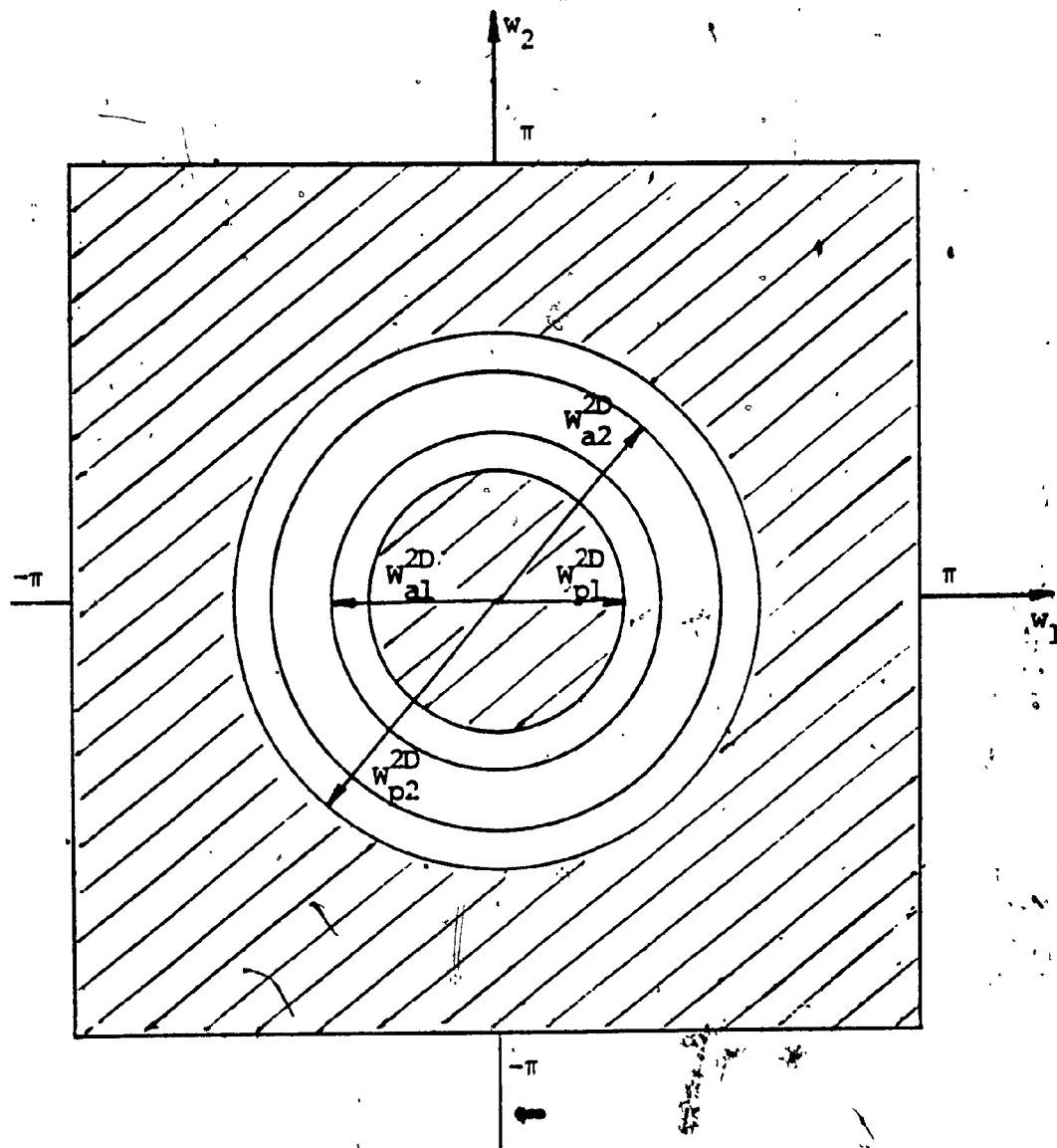


Figure 3.4 Passband and Stopband Boundaries of 2-D Circularly Symmetric Bandstop Filter

3.3 Prediction of the minimum number of pseudo-rotated filters required

It is often necessary to quantify the degree of circularity in 2-D digital filters but unfortunately circularity measures have not been proposed or defined in the past. In this section, such a measure will be developed and used for the prediction of the minimum number of rotations needed to achieve prescribed circularity in lowpass and highpass 2-D filters.

It is of interest to define the circularity of the filter with respect to the passband edge. Let us consider a typical contour plot for a loss of A_p^{2D} dB, as depicted in Fig. 3.5. Such a contour is clearly not circular and a parameter that measures its degree of circularity with respect to the circle of radius w_p^{2D} is needed. Fig. 3.6 shows the pattern obtained by plotting the actual radius versus angle for angles in the range 0° to 360° . For a properly designed 2-D filter, the mean of the radius of the actual passband boundary will be close to the radius of the ideal passband boundary, namely, w_p^{2D} . Therefore, a meaningful measure of circularity can be defined in terms of the variance

$$\sigma^2 = \frac{1}{k-1} \sum_{j=1}^k (w_{pj} - \bar{w}_p)^2$$

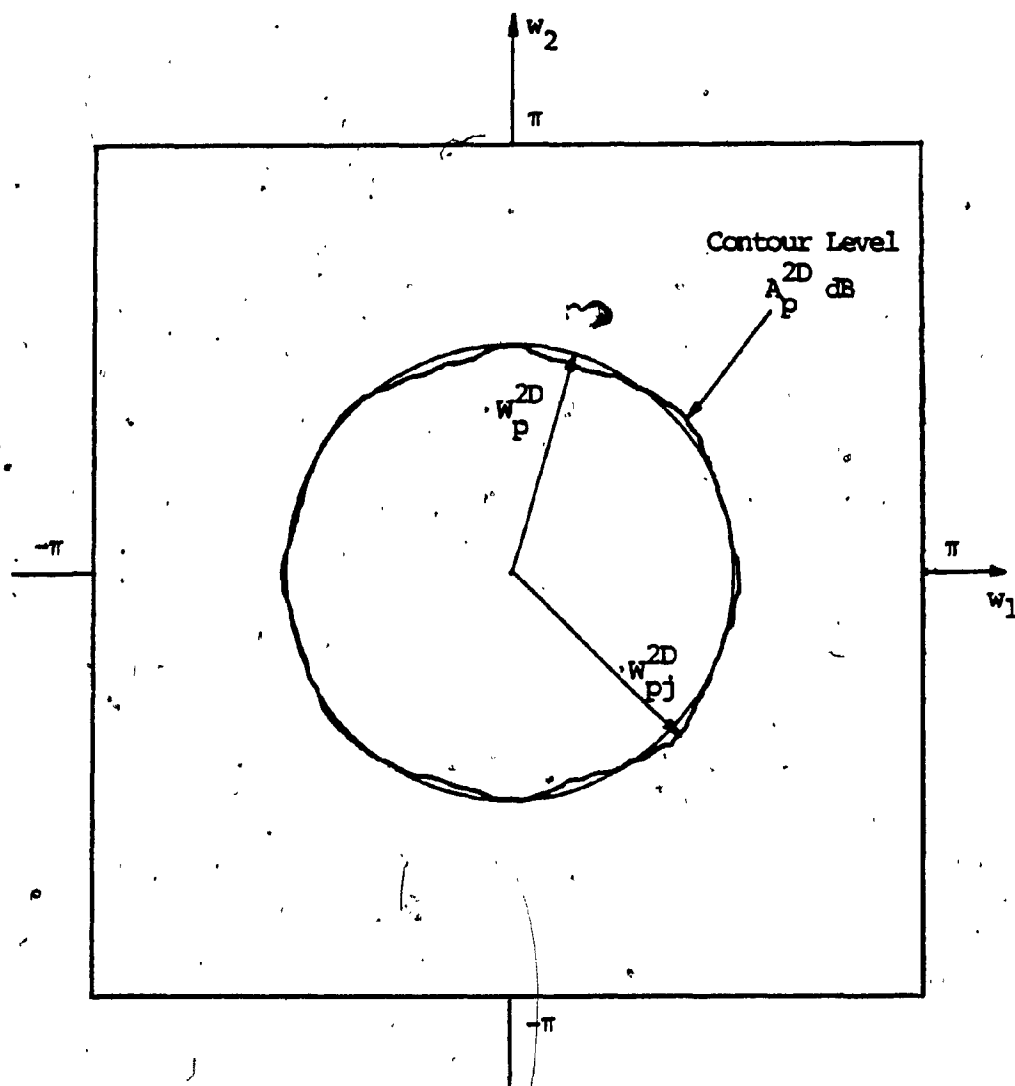


Figure 3.5 Actual and Ideal Passband Boundaries

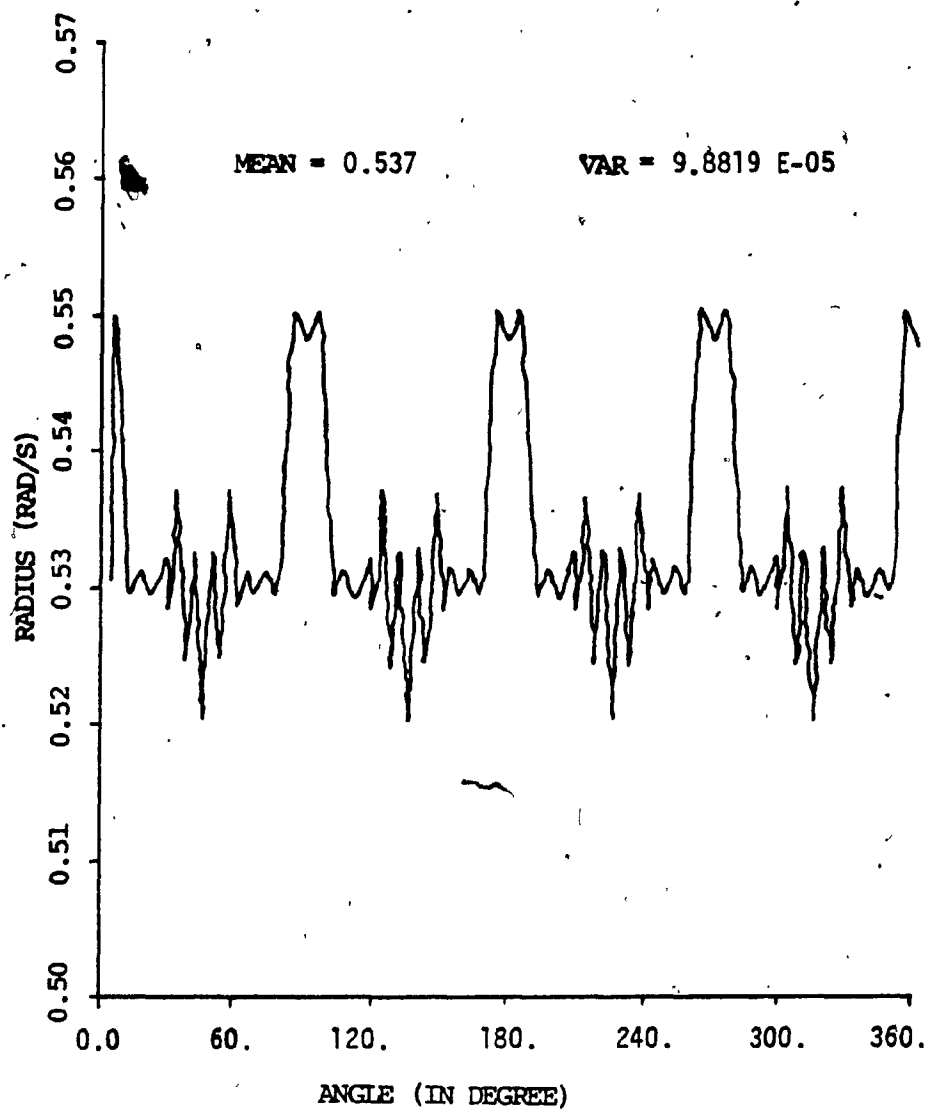


Figure 3.6 Radius of Actual Passband Boundary Versus Angle

where W_{pj} is the actual radius, \bar{W}_p is the mean of the actual radius, and k is the number of sample points on the actual passband boundary.

The variance σ^2 (or standard deviation σ) tends to vary with the type of filter, the number of rotations N , and the passband edge. In order to facilitate the prediction of the number of rotations needed to achieve a prescribed degree of circularity, an empirical formula was developed on the basis of information provided by the actual passband boundary of the 2-D filter. The variance was obtained for many prototype filters as a function of the passband edge for a fixed number of rotated filters N . This was then repeated for values of N in the range 1 to 15 for lowpass and for N in the range 1 to 5 for highpass filters. This procedure was carried out for Butterworth, Chebyshev, and elliptic lowpass as well as highpass filters. Then by means of regression, a prediction formula for σ^2 was deduced as

$$\sigma^2 = A_N + B_N x + C_N x^2 + D_N x^3 \quad (3.8)$$

where

$$x = \frac{2 \pi W_p^{2D}}{W_s} \quad (3.9)$$

is the normalized passband edge. The values of coefficients A_N , B_N , C_N , and D_N are given in Table 3.1 for lowpass

Table 3.1 Coefficients of the Variance (Lowpass Filters)

Filter Type	N	A_N	B_N	C_N	D_N
Butterworth	1	-.21690E-01	.76483E-01	-.63682E-01	.15654E-01
	2	-.60397E-02	.24350E-01	-.27961E-01	.99570E-02
	3	-.57304E-02	.23471E-01	-.28327E-01	.10682E-01
	4	-.60396E-02	.23983E-01	-.28905E-01	.11047E-01
	5	-.62773E-02	.24702E-01	-.29727E-01	.11409E-01
	6	-.60291E-02	.23748E-01	-.28869E-01	.11279E-01
	7	-.61915E-02	.24336E-01	-.29552E-01	.11531E-01
	8	-.62167E-02	.24419E-01	-.29648E-01	.11577E-01
	9	-.62850E-02	.24665E-01	-.29943E-01	.11704E-01
	10	-.62534E-02	.24544E-01	-.29867E-01	.11743E-01
	11	-.62147E-02	.24409E-01	-.29728E-01	.11698E-01
	12	-.61910E-02	.24327E-01	-.29690E-01	.11750E-01
	13	-.64754E-02	.25321E-01	-.30645E-01	.11967E-01
	14	-.64663E-02	.25289E-01	-.30635E-01	.11996E-01
	15	-.65431E-02	.25568E-01	-.30946E-01	.12117E-01
Chebyshev	1	-.23868E-01	.87334E-01	-.74194E-01	.18548E-01
	2	-.63659E-02	.26532E-01	-.30565E-01	.10891E-01
	3	-.68297E-02	.27529E-01	-.32234E-01	.11894E-01
	4	-.78380E-02	.30509E-01	-.35299E-01	.13009E-01
	5	-.63572E-02	.25088E-01	-.30149E-01	.11682E-01
	6	-.72418E-02	.27928E-01	-.32863E-01	.12512E-01
	7	-.74757E-02	.28698E-01	-.33603E-01	.12747E-01
	8	-.73504E-02	.28256E-01	-.33164E-01	.12634E-01
	9	-.73313E-02	.28168E-01	-.33058E-01	.12623E-01
	10	-.70043E-02	.26877E-01	-.31679E-01	.12259E-01
	11	-.72796E-02	.27820E-01	-.32583E-01	.12504E-01
	12	-.67988E-02	.26041E-01	-.30739E-01	.12012E-01
	13	-.69448E-02	.26658E-01	-.31451E-01	.12194E-01
	14	-.67034E-02	.25736E-01	-.30452E-01	.11914E-01
	15	-.67375E-02	.25635E-01	-.30544E-01	.11955E-01
Elliptic	1	-.21329E-01	.78859E-01	-.66642E-01	.16530E-01
	2	-.71438E-02	.28966E-01	-.32891E-01	.11535E-01
	3	-.65710E-02	.26288E-01	-.31326E-01	.11817E-01
	4	-.63688E-02	.25640E-01	-.30946E-01	.11887E-01
	5	-.68167E-02	.26712E-01	-.31889E-01	.12216E-01
	6	-.69898E-02	.27214E-01	-.32486E-01	.12478E-01
	7	-.68678E-02	.26821E-01	-.32210E-01	.12456E-01
	8	-.69186E-02	.27003E-01	-.32417E-01	.12534E-01
	9	-.69991E-02	.27277E-01	-.32714E-01	.12653E-01
	10	-.69516E-02	.27099E-01	-.32562E-01	.12656E-01
	11	-.69248E-02	.27004E-01	-.32465E-01	.12626E-01
	12	-.68942E-02	.26899E-01	-.32388E-01	.12647E-01
	13	-.71624E-02	.27818E-01	-.33257E-01	.12858E-01
	14	-.71117E-02	.27636E-01	-.33084E-01	.12830E-01
	15	-.71945E-02	.27913E-01	-.33351E-01	.12921E-01

filters and in Table 3.2 for highpass filters for different values of N . Note that in nonzero-phase filters N is the number of pseudo-rotated lowpass filters recursing in the $(+,+)$ direction whereas for zero-phase filters N is the number of pseudo-rotated lowpass filters recursing in the $(+,+)$ and the $(-,-)$ directions. In the case of highpass filters, N is the number of filters recursing on the $(+,+)$ direction since only zero-phase filters were considered.

Some care is needed when estimating σ^2 for $x < 0.5$ in lowpass filters and for $x < 1.0$ in highpass filters since no designs were carried out for these values of x . In order to obtain the minimum number of pseudo-rotated filters necessary to achieve a given degree of circularity, we increase the value of N from 1 until, the desired value of the variance is obtained. It is worthwhile to point out here that in the design of lowpass and highpass 2-D filters with passband edges greater than about 60 % of the Nyquist frequency, it is not possible to decrease the variance by increasing the value of N above unity and in actual fact the circularity starts to deteriorate when more than one pseudo-rotated filter is used in the $(+,+)$ direction. Thus, a rotation with an angle of 45° is good enough for these filters.

Tables 3.3 and 3.4 give the number of pseudo-rotated filters N for specific values of x for which the variance of the passband radii σ^2 is minimum in the case of lowpass and

Table 3.2 Coefficients of the Variance (Highpass Filters)

Filter Type	N	A_N	B_N	C_N	D_N
Butterworth	1	-.13852E+00	.31320E+00	-.22245E+00	.50495E-01
	2	-.73838E-01	.17172E+00	-.12855E+00	.31287E-01
	3	-.52157E-01	.12227E+00	-.93370E-01	.23433E-01
	4	-.45852E-01	.10693E+00	-.84645E-01	.21697E-01
	5	-.49350E-01	.11499E+00	-.87592E-01	.22040E-01
Chebyshev	1	-.98694E-01	.24370E+00	-.17906E+00	.41128E-01
	2	-.77584E-01	.17953E+00	-.13411E+00	.32737E-01
	3	-.45169E-01	.10927E+00	-.86776E-01	.22917E-01
	4	-.50439E-01	.11889E+00	-.92121E-01	.23801E-01
	5	-.65623E-01	.15157E+00	-.11474E+00	.28872E-01
Elliptic	1	-.14091E+00	.31130E+00	-.21346E+00	.46692E-01
	2	-.78221E-01	.17884E+00	-.13245E+00	.32298E-01
	3	-.53695E-01	.12654E+00	-.97778E-01	.25067E-01
	4	-.52949E-01	.12422E+00	-.95581E-01	.24434E-01
	5	-.60823E-01	.14106E+00	-.10740E+00	.27244E-01

Table 3.3 Value of N for Minimum Variance in 2-D Lowpass Filters

Filter Type \ x	0.5	1.0	1.5	2.0
Butterworth	12	4	1	1
Chebyshev	8	4	2	1
elliptic	11	4	2	1

Table 3.4 Value of N for Minimum Variance in 2-D Highpass Filters.

Filter Type \ x	1.0	1.5	2.0	2.8
Butterworth	5	2	1	1
Chebyshev	5	2	1	1
elliptic	5	3	1	1

highpass Butterworth, Chebyshev and elliptic filters. The usefulness of our prediction formula will be demonstrated later by means of examples.

3.4 Prediction of 1-D lowpass digital filter specifications

The problem which we want to solve here is to deduce the specifications of the 1-D digital filter from the specifications of the 2-D digital filter. If this can be done, the procedures given in [42] can be used to obtain the specifications of the desired prototype analog filter. This can then be transformed into a 2-D pseudo-rotated digital filter satisfying prescribed specifications.

Given the 2-D digital filter specifications defined in Sec. 3.2, we want to deduce the 1-D digital filter specifications given below :

A_p^{1D} = maximum passband ripple in dB
 A_a^{1D} = minimum stopband loss in dB
 ω_p^{1D} = passband edge in rad/s
 ω_a^{1D} = stopband edge in rad/s

Initially the rotation angles need to be determined. If N different rotation angles are to be used we select the

angles

$$\alpha_i, -\alpha_i, 180^\circ - \alpha_i, 180^\circ + \alpha_i, i=1, N$$


where $0^\circ < \alpha_i < 90^\circ$. To obtain α_i , we divide the first quadrant into N equally spaced sectors such that

$$\alpha_1 = \frac{90}{N+1}, \quad \alpha_i = i \alpha_1 \quad \text{for } i=2, N \quad (3.10)$$

This procedure leads to the same variations of the 2-D amplitude response with respect to both the frequency variables w_1 and w_2 .

Extensive experimentation has shown that a filter rotated by angles in the range $(0^\circ, 90^\circ)$ has a lowpass amplitude response on line $w_1 = w_2$ and an allpass amplitude response on line $w_1 = -w_2$ of the 2-D frequency plane. Similarly, a filter rotated by angles in the range $(-90^\circ, 0^\circ)$, has a lowpass amplitude response on line $w_1 = -w_2$ and an allpass amplitude response on line $w_1 = w_2$.

3.4.1 Prediction of the minimum stopband attenuation



Extensive experimentation has shown that when a filter is rotated by angles in the range $(-90^\circ, 90^\circ)$ the following effects occur :

i) The stopband attenuation in sectors $(0^\circ, 90^\circ)$ and $(180^\circ, 270^\circ)$ is approximately dictated by the number of cascaded filters N whose rotation angles are in the range $(0^\circ, 90^\circ)$. These filters have little effect on the stopband attenuation in sectors $(90^\circ, 180^\circ)$ and $(270^\circ, 360^\circ)$.

ii) The N cascaded filters rotated by angles in the range $(-90^\circ, 0^\circ)$ dominate the stopband attenuation in sectors $(90^\circ, 180^\circ)$ and $(270^\circ, 360^\circ)$. These filters also have little effect in the stopband attenuation in sectors $(0^\circ, 90^\circ)$ and $(180^\circ, 270^\circ)$.

Based on these observations, we can derive the minimum stopband attenuation required for the 1-D digital filter which is equal to the minimum stopband attenuation of the prototype analog lowpass filter. For rotation angles in the range $(-90^\circ, 90^\circ)$, the minimum stopband attenuation in the 2-D digital filter is given by

$$A_a^{2D} \approx \sum_{i=1}^N A_{ai}^{1D} \quad (3.11)$$

where A_{ai}^{1D} is the minimum stopband attenuation in dB of the prototype analog filter that has been rotated by an angle α_i , $i=1, N$. If we assume that all pseudo-rotated filters contribute equally to the stopband attenuation, i.e., $A_{a1}^{1D} = A_{a2}^{1D} = \dots = A_a^{1D}$, then Eqn. 3.11 gives the minimum stopband

attenuation of the prototype analog filter as

$$A_a^{1D} \approx \frac{A_a^{2D}}{N} \quad (3.12)$$

If the analog filter is rotated by angles in the range $(0^\circ, 360^\circ)$ in order to obtain a zero-phase 2-D pseudo-rotated filter, we have

$$A_a^{2D} \approx \sum_{i=1}^{2N} A_{ai}^{1D} \quad (3.13)$$

since filters rotated by angles in the range $(90^\circ, 270^\circ)$ have the same stopband attenuation as filters rotated in the range $(-90^\circ, 90^\circ)$. On assuming equal contributions, we get the minimum stopband attenuation of the prototype analog filter as

$$A_a^{1D} \approx \frac{A_a^{2D}}{2N} \quad (3.14)$$

3.4.2 Prediction of the maximum passband ripple

As in the previous section, we have here two basic contributions, namely, contributions by filters rotated by angles in the range $(0^\circ, 90^\circ)$ and contributions by filters rotated by angles in the range $(-90^\circ, 0^\circ)$. However, here the type of filter (e.g. Butterworth, Bessel, Chebyshev or

elliptic) should be taken into account. If the prototype analog filter is a Butterworth or Bessel filter and the rotation angles are in the range $(-90^\circ, 90^\circ)$, the following observations can be made :

- i) The N cascaded filters rotated by angles in the range $(0^\circ, 90^\circ)$ dominate the passband attenuation in the sectors $(0^\circ, 90^\circ)$ and $(180^\circ, 270^\circ)$
- ii) The N cascaded filters rotated by angles in the range $(-90^\circ, 0^\circ)$ dominate the passband attenuation in the sectors $(90^\circ, 180^\circ)$ and $(270^\circ, 360^\circ)$

As for the calculation of minimum stopband attenuation, the maximum passband attenuation is given by

$$A_p^{2D} \approx \sum_{i=1}^N A_{pi}^{1D} \quad (3.15)$$

where A_{pi}^{1D} is the contribution to the passband attenuation in dB of the prototype analog lowpass filter that has been rotated by an angle α_i , $i=1, N$. Assuming equal contributions for all pseudo-rotated filters, i.e., $A_{p1}^{1D} = A_{p2}^{1D} = \dots = A_p^{1D}$, the maximum passband ripple of the prototype analog filter, can be deduced as

$$A_p^{1D} \approx \frac{A_p^{2D}}{N} \quad (3.16)$$

If the prototype filter is to be rotated by angles in the range $(0^\circ, 360^\circ)$ as in the case of zero-phase 2-D filters, then the maximum passband ripple of 1-D analog filter is obtained as

$$A_p^{1D} \approx \frac{A_p^{2D}}{2N} \quad (3.17)$$

In the case where the prototype analog filter has an equiripple passband response, as in Chebyshev and elliptic filters, all cascaded pseudo-rotated filters contribute to the passband attenuation. Consequently, the maximum passband ripple of the 2-D filter is given by

$$A_p^{2D} \approx \sum_{i=1}^{2N} A_{pi}^{1D} \quad (3.18)$$

and since at some frequency point all the pseudo-rotated filters will contribute their maximum passband attenuation, the maximum passband ripple for the prototype analog filter is obtained as

$$A_p^{1D} \approx \frac{A_p^{2D}}{2N} \quad (3.19)$$

In the case where the filter is rotated by angles in the range $(0^\circ, 360^\circ)$, i.e., for zero-phase filters, the

maximum passband ripple of the analog prototype filter is given by

$$A_p^{1D} \approx \frac{A_p^{2D}}{4N} \quad (3.20)$$

The above formulas for the prediction of the maximum passband attenuation and minimum stopband attenuation of the filter are very general. If they are applied to any prototype analog filter, the resulting characteristics turn out to be very close to the desired values. However, experience has shown that a small shift of the stopband edge of the 1-D digital filter is necessary in order to satisfy prescribed amplitude specifications for any prototype analog filter used. Nevertheless, by making use of linear regression the formula

$$W_a^{1D} = \frac{W_a^{2D} + 0.03 \frac{W_s}{2\pi}}{1.1781} \quad (3.21)$$

was deduced which gives the necessary correction in the stopband edge. This formula was deduced by computing W_a^{1D} for many values of W_a^{2D} and for many Butterworth, Chebyshev and elliptic prototype filters.

3.5 Design of 1-D analog filter

Since the specifications of the 1-D digital filter can be deduced as shown in Sec. 3.4, the specifications of the 1-D prototype analog filter can be deduced as described in [42] by taking the warping effect into account.

3.6 Design Procedure

A 2-D circularly symmetric pseudo-rotated lowpass digital filter that meets prescribed amplitude specifications can be designed by using the following procedure :

Butterworth filters

- 1) Choose the number of rotation angles per quadrant N to achieve prescribed circularity using Eqn. 3.8.
- 2) Use Eqns. 3.12 and 3.16 to predict A_a^{1D} and A_p^{1D} , respectively, for a nonzero-phase filter or Eqns. 3.14 and 3.17, respectively, for a zero-phase filter.
- 3) Predict w_a^{1D} using Eqn. 3.21 and assume that $w_p^{1D} = w_p^{2D}$.
- 4) Design the analog lowpass filter as shown in [42].

- 5) Rotate the analog filter by the desired angles using Eqns. 2.19 - 2.21 in order to obtain the 2-D transfer function of the cascaded filters given in Eqn. 2.18.

Chebyshev or elliptic filters

- 1) Choose the number of rotation angles per quadrant N to achieve prescribed circularity using Eqn. 3.8.
- 2) Use Eqns. 3.12 and 3.19 to predict A_a^{1D} and A_p^{1D} , respectively, for a nonzero-phase filter or Eqns. 3.14 and 3.20, respectively, for a zero-phase filter.
- 3) Predict w_a^{1D} using Eqn. 3.21 and assume that $w_p^{1D} = w_p^{2D}$.
- 4) Design the analog filter as shown in [42].
- 5) Rotate the prototype filter by the desired angles in order to obtain the transfer function in Eqn. 2.18 by using the Eqns. 2.19 - 2.21.

The effectiveness of the above design procedures is illustrated by the following example.

Example 3.1 (A1 to A5)

Several 2-D digital lowpass filters were designed having circular symmetry and zero-phase. The desired 2-D specifications are given in Table 3.5. For each

Table 3.5 2-D Lowpass-Filter Specifications

Example	A_p^{2D} (dB)	A_a^{2D} (dB)	W_p^{2D} (rad/s)	W_a^{2D} (rad/s)	σ^2 (rad/s) ²
A1	0.4	40.0	0.5	1.0	10^{-4}
A2	0.4	40.0	1.0	1.5	10^{-3}
A3	0.4	40.0	1.5	2.0	5×10^{-3}
A4	0.5	45.0	1.0	1.6	5×10^{-3}
A5	0.6	50.0	1.0	1.7	10^{-3}

specification Butterworth, Chebyshev and elliptic designs were obtained. Using the prediction formulas, the 1-D digital-filter specifications were obtained as shown in Tables 3.6 to 3.8. Making use of these specifications, the 1-D analog filters were designed using the method in [42]. Subsequently, on using the proposed design procedure the results shown in Tables 3.9 to 3.11 were obtained for Butterworth, Chebyshev and elliptic filters, respectively. As can be seen, the desired specifications have been met in all examples. In addition, the actual circularity measure of each designed filter is very close to the specified value.

3.7 Design of highpass filters

The design of pseudo-rotated highpass filters is accomplished by finding a prototype analog highpass filter which after transformation gives rise to a 2-D digital filter that meets desired specifications. As in the case of lowpass filters, we are interested in deriving expressions for the prediction of the 1-D highpass digital-filter specifications.

First, we divide the first quadrant into N equally-spaced sectors as before in which case the rotation angles

Table 3.6 1-D Digital-Filter Specifications (Butterworth Filters)

Example	A_p^{1D} (dB)	A_a^{1D} (dB)	W_p^{1D} (rad/s)	W_a^{1D} (rad/s)	Rotation Angles
A1	0.04	4.0	0.5	0.874	$15^\circ, 30^\circ$ $45^\circ, 60^\circ, 75^\circ$
A2	0.1	10.0	1.0	1.298	$30^\circ, 60^\circ$
A3	0.2	20.0	1.5	1.723	45°
A4	0.125	11.25	1.0	1.383	$30^\circ, 60^\circ$
A5	0.15	12.5	1.0	1.468	$30^\circ, 60^\circ$

Table 3.7 1-D Digital-Filter Specifications (Chebyshev Filters)

Example	A_p^{1D} (dB)	A_a^{1D} (dB)	W_p^{1D} (rad/s)	W_a^{1D} (rad/s)	Rotation Angles
A1	0.0167	3.33	0.5	0.874	$12^\circ, 26^\circ, 38^\circ$ $52^\circ, 64^\circ, 78^\circ$
A2	0.05	10.0	1.0	1.298	$30^\circ, 60^\circ$
A3	0.1	20.0	1.5	1.723	45°
A4	0.0625	11.25	1.0	1.383	$30^\circ, 60^\circ$
A5	0.075	12.5	1.0	1.468	$30^\circ, 60^\circ$

Table 3.8 1-D Digital-Filter Specifications (Elliptic Filters)

Example	A_p^{1D} (dB)	A_g^{1D} (dB)	W_p^{1D} (rad/s)	W_g^{1D} (rad/s)	Rotation Angles
A1	0.02	4.0	0.5	0.874	15°, 30° 45°, 60°, 75°
A2	0.05	10.0	1.0	1.298	30°, 60°
A3	0.1	20.0	1.5	1.723	45°
A4	0.0625	11.25	1.0	1.383	30°, 60°
A5	0.075	12.5	1.0	1.468	30°, 60°

Table 3.9 Results Obtained for Butterworth Filters

Example	A_p^{2D} (dB)	A_g^{2D} (dB)	σ^2 (rad/s) ²
A1	0.385	81.56	6.789×10^{-5}
A2	0.267	55.23	2.716×10^{-4}
A3	0.187	50.56	2.487×10^{-3}
A4	0.288	60.75	2.349×10^{-4}
A5	0.330	70.57	2.198×10^{-4}

Table 3.10 Results Obtained for Chebyshev Filters

Example	$A_p^{2D} \text{ (dB)}$	$A_a^{2D} \text{ (dB)}$	$\sigma^2 \text{ (rad/s)}^2$
A1	0.379	54.04	9.882×10^{-5}
A2	0.393	50.44	4.362×10^{-4}
A3	0.321	58.68	2.569×10^{-3}
A4	0.486	76.59	4.365×10^{-4}
A5	0.417	61.56	4.821×10^{-4}

Table 3.11 Results Obtained for Elliptic Filters

Example	A_p^{2D} (dB)	A_s^{2D} (dB)	σ^2 (rad/s) ²
A1	0.374	92.43	9.728×10^{-5}
A2	0.359	64.00	4.653×10^{-4}
A3	0.390	56.54	2.416×10^{-3}
A4	0.315	55.60	1.350×10^{-4}
A5	0.372	75.03	1.092×10^{-4}

are given by Eqn. 3.10. After obtaining the specifications A_p^{1D} , A_a^{1D} , W_p^{1D} and W_a^{1D} we design the analog prototype filter as proposed in [42]. The 2-D digital filter is then designed following the procedures in the previous chapter.

Extensive experimental results have shown that a filter rotated by angles in the range $(0^\circ, 90^\circ)$ or $(180^\circ, 270^\circ)$ has a highpass amplitude response on line $w_1 = w_2$ and an allstop amplitude response on line $w_1 = -w_2$ of the 2-D frequency plane. For filters whose rotation angles are in the interval $(90^\circ, 180^\circ)$ or $(270^\circ, 360^\circ)$, a highpass amplitude response is obtained on line $w_1 = -w_2$ and an allstop amplitude response is obtained on line $w_1 = w_2$.

In the interconnection of pseudo-rotated highpass filters given in Fig. 2.7, there are combinations of filters in cascade and parallel. This unique way of combining pseudo-rotated filters makes the stopband and passband attenuations independent of the number of rotations. Actually, the attenuation of the overall filter is mostly dictated by the cascaded filters represented by H^{++} and H^{--} (or H^{+-} and H^{-+}) in Fig. 2.7. Therefore, for any type of filter

$$A_p^{2D} = \sum_{i=1}^2 A_{pi}^{1D} \quad (3.22)$$

$$A_a^{2D} = \sum_{i=1}^2 A_{ai}^{1D} \quad (3.23)$$

where A_{p1}^{1D} and A_{a1}^{1D} are specifications of H^{++} (or H^{+-}), A_{p2}^{1D} and A_{a2}^{1D} are specifications of H^{--} (or H^{-+}), and A_p^{2D} and A_a^{2D} are specifications of the resulting 2-D highpass digital filter.

Now if the contributions of H^{++} and H^{--} (or H^{+-} and H^{-+}) are equal, i.e., $A_{p1}^{1D} = A_{p2}^{1D}$ and $A_{a1}^{1D} = A_{a2}^{1D}$ we can write

$$A_p^{1D} \approx \frac{A_p^{2D}}{2} \quad (3.24)$$

$$A_a^{1D} \approx \frac{A_a^{2D}}{2} \quad (3.25)$$

These formulas give good predictions for the maximum passband ripple and the minimum stopband attenuation of the 1-D digital filter in the case of Butterworth filters. In Chebyshev and elliptic filters, however, these formulas do not give accurate predictions. Extensive experimental results have shown that, in the case of Chebyshev improved results can be obtained by using the formulas

$$A_p^{1D} \approx \frac{A_p^{2D}}{3} \quad (3.26)$$

$$A_a^{1D} \approx \frac{A_a^{2D}}{2} \quad (3.27)$$

On the other, in the case of elliptic filters improved results can be obtained by using the formulas

$$A_p^{1D} \approx \frac{A_p^{2D}}{3} \quad (3.28)$$

$$A_a^{1D} \approx \frac{2 A_a^{2D}}{3} \quad (3.29)$$

These formulas give reasonable predictions for the maximum passband ripple and the minimum stopband attenuation of the 1-D digital filter. Since these formulas are based on approximations, the 2-D digital filters obtained may violate the desired specifications. In the case of lowpass filters, it is possible to adjust the stopband edge of the 1-D digital filter w_a^{1D} through the use of an empirical formula so as to ensure a better coincidence

between the desired 2-D specifications and the actual specifications achieved (see Sec. 3.4). Similarly, in the case of highpass filters, the passband edge of the 1-D digital filter w_p^{1D} can be adjusted through the use of the following empirical formulas :

i) Butterworth filters :

$$w_p^{1D} = \frac{w_p^{2D} - \frac{0.09 - 0.175N + 0.02N^2}{2\pi} w_s}{1.167 + 0.09N} \quad (3.30)$$

where N is the number of rotation angles in the first quadrant

ii) Chebyshev filters :

$$w_p^{1D} = \frac{w_p^{2D} - \frac{0.083 - 0.16N + 0.02N^2}{2\pi} w_s}{1.26 + 0.0313N + 0.005N^2} \quad (3.31)$$

iii) Elliptic filters :

$$w_p^{1D} = \frac{w_p^{2D} - \frac{0.08 - 0.18N + 0.022N^2}{2\pi} w_s}{1.26 + 0.04N - 0.06N^2} \quad (3.32)$$

These formulas were deduced by first using linear regression between w_p^{2D} and w_p^{1D} for individual values of N . Then the coefficients of the linear model obtained were interpolated by using multiple regression on the number of pseudo-rotated filters employed.

At this point all the parameters of the 1-D digital filter are known and hence the 1-D analog filter can be designed using the method in [42].

A 2-D circularly symmetric /pseudo-rotated highpass digital filter that meets prescribed amplitude specifications can be designed by using the following procedure :

- 1) Determine the number of rotations per quadrant N to achieve prescribed circularity using Eqn. 3.8.
- 2) Predict specifications A_p^{1D} , A_a^{1D} and w_p^{1D} by using Eqns. 3.24, 3.25 and 3.30 for Butterworth filters, Eqns 3.26, 3.27 and 3.31 for Chebyshev filters, and Eqns. 3.28, 3.29 and 3.32 for elliptic filters. In addition, assume that $w_a^{1D} = w_a^{2D}$.
- 3) Design the 1-D analog highpass filter by the method in [42] using A_p^{1D} , A_a^{1D} , w_p^{1D} , w_a^{1D} and w_s .
- 4) Use Eqns. 2.19 - 2.21 to deduce the 2-D transfer function in Eqn. 2.18.
- 5) Interconnect the cascaded filters as it is shown in Fig. 2.7.

Example 3.2 (B1 to B5)

The above procedure was used to design several 2-D circularly symmetric zero-phase pseudo-rotated highpass digital filters. Table 3.12 gives the desired set of specifications. Butterworth, Chebyshev and elliptic designs were obtained for each set of specifications. The 1-D digital specifications for the various types of filters are given in Tables 3.13 to 3.15. Tables 3.16 to 3.18 show the results obtained for Butterworth, Chebyshev and elliptic filters, respectively and, as can be seen, the desired specifications are met in all examples. In addition, the circularity measures are close to the specified values.

3.8 Design of bandpass and bandstop filters

The design of bandpass and bandstop filters, can be accomplished by using a combination of lowpass and highpass filters which are designed to satisfy appropriate specifications.

The design of a bandpass filter satisfying the specifications of Sec. 3.2 (see Fig. 3.3) can be accomplished by using the following procedure :

Table 3.12 2-D Highpass-Filter Specifications

Example	A_p^{2D} (dB)	A_a^{2D} (dB)	W_p^{2D} (rad/s)	W_a^{2D} (rad/s)	σ^2 (rad/s) ²
B1	0.4	45.0	1.0	0.5	5×10^{-4}
B2	0.4	50.0	1.5	1.0	5×10^{-3}
B3	0.5	40.0	2.0	1.5	5×10^{-3}
B4	0.6	45.0	2.0	1.2	5×10^{-3}
B5	0.8	40.0	1.5	0.8	10^{-3}

Table 3.13 1-D Digital-Filter Specifications (Butterworth Filters)

Example	A_p^{1D} (dB)	A_a^{1D} (dB)	W_p^{1D} (rad/s)	W_a^{1D} (rad/s)	Rotation Angles
B1	0.2	22.5	1.06	0.55	15°, 30° 45°, 60°, 75°
B2	0.2	25.0	1.42	1.05	30°, 60°
B3	0.25	20.0	1.76	1.55	45°
B4	0.3	22.5	1.76	1.25	45°
B5	0.4	20.0	1.42	0.85	30°, 60°

Table 3.14 1-D Digital-Filter Specifications (Chebyshev Filters)

Example	A_p^{LD} (dB)	A_a^{LD} (dB)	W_p^{LD} (rad/s)	W_a^{LD} (rad/s)	Rotation Angles
B1	0.133	22.5	0.94	0.55	15°, 30° 45°, 60°, 75°
B2	0.133	25.0	1.272	1.05	30°, 60°
B3	0.167	20.0	1.6	1.55	45°
B4	0.2	22.5	1.6	1.25	45°
B5	0.267	20.0	1.272	0.85	30°, 60°

Table 3.15 1-D Digital-Filter Specifications (Elliptic Filters)

Example	A_p^{1D} (dB)	A_a^{1D} (dB)	W_p^{1D} (rad/s)	W_a^{1D} (rad/s)	Rotation Angles
B1	0.133	30.0	1.045	0.55	15°, 30° 45°, 60°, 75°
B2	0.133	33.34	1.43	1.05	22.5° 45°, 67.5°
B3	0.167	26.67	1.733	1.55	45°
B4	0.2	30.0	1.733	1.25	45°
B5	0.267	26.67	1.43	0.85	22.5° 45°, 67.5°

Table 3.16 Results Obtained for Butterworth Filters

Example	A_p^{2D} (dB)	A_a^{2D} (dB)	σ^2 (rad/s) ²
B1	0.1739	55.65	1.095×10^{-4}
B2	0.3867	57.96	1.222×10^{-4}
B3	0.2700	81.13	3.458×10^{-4}
B4	0.4624	64.57	8.873×10^{-5}
B5	0.6252	54.38	7.474×10^{-5}

Table 3.17 Results Obtained for Chebyshev Filters

Example	A_p^{2D} (dB)	A_a^{2D} (dB)	σ^2 (rad/s) ²
B1	0.1416	42.07	1.900×10^{-4}
B2	0.2679	77.44	1.223×10^{-3}
B3	0.3305	97.02	2.550×10^{-3}
B4	0.3976	71.53	2.346×10^{-3}
B5	0.2483	65.08	3.058×10^{-4}

Table 3.18 Results Obtained for Elliptic Filters

Example	A_p^{2D} (dB)	A_a^{2D} (dB)	σ^2 (rad/s) ²
B1	0.3826	73.18	1.575×10^{-4}
B2	0.3988	75.90	6.712×10^{-4}
B3	0.3129	57.28	8.833×10^{-4}
B4	0.4088	67.99	8.296×10^{-4}
B5	0.1000	43.57	7.903×10^{-5}

- 1) Design a 2-D circularly symmetric zero-phase lowpass filter with specifications given by

$$\begin{aligned}\tilde{A}_p^{2D} &= \frac{A_p^{2D}}{2} \\ \tilde{A}_a^{2D} &= A_a^{2D}\end{aligned}\quad (3.33)$$

$$W_p^{2D} = W_{p2}^{2D}$$

$$W_a^{2D} = W_{a2}^{2D}$$

- 2) Design a 2-D circularly symmetric highpass filter with specifications given by

$$\begin{aligned}\tilde{A}_p^{2D} &= \frac{A_p^{2D}}{2} \\ \tilde{A}_a^{2D} &= A_a^{2D}\end{aligned}\quad (3.34)$$

$$W_p^{2D} = W_{p1}^{2D}$$

$$W_a^{2D} = W_{a1}^{2D}$$

- 3) Cascade the lowpass and highpass filters to obtain the desired 2-D circularly symmetric bandpass filter.

The design of a 2-D bandstop filter satisfying the specifications of Sec. 3.2 (Fig. 3.4) can be

accomplished by using the following procedure :

- 1) Design a 2-D circularly symmetric lowpass filter with specifications given by

$$\tilde{A}_p^{2D} = A_p^{2D}$$

$$\tilde{A}_a^{2D} = A_a^{2D}$$

(3.35)

$$W_p^{2D} = W_{p1}^{2D}$$

$$W_a^{2D} = W_{a1}^{2D}$$

- 2) Design a circularly symmetric highpass 2-D filter with specifications given by

$$\tilde{A}_p^{2D} = A_p^{2D}$$

$$\tilde{A}_a^{2D} = A_a^{2D}$$

(3.36)

$$W_p^{2D} = W_{p2}^{2D}$$

$$W_a^{2D} = W_{a2}^{2D}$$

- 3) Connect the lowpass and highpass filters in parallel to obtain the desired circularly symmetric bandstop 2-D filter.

Example 3.3 (C1 to C2)

The above procedure was used to design a bandpass and a bandstop filter. The design specifications are given in Table 3.19. Assuming elliptic designs, the specifications of the 1-D digital filters are obtained as shown in Table 3.20.

Table 3.21 shows the results obtained. As can be seen, the designs obtained meet the desired specifications.

3.9 Conclusions

In this chapter, the design of 2-D pseudo-rotated digital filters satisfying prescribed amplitude specifications was investigated. First, the characteristics of 2-D digital filters were defined. Then a circularity measure was defined and used for the prediction of the minimum number of pseudo-rotated filters to achieve filters with prescribed degree of circularity. Subsequently, prediction formulas were deduced which give the specifications of the 1-D digital filter, if prescribed

Table 3.19 2-D Bandpass- and Bandstop-Filter Specifications

Example	Filter Type	A_p^{2D} (dB)	A_a^{2D} (dB)	W_{p1}^{2D} (rad/s)	W_{p2}^{2D} (rad/s)	W_{a1}^{2D} (rad/s)	W_{a2}^{2D} (rad/s)	σ^2 (rad/s) ²
C1	Bandpass	0.4	40.0	1.0	1.5	0.5	2.0	5×10^{-3}
C2	Bandstop	0.4	40.0	0.5	2.0	1.0	1.5	5×10^{-3}

Table 3.20 1-D Digital-Filter Specifications (Bandpass and Bandstop Filters)

Example	Filter Type	A_p^{ID} (dB)	A_a^{ID} (dB)	W_p^{ID} (rad/s)	W_a^{ID} (rad/s)	N	Rotation Angles
C1	Lowpass	0.05	10.0	1.5	1.723	2	30°, 60°
	Highpass	0.133	26.67	0.905	0.55	2	30°, 60°
C2	Lowpass	0.05	10.0	0.5	0.874	2	30°, 60°
	Highpass	0.133	26.67	1.605	1.55	1	45°

Table 3.21 Results Obtained for Bandpass and Bandstop Filters

Example	A_p^{2D} (dB)	A_a^{2D} (dB)	σ^2 (rad/s) ²
C1	0.3549	41.02	1.719×10^{-3}
C2	0.4065	57.03	2.184×10^{-3}

amplitude specifications are to be achieved in the 2-D digital filter. Once the specifications of the 1-D digital filter are known, those of the 1-D analog prototype filter can readily be deduced as in [42] and, consequently, the design of the 2-D filter can be carried out.

This chapter dealt with step-by-step design procedures which can be used to design lowpass, highpass, bandpass, and bandstop filters. These procedures have been used to design many filters of different types. The results obtained show that prescribed amplitude specifications can easily be achieved in Butterworth, Chebyshev, and elliptic filters. These procedures can readily be used to construct a computer-aided filter-design package which can be used for the design of 2-D circularly symmetric pseudo-rotated filters.

CHAPTER 4OPTIMIZATION OF PSEUDO-ROTATED FILTERS4.1 Introduction

An alternative approach for the design of circularly symmetric 2-D digital filters is through the use of optimization techniques [25], [27] - [29], [31], [33]. This approach is effective if the band edges are fixed and the passband loss is to be minimized and/or the stopband loss is to be maximized. The main disadvantage of the approach is that the filter order needed to satisfy prescribed amplitude specifications is not known a priori and, therefore, extensive trial and error is necessary before satisfactory performance can be achieved. By contrast, the method of pseudo-rotated filters described in Chapter 3 leads readily to filters satisfying prescribed amplitude specifications.

In this chapter, a standard optimization method is applied in conjunction with the method of pseudo-rotated filters for the design of 2-D circularly symmetric filters. Our purpose is to investigate to what extent improvements can be brought about in pseudo-rotated filters through the use of optimization techniques. Desirable improvements are a reduction in the number of cascaded sections, a reduction

in the maximum passband ripple, an increase in the minimum stopband loss, and an increase in the degree of circularity.

The procedure followed consists of two steps. First, a pseudo-rotated filter satisfying prescribed amplitude specifications is designed. Then by using the transfer function coefficients obtained as initial values in an optimization procedure, an alternative design is obtained. The optimization is carried out by using the sequential unconstrained minimization technique (SUMT) due to Fiacco and McCormick [43] - [44]. Stability of the filter is maintained by using constraints.

In the optimization procedure the phase is not considered. Nevertheless, zero-phase filters can easily be obtained by cascading the optimized 2-D filter which recurses in the $(+,+)$ and $(+,-)$ directions with a filter that recurses in the $(-,-)$ and $(-,+)$ directions. The transfer function coefficients of the latter filter can be deduced from the coefficients of the transfer function of the optimized filter.

4.2 The design problem

A 2-D transfer function obtained by the rotation method of Chapter 3 can be written as

$$H(z_1, z_2) = H_0 \prod_{n=1}^N H_n(z_1, z_2) \quad (4.1)$$

where

$$H_n(z_1, z_2) = \frac{a_{11n} + a_{21n}z_1 + a_{12n}z_2 + a_{22n}z_1z_2}{b_{11n} + b_{21n}z_1 + b_{12n}z_2 + b_{22n}z_1z_2} \quad (4.2)$$

Coefficients $a_{11n}, \dots, b_{22n}, n=1, N$ are calculated by using Eqn. 2.21. Such a transfer function represents a stable filter if [18]

$$\begin{aligned} C_{1n} &= |b_{11n}| - |b_{12n}| > 0 \\ C_{2n} &= |b_{12n} + b_{11n}| - |b_{21n} + b_{22n}| > 0 \\ C_{3n} &= |b_{12n} + b_{11n}| - |b_{21n} - b_{22n}| > 0 \end{aligned} \quad (4.3)$$

These constraints ensure that the filter is stable if recursion is carried out in the $(+, +)$ direction. Since circular symmetry is of interest, the analog filter has to be rotated in the $(+, +)$ and $(+, -)$ directions. The constraints imposed on the coefficients of the transfer function for a filter that recurses in the $(+, -)$ direction can be derived from Eqn. 4.3 by interchanging b_{11n} and b_{12n} . The constraints in Eqn. 4.3 do not exclude

singularities of the second kind. Nevertheless, the existence of such singularities can be detected by checking the transfer function at points $(+1,+1)$, $(+1,-1)$, $(-1,+1)$ and $(-1,-1)$ of the (z_1, z_2) plane.

4.2.1 The objective function

If D is the desired amplitude response and $H_0 > 0$ then the error in the amplitude response at point (w_1, w_2) is given by

$$f_k = H_0 \sum_{n=1}^N (G_n - D) \quad (4.4)$$

where $k = \{ (i, j) , i=1, I , j=1, J \}$ is the index assigned to the grid point (w_1, w_2) of the frequency plane and

$$G_n = |H_n(e^{jw_1}, e^{jw_2})| \quad (4.5)$$

Function f_k is dependent on the parameters $\{ a_{11n}, a_{21n}, \dots, b_{11n}, \dots, b_{22n} \}$. These parameters can be represented by the vector

$$\begin{aligned} \underline{x} &= [x_1 \ x_2 \ \dots \ x_M]^T \\ &= [a_{111}^R \ a_{111}^I \ a_{211}^R \ a_{211}^I \ \dots \ b_{111}^R \ b_{111}^I \ \dots]^T \end{aligned}$$

where superscripts R and I denote the real and imaginary parts, respectively, of the coefficients. M is the number of optimization variables in the transfer function of Eqn.

4.1.

An objective function can be defined as the sum of the squares of the errors and is given by

$$f(\underline{x}) = \sum_{k=1}^K w_k^2 f_k^2 = \sum_{k=1}^K w_k^2 \left[\left| H_{0k} - \prod_{n=1}^M H_n \right| - D \right]^2 \quad (4.6)$$

where w_k is a weighting function for emphasizing errors of importance in the formulation of the problem.

The optimization problem of interest is to obtain the vector \underline{x} which minimizes $f(\underline{x})$ subject to the constraints in Eqn. 4.3.

4.2.2 The optimization method

The method used here for the minimization of $f(\underline{x})$ is the sequential unconstrained minimization technique (SUMT) due to Fiacco and McCormick [43] - [44]. SUMT is based on a variable metric method which is a modification of the Fletcher-Powell optimization method [44]. At each iteration of the minimization, the vector \underline{x} is updated by using the

gradient and an estimation of the Hessian matrix of the objective function is deduced. A Fortran program based on this method is given in [45]. The original method uses the golden-section line search but in order to speed up the optimization process, the inexact line search due to Fletcher [46] has been incorporated in the program. Constraints can be incorporated in the SUMT method by adding to the objective function $f(\underline{x})$, a function of the constraints that acts as a penalty function. The penalty function becomes very high if \underline{x} is close to the nonfeasible region and negligible if \underline{x} is far from this region. The modified objective function is

$$\tilde{f}(\underline{x}_k) = f(\underline{x}_k) - r^k \sum_{p=1}^P \ln(C_p(\underline{x}_k)) \quad (4.7)$$

where $C_p(\underline{x})$ is a constraint (C_{1n} , C_{2n} and C_{3n}); P is the number of constraints and r^k is a positive constant such that at each iteration k of the minimization procedure, $r^1 < r^2 < \dots$

4.2.3 Derivatives of the objective function

As was stated earlier, SUMT uses the gradient of the objective function for the estimation of the Hessian matrix and in the minimization process itself. The gradient of the objective function can be deduced from the first derivatives

of the unconstrained objective function and the first derivatives of the constraints. If x_n belongs to the first-order section n then from Eqn. 4.5

$$\frac{\partial f(\underline{x})}{\partial x_n} = \sum_{k=1}^K w_k^2 \left(H_0 \left| \prod_{n=1}^N H_n \right|^{-D} \right) H_0 \left| \prod_{n=1}^N H_n \right| F_n \quad (4.8)$$

where

$$H_n = \frac{N_n}{D_n} \quad (4.9)$$

and F_n is a real number which can be obtained as follows :

i) If x_n is a coefficient in the numerator polynomial N_n

$$F_n = \text{Re} \left[\frac{1}{N_n} \frac{\partial N_n}{\partial x_n} \right] \quad (4.10)$$

ii) If x_n is a coefficient in the denominator polynomial D_n

$$F_n = \text{Re} \left[-\frac{1}{D_n} \frac{\partial D_n}{\partial x_n} \right] \quad (4.11)$$

Multiplier constant H_0 can be made an element of the vector \underline{x} . However, this tends to slow the optimization process. Alternatively, H_0 can be fixed for each change of \underline{x} . In this case, H_0 can be calculated such that

$$\frac{\partial f(\underline{x})}{\partial H_0} = 0$$

or

$$H_0 = \frac{\sum_{k=1}^K w_k^2 D \left| \prod_{n=1}^N H_n \right|}{\sum_{k=1}^K w_k^2 \left| \prod_{n=1}^N H_n \right|} \quad (4.12)$$

The derivatives of the constraints of Eqn. 4.3 which are necessary for the SUMT algorithm can be deduced as follows :

$$\begin{aligned} \frac{\partial C_{1n}}{\partial \text{Re}(b_{11})} &= \frac{\text{Re}(b_{11})}{|b_{11}|} & \frac{\partial C_{2n}}{\partial \text{Im}(b_{11})} &= y_1 \frac{\text{Im}(b_{11})}{|b_{11}+b_{12}|} \\ \frac{\partial C_{1n}}{\partial \text{Im}(b_{11})} &= \frac{\text{Im}(b_{11})}{|b_{11}|} & \frac{\partial C_{2n}}{\partial \text{Re}(b_{12})} &= x_1 \frac{\text{Re}(b_{12})}{|b_{11}+b_{12}|} \\ \frac{\partial C_{1n}}{\partial \text{Re}(b_{12})} &= -\frac{\text{Re}(b_{12})}{|b_{12}|} & \frac{\partial C_{2n}}{\partial \text{Im}(b_{12})} &= y_1 \frac{\text{Im}(b_{12})}{|b_{11}+b_{12}|} \\ \frac{\partial C_{1n}}{\partial \text{Im}(b_{12})} &= -\frac{\text{Im}(b_{12})}{|b_{12}|} & \frac{\partial C_{2n}}{\partial \text{Re}(b_{21})} &= -x_2 \frac{\text{Re}(b_{21})}{|b_{21}+b_{22}|} \\ \frac{\partial C_{2n}}{\partial \text{Re}(b_{11})} &= x_1 \frac{\text{Re}(b_{11})}{|b_{11}+b_{12}|} & \frac{\partial C_{2n}}{\partial \text{Im}(b_{21})} &= -y_2 \frac{\text{Im}(b_{21})}{|b_{21}+b_{22}|} \end{aligned} \quad (4.13)$$

$$\frac{\partial C_{2n}}{\partial \operatorname{Re}(b_{22})} = -x_2 \frac{\operatorname{Re}(b_{22})}{|b_{21}+b_{22}|}$$

$$\frac{\partial C_{2n}}{\partial \operatorname{Im}(b_{22})} = -y_2 \frac{\operatorname{Im}(b_{22})}{|b_{21}+b_{22}|}$$

$$\frac{\partial C_{3n}}{\partial \operatorname{Re}(b_{11})} = x_1 \frac{\operatorname{Re}(b_{11})}{|b_{11}+b_{12}|}$$

$$\frac{\partial C_{3n}}{\partial \operatorname{Im}(b_{11})} = y_1 \frac{\operatorname{Im}(b_{11})}{|b_{11}+b_{12}|}$$

$$\frac{\partial C_{3n}}{\partial \operatorname{Re}(b_{12})} = x_1 \frac{\operatorname{Re}(b_{12})}{|b_{11}+b_{12}|}$$

$$\frac{\partial C_{3n}}{\partial \operatorname{Im}(b_{12})} = y_1 \frac{\operatorname{Im}(b_{12})}{|b_{11}+b_{12}|}$$

$$\frac{\partial C_{3n}}{\partial \operatorname{Re}(b_{21})} = -x_3 \frac{\operatorname{Re}(b_{21})}{|b_{21}-b_{22}|}$$

$$\frac{\partial C_{3n}}{\partial \operatorname{Im}(b_{21})} = -y_3 \frac{\operatorname{Im}(b_{21})}{|b_{21}-b_{22}|}$$

$$\frac{\partial C_{3n}}{\partial \operatorname{Re}(b_{22})} = x_3 \frac{\operatorname{Re}(b_{22})}{|b_{21}-b_{22}|}$$

$$\frac{\partial C_{3n}}{\partial \operatorname{Im}(b_{22})} = y_3 \frac{\operatorname{Im}(b_{22})}{|b_{21}-b_{22}|}$$

where

$$x_1 = 2(\operatorname{Re}(b_{11})+\operatorname{Re}(b_{12})) \quad , \quad y_1 = 2(\operatorname{Im}(b_{11}+b_{12}))$$

$$x_2 = 2(\operatorname{Re}(b_{21})+\operatorname{Re}(b_{22})) \quad , \quad y_2 = 2(\operatorname{Im}(b_{21}+b_{22}))$$

$$x_3 = 2(\operatorname{Re}(b_{21})-\operatorname{Re}(b_{22})) \quad , \quad y_3 = 2(\operatorname{Im}(b_{21}-b_{22}))$$

4.3 Design of lowpass filters

In this section the method of Sec. 4.2 is applied to the design of circularly symmetric lowpass filters. Let W_p and W_a be the passband edge and stopband edge of the filter, respectively, and let the required rotation angles be equally spaced in the sector $(-90^\circ, 90^\circ)$ such that

$$\alpha_1 = \frac{90}{N+1}, \quad \alpha_n = n \alpha_1, \quad n=2, N$$

where N is the number of pseudo-rotated filters recursing in the $(+,+)$ direction

The error function must be evaluated over a relatively dense grid of the frequency plane, and since a circularly symmetric amplitude response is required, the grid points can be chosen on circles centred at the origin. No particular symmetry in the coefficients is assumed and hence the grid points can be distributed over the region $0 < w_1 < W_s/2$ and $-W_s/2 < w_2 < W_s/2$ where W_s is the sampling frequency. The grid points can be chosen as

$$w_1 = R_k \cos(\theta_k) \quad (4.14)$$

$$w_2 = R_k \sin(\theta_k)$$

where θ_k is taken over ten equally spaced sectors in the range $(-90^\circ, 90^\circ)$ such that

$$\theta_k = \frac{\pi}{2} + (k-1) \frac{\pi}{10}, \quad k=1, 11 \quad (4.15)$$

and

$$R = \begin{cases} W_p Y_{1k} & \text{for } R \leq W_p \\ W_p + (W_a - W_p) Y_{2k} & \text{for } W_p < R < W_a \\ W_a + (\pi - W_a) Y_{3k} & \text{for } R \geq W_a \end{cases} \quad (4.16)$$

where Y_{1k} , Y_{2k} and Y_{3k} assume the values 0.05, 0.1, 0.2, 0.4, 0.6, 0.8, 0.9 and 1.0

The desired amplitude response is assumed to be

$$D = \begin{cases} 1 & \text{for } R \leq W_p \\ e^{-11.5u} & \text{for } W_p < R < W_a \\ 0 & \text{for } R \geq W_a \end{cases} \quad (4.17)$$

where u can assume values between 0 and 1.

4.3.1 Design examples and results

The above approach was used to design six fourth-order elliptic lowpass filters. The rotation angles were 30° , 60° , -30° and -60° , that is, only recursion directions $(+,+)$ and $(+,-)$ were used. In each case, the 2-D filter comprised

16 first-order sections with complex coefficients. These sections were grouped into 8 second-order filter sections having real coefficients (see Chapter 5). Four of these filters recurse in the (+,+) direction and the remaining four recurse in the (+,-) direction.

Several optimized designs were obtained for each pseudo-rotated elliptic filter in order to determine whether improved designs can be obtained with reduced number of cascaded sections. The various possibilities considered are as follows :

- I) 8 sections with $R_1 = 4$ and $R_2 = 4$
- II) 7 sections with $R_1 = 4$ and $R_2 = 3$
- III) 6 sections with $R_1 = 3$ and $R_2 = 3$
- IV) 5 sections with $R_1 = 3$ and $R_2 = 2$
- V) 4 sections with $R_1 = 2$ and $R_2 = 2$

Parameters R_1 and R_2 are the numbers of sections recursing in the (+,+) and (+,-) directions, respectively.

Table 4.1 shows the specifications assumed for the design of the 2-D pseudo-rotated filters (Examples 1 to 6). By using the transfer function coefficients of the pseudo-rotated designs as the initial values of x , optimized designs were obtained for the five filter configurations

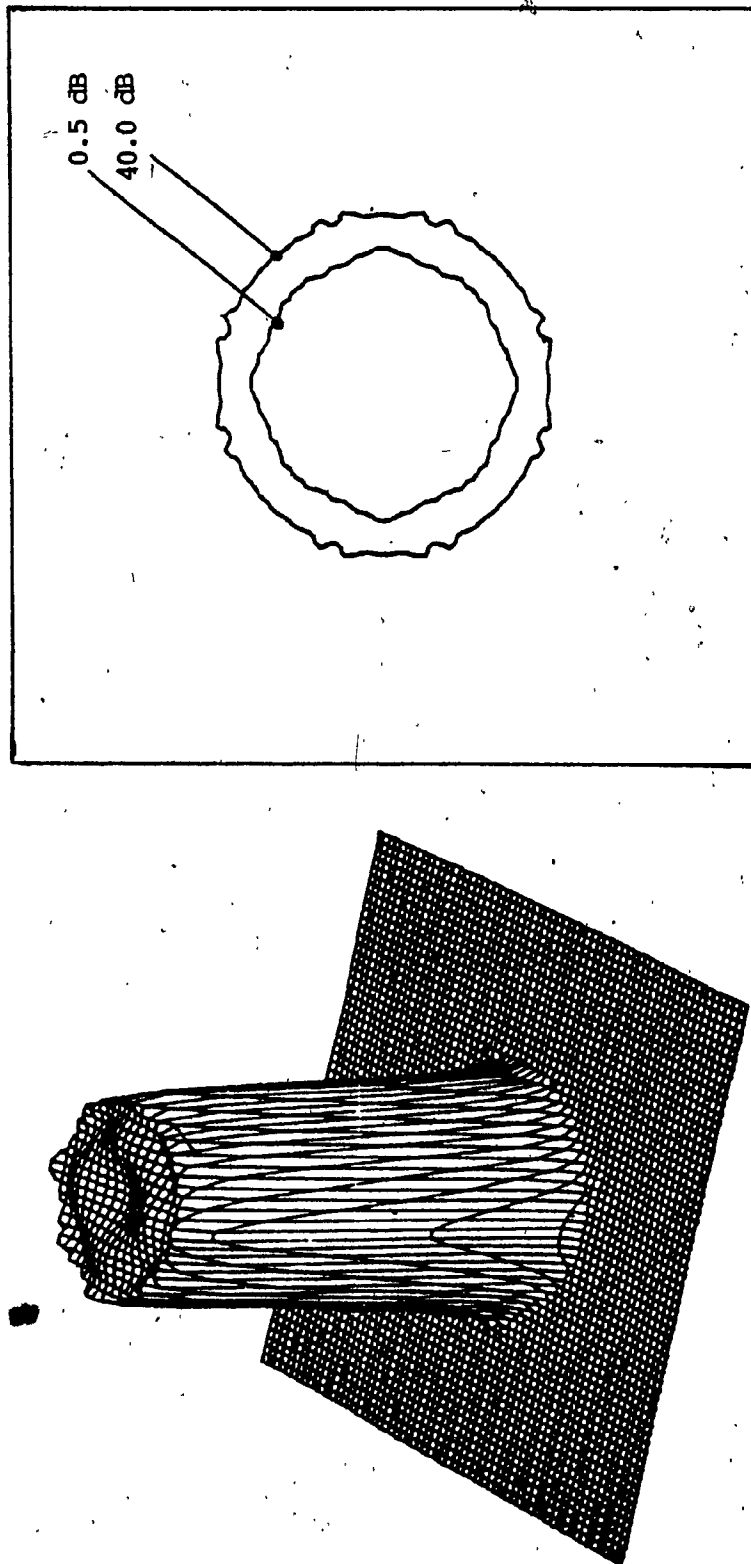
Table 4.1 Design Specifications for the 2-D Digital Filters

Example	A_p^{2D} (dB)	A_a^{2D} (dB)	W_p^{2D} (rad/s)	W_a^{2D} (rad/s)
1	0.5	40.0	1.0	1.5
2	0.4	40.0	1.3	2.0
3	0.5	45.0	1.0	1.6
4	0.6	50.0	1.0	1.7
5	0.4	45.0	0.5	1.0
6	0.4	40.0	2.0	2.8

listed above. Figs. 4.1 to 4.6 show the amplitude responses and contour plots obtained for the pseudo-rotated filter and the five optimized configurations of Example 1. Tables 4.2 - 4.7 show the actual maximum passband ripple and the minimum stopband attenuation for the pseudo-rotated filters and for the optimized designs.

As can be seen from these tables, all the optimized designs are violating the specifications in the passband and/or the stopband region. However, these designs are almost always more circularly symmetric than the original pseudo-rotated filters. An exception to this rule occurs in the Example 6 where the circularity of the pseudo-rotated and optimized filters are similar. This is consistent with some results in Chapter 3 where the circularity could not be improved by increasing the number of sections, if w_p^{2D} was greater than 60% of the Nyquist frequency.

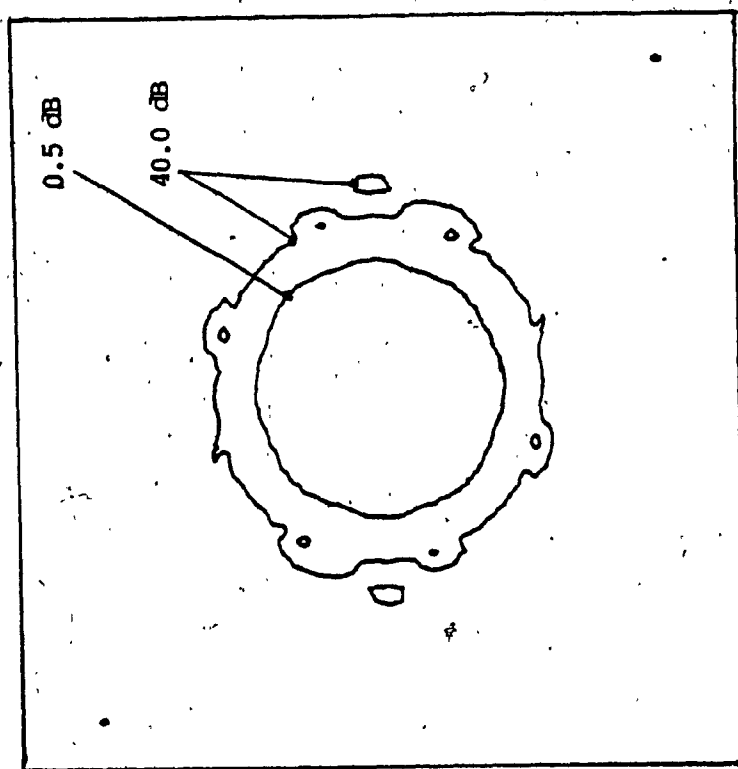
These results show that the method of pseudo-rotated filters described in Chapter 3 yields near optimal elliptic designs. In addition, the amount of computation needed is only a small fraction of that needed by the optimization method.



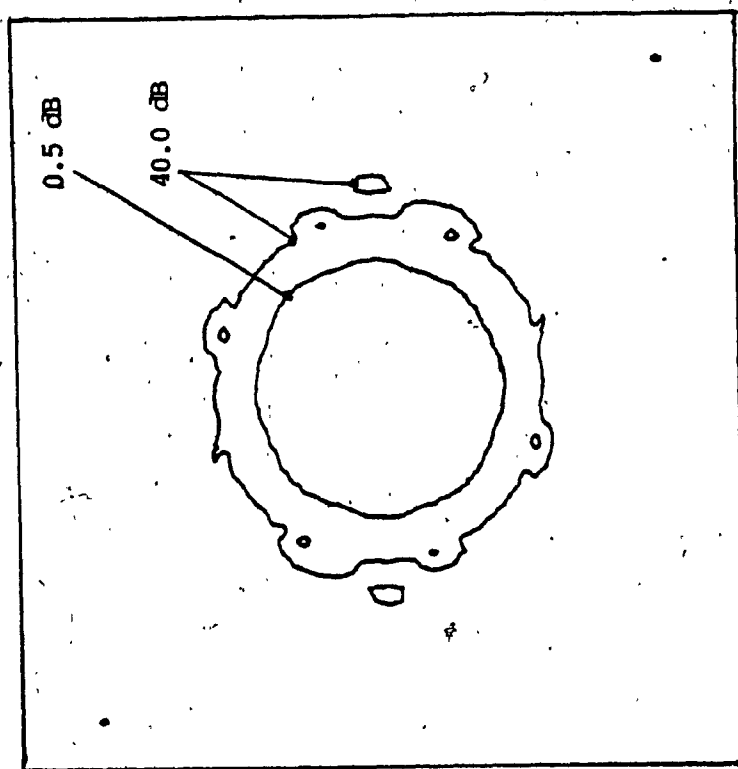
(a)

(b)

Figure 4.1 (a) 3-D Plot (Pseudo-Rotated Design), (b) Corresponding Contour Plots for Attenuations of 0.5 dB and 40.0 dB.



(a)



(b)

Figure 4.2 (a) 3-D Plot (Example 1, Configuration I), (b) Corresponding Contour Plots for Attenuations of 0.5 dB and 40.0 dB.

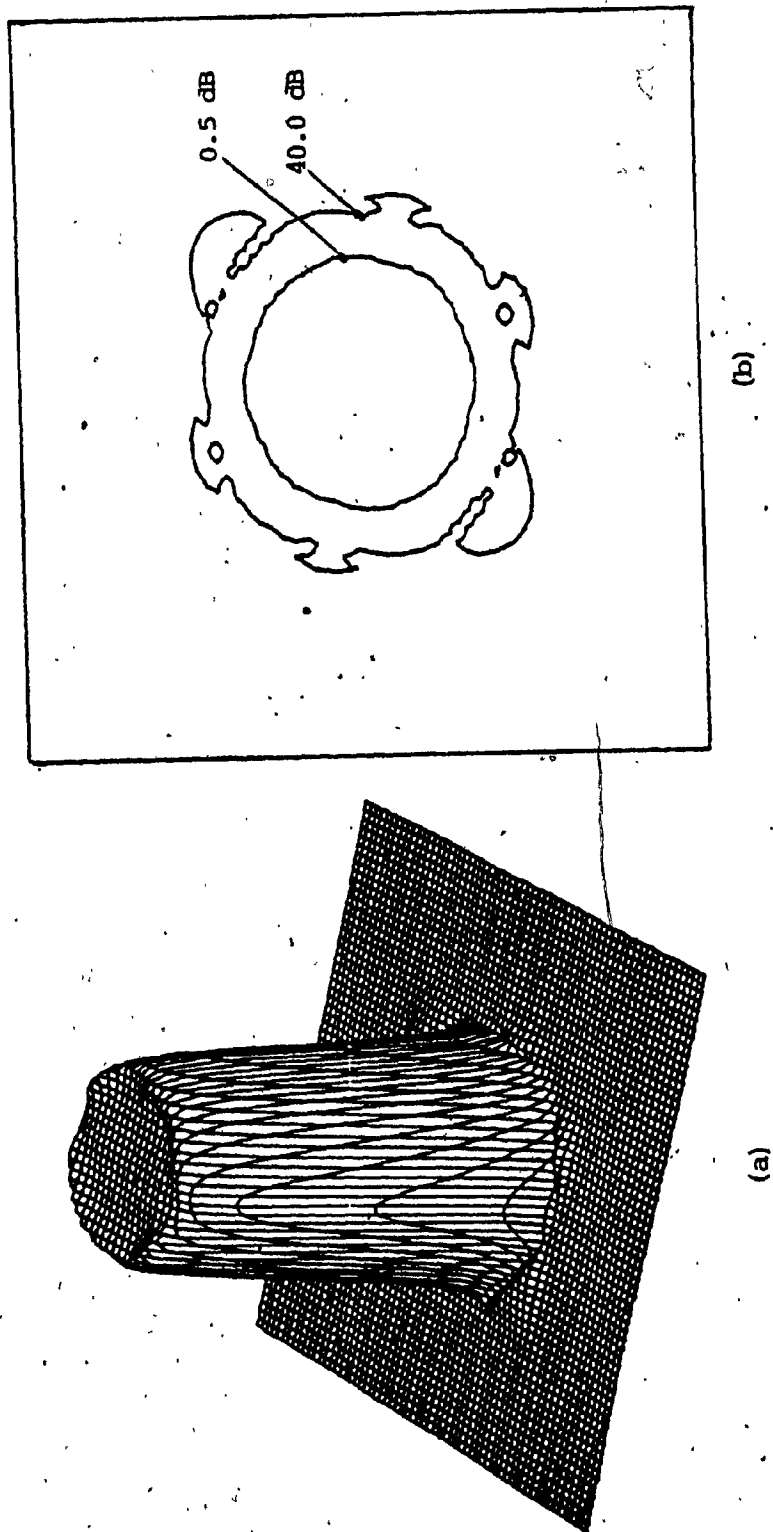
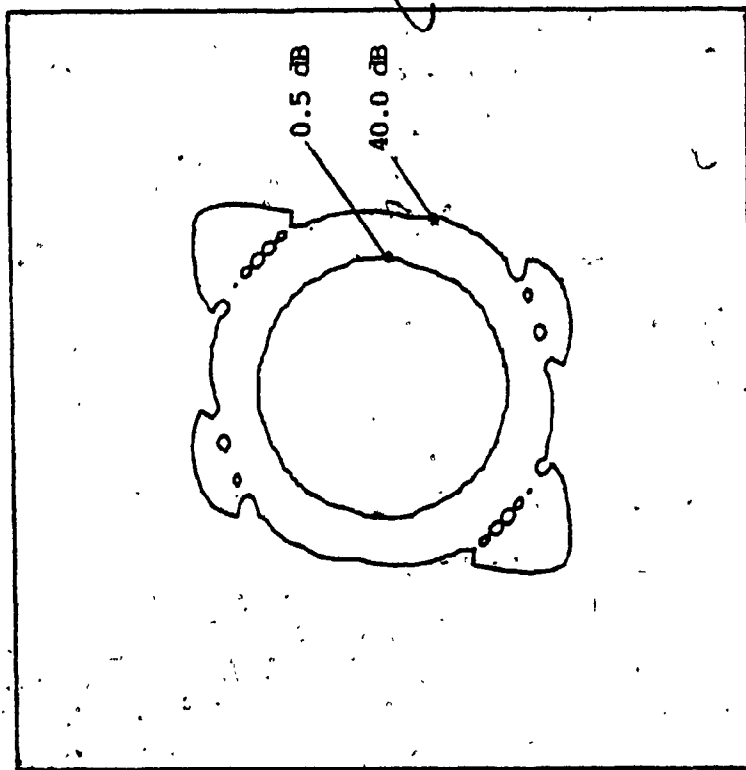
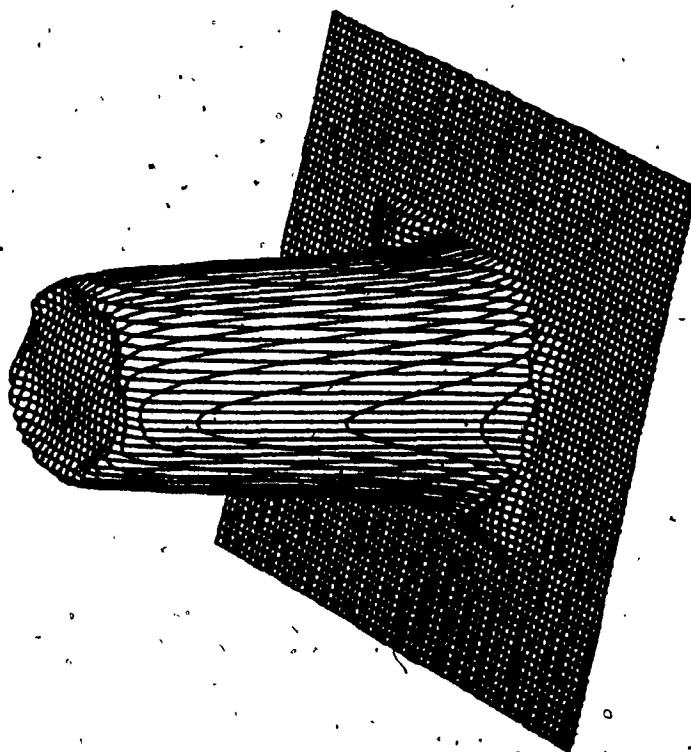


Figure 4.3 (a) 3-D Plot (Example 1, Configuration II), (b) Corresponding Contour Plots for Attenuations of 0.5 dB and 40.0 dB.

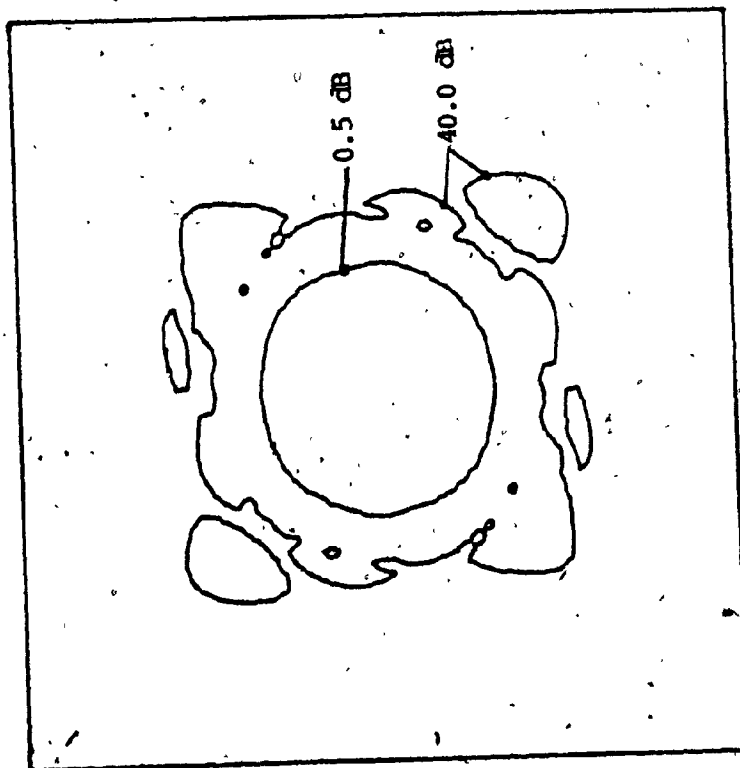


(a)



(b)

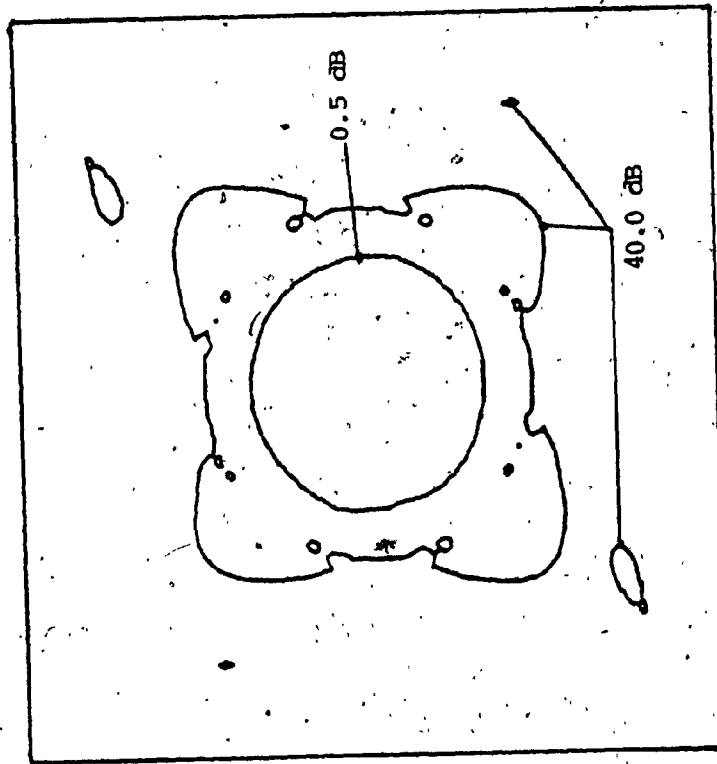
Figure 4.4 (a) 3-D Plot (Example 1, Configuration III), (b) Corresponding Contour Plots for Attenuations of 0.5 dB and 40.0 dB.



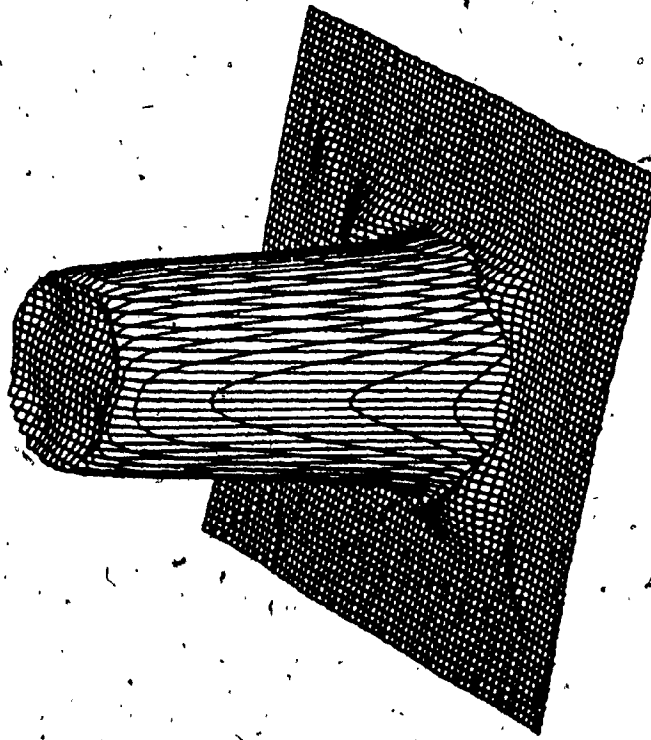
(a)

(b)

Figure 4.5 (a) 3-D Plot (Example 1, Configuration IV), (b) Corresponding Contour Plots for Attenuations of 0.5 dB and 40.0 dB.



(b)



(a)

Figure 4.6 (a) 3-D Plot (Example 1, Configuration V), (b) Corresponding Contour Plots for Attenuations of 0.5 dB and 40.0 dB.

Table 4.2 Actual Losses and Variance at the Passband Edge
(Pseudo-Rotated and Optimized Designs of Example 1)

Configuration	A_p^{2D} (dB)	A_a^{2D} (dB)	σ^2 (rad/s) ²
Rotated Filters	0.4296	41.05	1.094×10^{-2}
I	0.3834	27.88	8.642×10^{-3}
II	0.4020	32.83	8.654×10^{-3}
III	0.3628	29.65	8.685×10^{-3}
IV	0.4233	27.35	1.287×10^{-2}
V	0.2810	26.44	4.700×10^{-3}

Table 4.3 Actual Losses and Variance at the Passband Edge
(Pseudo-Rotated and Optimized Designs of Example 2)

Configuration	A_p^{2D} (dB)	A_a^{2D} (dB)	σ^2 (rad/s) ²
Rotated Filters	0.2310	53.36	2.310×10^{-2}
I	0.3189	26.40	8.630×10^{-4}
II	0.3924	23.36	3.420×10^{-3}
III	0.3741	27.22	3.530×10^{-3}
IV	0.2544	26.49	8.842×10^{-4}
V	0.2328	27.76	4.685×10^{-4}

Table 4.4 Actual Losses and Variance at the Passband Edge
(Pseudo-Rotated and Optimized Designs of Example 3)

Configuration	A_p^{2D} (dB)	A_a^{2D} (dB)	σ^2 (rad/s) ²
Rotated Filters	0.4573	54.30	1.283×10^{-2}
I	0.3752	28.11	1.468×10^{-3}
II	0.4538	25.44	8.573×10^{-3}
III	0.3741	23.64	3.686×10^{-3}
IV	0.3644	25.50	4.044×10^{-3}
V	0.2557	23.89	2.052×10^{-3}

Table 4.5 Actual Losses and Variance at the Passband Edge
(Pseudo-Rotated and Optimized Designs of Example 4)

Configuration	A_p^{2D} (dB)	A_a^{2D} (dB)	σ^2 (rad/s) ²
Rotated Filters	0.5045	67.14	1.634×10^{-2}
I	0.2883	37.95	1.065×10^{-3}
II	0.4102	30.19	7.524×10^{-3}
III	0.4269	30.92	5.858×10^{-3}
IV	0.3775	32.07	4.467×10^{-3}
V	0.2427	32.52	1.738×10^{-3}

Table 4.6 Actual Losses and Variance at the Passband Edge
(Pseudo-Rotated and Optimized Designs of Example 5)

Configuration	A_p^{2D} (dB)	A_a^{2D} (dB)	σ^2 (rad/s) ²
Rotated Filters	0.3659	60.27	1.565×10^{-2}
I	0.3456	29.93	1.405×10^{-3}
II	0.4585	25.45	2.083×10^{-3}
III	0.3930	26.49	1.994×10^{-3}
IV	0.5792	24.93	3.174×10^{-3}
V	0.3231	25.81	1.496×10^{-2}

Table 4.7 Actual Losses and Variance at the Passband Edge
(Pseudo-Rotated and Optimized Designs of Example 6)

Configuration	A_p^{2D} (dB)	A_a^{2D} (dB)	σ^2 (rad/s) ²
Rotated Filters	0.2500	41.95	2.935×10^{-3}
I	0.3652	33.77	3.493×10^{-3}
II	0.4363	33.86	3.678×10^{-3}
III	0.4545	35.33	3.682×10^{-3}
IV	0.4415	26.28	1.067×10^{-2}
V	0.4259	29.12	4.355×10^{-3}

4.4 Conclusions

In this chapter an attempt has been made to see if improvements can be brought about in pseudo-rotated designs through the use of an optimization technique. The optimization technique used was SUMT and a least-squares objective function has been assumed.

Several elliptic lowpass filters were first designed by using the method of pseudo-rotated filters described in Chapter 3. Then several configurations of the pseudo-rotated filters, each with decreasing number of sections were optimized to see if more economical and/or improved designs can be obtained. The results have shown that, in general, the maximum passband ripple is increased and/or the minimum stopband loss is reduced. The degree of circularity, however, is usually improved. In effect, the method of Chapter 3 appears to yield near-optimal approximations for the required specifications. This is to be expected, however, since the predictions of Chapter 3 lead to the lowest-order elliptic (or optimal) analog filter which, when used as prototype, will lead to the 2-D digital filter that will just satisfy the required specifications.

Unlike optimization methods, the method of pseudo-rotated filters entails an insignificant amount of computation by comparison, and since it readily yields filters that satisfy the required specifications, it is to be preferred in practice.

CHAPTER 5

REALIZATION AND IMPLEMENTATION OF PSEUDO-ROTATED FILTERS

5.1 Introduction

In the previous chapters the solution of the approximation problem in 2-D pseudo-rotated digital filters has been considered; and several procedures have been developed for the design of pseudo-rotated filters satisfying prescribed amplitude specifications. These procedures lead to the desired 2-D discrete transfer function.

In this chapter the realization of the 2-D discrete transfer function is considered. Two types of realizations are considered, namely, direct and wave realizations. In direct realizations, the transfer function is realized by means of first- and second-order sections connected in cascade or in parallel, and in wave realizations a 2-D structure is deduced from a corresponding 1-D analog filter by using the wave characterization [42].

In addition, the software implementation of pseudo-rotated digital filters is considered and several issues pertaining to the implementation are delineated.

5.2 Direct realization

The 2-D discrete transfer function obtained by the method of pseudo-rotation can be realized in terms of the direct realization. This is accomplished by obtaining an equivalent 2-D discrete transfer function having real coefficients. Then a structure realizing the 2-D transfer function is chosen.

5.2.1 Rearrangement of the transfer function coefficients

The procedure described in Sec. 2.4 gives the transfer function of a single pseudo-rotated filter as

$$H(z_1, z_2) = H_0 \frac{\prod_{i=1}^{M_N} (a_{11i} + a_{21i}z_1^{-1} + a_{12i}z_2^{-1} + a_{22i}z_1^{-1}z_2^{-1})}{\prod_{i=1}^{M_D} (b_{11i} + b_{21i}z_1^{-1} + b_{12i}z_2^{-1} + b_{22i}z_1^{-1}z_2^{-1})} \quad (5.1)$$

The numerator and denominator coefficients of the transfer function are usually complex since they are functions of a complex zeros and poles, respectively, of the 1-D analog filter. Hence, in order to obtain realizations with real multiplier constants it is necessary to express the transfer function of Eqn. 5.1 in terms of real coefficients.

For a pseudo-rotated filter section characterized by

$$H_i(z_1, z_2) = \frac{a_{11i} + a_{21i}z_1^{-1} + a_{12i}z_2^{-1} + a_{22i}z_1^{-1}z_2^{-1}}{b_{11i} + b_{21i}z_1^{-1} + b_{12i}z_2^{-1} + b_{22i}z_1^{-1}z_2^{-1}}$$

there is a pseudo-rotated filter section characterized by

$$H_j(z_1, z_2) = \frac{a_{11i}^* + a_{21i}^*z_1^{-1} + a_{12i}^*z_2^{-1} + a_{22i}^*z_1^{-1}z_2^{-1}}{b_{11i}^* + b_{21i}^*z_1^{-1} + b_{12i}^*z_2^{-1} + b_{22i}^*z_1^{-1}z_2^{-1}}$$

Hence for each set of coefficients

$$\{ a_{11i}, a_{21i}, a_{12i}, a_{22i}, b_{11i}, b_{21i}, b_{12i}, b_{22i} \}$$

there exists a corresponding set of coefficients

$$\{ a_{11i}^*, a_{21i}^*, a_{12i}^*, a_{22i}^*, b_{11i}^*, b_{21i}^*, b_{12i}^*, b_{22i}^* \}$$

and by combining the two first-order transfer functions, a second-order transfer function can be obtained which has real coefficients. These transfer functions can be obtained by using the following procedure :

- 1) Obtain the poles and zeros of the 1-D analog filter and arrange complex pairs of zeros and poles together.
- 2) Calculate the coefficients of the first-order pseudo-rotated sections for the complex zeros and poles.
- 3) Repeat (2) for the real zeros and poles.
- 4) Combine complex conjugate pairs of coefficients to obtain second-order transfer functions with real coefficients.

If we let

N_{ZR} = number of real zeros

N_{ZC} = number of complex zeros

N_{PR} = number of real poles

N_{PC} = number of complex poles

then from Eqn. 5.1, we have

$$M_N = N_{ZR} + N_{ZC}$$

$$M_D = N_{PR} + N_{PC} \quad (5.2)$$

where $M_D \geq M_N$.

By combining the first-order transfer functions with complex coefficients, we obtain the 2-D discrete transfer function

$$\begin{aligned}
 H(z_1, z_2) = H_0 & \left[\frac{\prod_{i=1}^{N_{Z2}} A_{11i} + A_{21i} z_1^{-1} + A_{12i} z_2^{-1} + A_{22i} z_1^{-1} z_2^{-1} + A_{31i} z_1^{-2}}{\prod_{i=1}^{N_{P2}} B_{11i} + B_{21i} z_1^{-1} + B_{12i} z_2^{-1} + B_{22i} z_1^{-1} z_2^{-1} + B_{31i} z_1^{-2}} \right. \\
 & \left. \frac{+ A_{13i} z_2^{-2} + A_{32i} z_1^{-2} z_2^{-1} + A_{23i} z_1^{-1} z_2^{-2} + A_{33i} z_1^{-2} z_2^{-2}}{+ B_{13i} z_2^{-2} + B_{32i} z_1^{-2} z_2^{-1} + B_{23i} z_1^{-1} z_2^{-2} + B_{33i} z_1^{-2} z_2^{-2}} \right] \times \\
 & \left[\frac{\prod_{i=1}^{N_{ZR}} a_{11i} + a_{21i} z_1^{-1} + a_{12i} z_2^{-1} + a_{22i} z_1^{-1} z_2^{-1}}{\prod_{i=1}^{N_{PR}} b_{11i} + b_{21i} z_1^{-1} + b_{12i} z_2^{-1} + b_{22i} z_1^{-1} z_2^{-1}} \right] \times \quad (5.3) \\
 & \left[\left(1 + \frac{4c}{T^2}\right) + \left(1 - \frac{4c}{T^2}\right) z_1^{-1} + \left(1 - \frac{4c}{T^2}\right) z_2^{-1} + \left(1 + \frac{4c}{T^2}\right) z_1^{-1} z_2^{-1} \right]^{M_D - M_N}
 \end{aligned}$$

where coefficients $\{a_{11}, a_{21}, \dots, b_{11}, \dots, b_{22}\}$ are given by the relations in Eqn. 2.21, and

$$N_{Z2} = \frac{N_{ZC}}{2} \quad N_{P2} = \frac{N_{PC}}{2} \quad (5.4)$$

$$A_{11i} = |a_{11j}|^2$$

$$A_{21i} = 2 \operatorname{Re}(a_{21j} a_{11j}^*)$$

$$A_{12i} = 2 \operatorname{Re}(a_{12j} a_{11j}^*)$$

$$A_{22j} = 2 \operatorname{Re}(a_{11j} a_{22j}^* + a_{12j} a_{21j}^*)$$

$$A_{31i} = |a_{21j}|^2$$

(5.5)

$$A_{13i} = |a_{12j}|^2$$

$$A_{32i} = 2 \operatorname{Re}(a_{21j} a_{22j}^*)$$

$$A_{23i} = 2 \operatorname{Re}(a_{12j} a_{22j}^*)$$

$$A_{33i} = |a_{22j}|^2$$

for $j=1, N_{ZC}, i=1, N_{Z2}$, and

$$B_{11i} = |b_{11j}|^2$$

$$B_{21i} = 2 \operatorname{Re}(b_{21j} b_{11j}^*)$$

$$B_{12i} = 2 \operatorname{Re}(b_{12j} b_{11j}^*)$$

$$B_{22j} = 2 \operatorname{Re}(b_{11j} b_{22j}^* + b_{12j} b_{21j}^*)$$

$$B_{31i} = |b_{21j}|^2$$

(5.6)

$$B_{13i} = |b_{12j}|^2$$

$$B_{32i} = 2 \operatorname{Re}(b_{21j} b_{22j}^*)$$

$$B_{23i} = 2 \operatorname{Re}(b_{12j} b_{22j}^*)$$

$$B_{33i} = |b_{22j}|^2$$

for $j=1, N_{PC}, i=1, N_{P2}$

The relationship between i and j is such that the first and the second ($i=1,2$), the third and fourth ($i=3,4$), etc. set of coefficients

$$\{ a_{11}, \dots, a_{22} \}$$

will generate the first ($j=1$), second ($j=2$), etc. set of coefficients

$$\{ A_{11}, \dots, A_{33} \}$$

Similarly, the denominator coefficients can be generated.

Now by dividing all the coefficients of the second-order transfer functions in Eqn. 5.3 by B_{11} and all the coefficients of the first-order in Eqn. 5.3 by b_{11} we obtain

$$H(z_1, z_2) = \prod_{i=1}^{N_{PR}} H_{1i}(z_1, z_2) \prod_{i=1}^{N_{P2}} H_{2i}(z_1, z_2) \quad (5.7)$$

where

$$H_{11}(z_1, z_2) = \frac{a'_{11} + a'_{21}z_1^{-1} + a'_{12}z_2^{-1} + a'_{22}z_1^{-1}z_2^{-1}}{1 + b'_{21}z_1^{-1} + b'_{12}z_2^{-1} + b'_{22}z_1^{-1}z_2^{-1}} \quad (5.8)$$

$$H_{21}(z_1, z_2) = \frac{A'_{11} + A'_{21}z_1^{-1} + A'_{12}z_2^{-1} + A'_{22}z_1^{-1}z_2^{-1} + A'_{31}z_1^{-2} + A'_{13}z_2^{-2} + A'_{32}z_1^{-2}z_2^{-1} + A'_{23}z_1^{-1}z_2^{-2} + A'_{33}z_1^{-2}z_2^{-2}}{1 + B'_{21}z_1^{-1} + B'_{12}z_2^{-1} + B'_{22}z_1^{-1}z_2^{-1} + B'_{31}z_1^{-2} + B'_{13}z_2^{-2} + B'_{33}z_1^{-2}z_2^{-2} + B'_{32}z_1^{-2}z_2^{-1} + B'_{23}z_1^{-1}z_2^{-2}} \quad (5.9)$$

In effect, pseudo-rotated filters can be realized in terms of a cascade and/or a parallel arrangement of low-order filter sections. As it is well known [47], such a realization leads to reduced sensitivity to coefficient quantization relative to a direct realization of the transfer function as a high-order single section.

Example 1

As an example, let us consider an elliptic lowpass analog filter characterized by

$$H(s) = K \frac{s - z_1}{s - p_1} \frac{s - z_1^*}{s - p_1^*} \frac{1}{s - p_2} \quad (5.10)$$

where z_1 and p_1 are complex and p_2 is real.

Using β as a rotation angle, the following 2-D digital transfer function is obtained

$$H(z_1, z_2) = K \frac{\prod_{i=1}^2 (a_{11i} + a_{21i}z_1 + a_{12i}z_2 + a_{22i}z_1z_2)}{\prod_{i=1}^2 (b_{11i} + b_{21i}z_1 + b_{12i}z_2 + b_{22i}z_1z_2)} \quad (5.11)$$

$$\frac{(1 + \frac{4c}{T^2}) + (1 - \frac{4c}{T^2})z_1 + (1 - \frac{4c}{T^2})z_2 + (1 + \frac{4c}{T^2})z_1z_2}{b_{113} + b_{213}z_1 + b_{123}z_2 + b_{223}z_1z_2}$$

5.2.2 Digital structures

At this stage some differences between the shift operators z_1^{-1} and z_2^{-1} will be pointed out. Let us suppose that the input data is being scanned column by column as indicated in Fig. 5.1. The delay operator z_2^{-1} will be implemented by a single register as in 1-D digital filters. However, since the scanning is performed one column at a time, the values of each element of that column have to be preserved in the delay operator z_1^{-1} for the calculations of elements of successive columns. Consequently, this delay operator must be implemented in terms of a memory consisting of a number of registers equal to the number of elements of a column.

In the case where scanning is performed row by row, z_1^{-1} is implemented in terms of a single register and z_2^{-1} is implemented in terms of a set of registers.

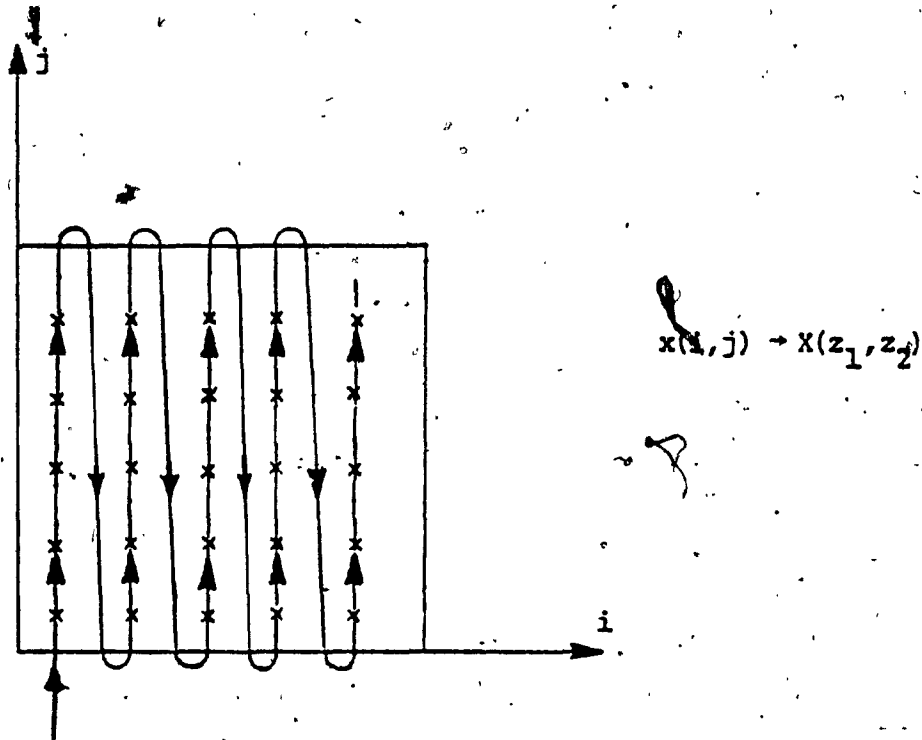


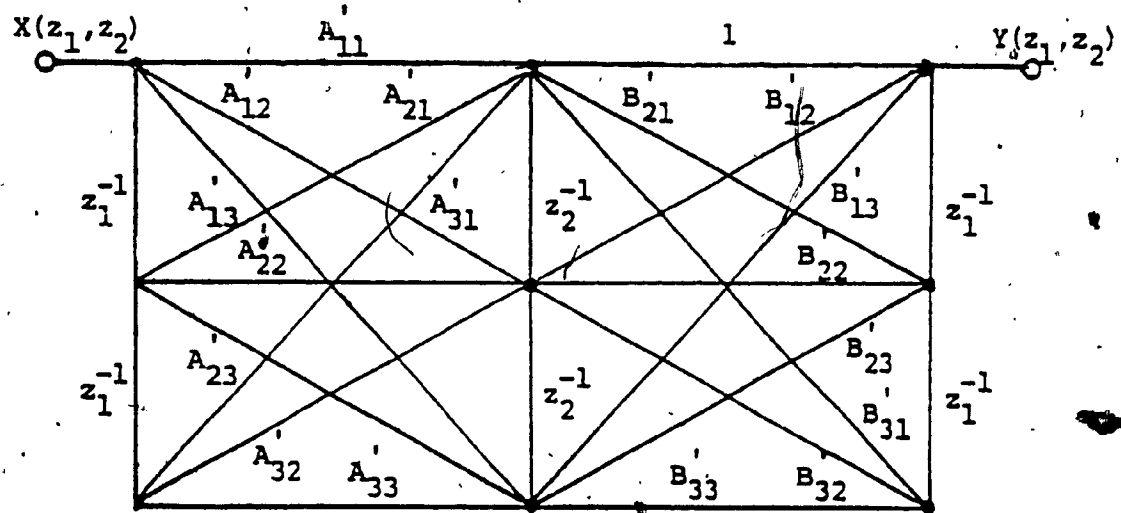
Figure 3.1 Scanning the Input Data Column by Column.

Before a 2-D digital structure is chosen, a decision must be made as to whether the scanning will be performed row by row or column by column. If the scanning is to be performed row by row, the number of delay operators z_2^{-1} should be minimized and if it is to be performed column by column, the number of delay operators z_1^{-1} should be minimized.

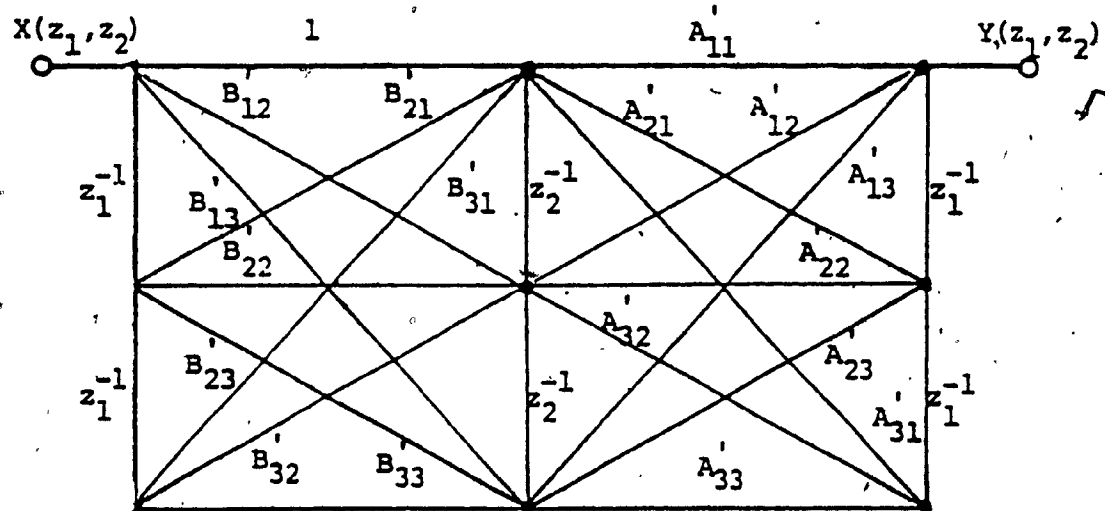
The 2-D direct realizations that minimize the numbers of z_2^{-1} are given in Figs. 5.2(a) and (b) for the second-order sections and in Figs. 5.3(a) and (b) for the first-order sections. The 2-D direct realizations that minimize the number of delay operators z_1^{-1} can easily be obtained from Figs. 5.2 and 5.3 by interchanging z_1^{-1} and z_2^{-1} . Though these are not new structures, they have been included here just to point out the difference between the delay operators and for comparison with the wave realization of pseudo-rotated filters described below.

5.3 Wave realization of pseudo-rotated filters

The wave characterization has been used extensively in the past for the realization of low-sensitivity 1-D digital filters. In this section it is shown that the wave characterization can also be applied for the realization of 2-D pseudo-rotated digital filters.



(a)



(b)

Figure 5.2 (a) Flowgraph Representation of a Second-Order Section for Scanning the Input Data Row by Row, (b) The Transpose Flowgraph

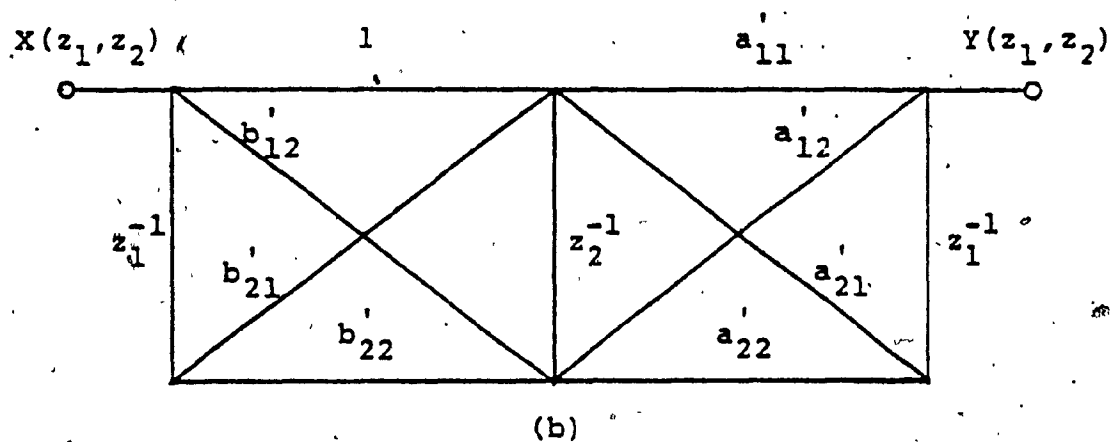
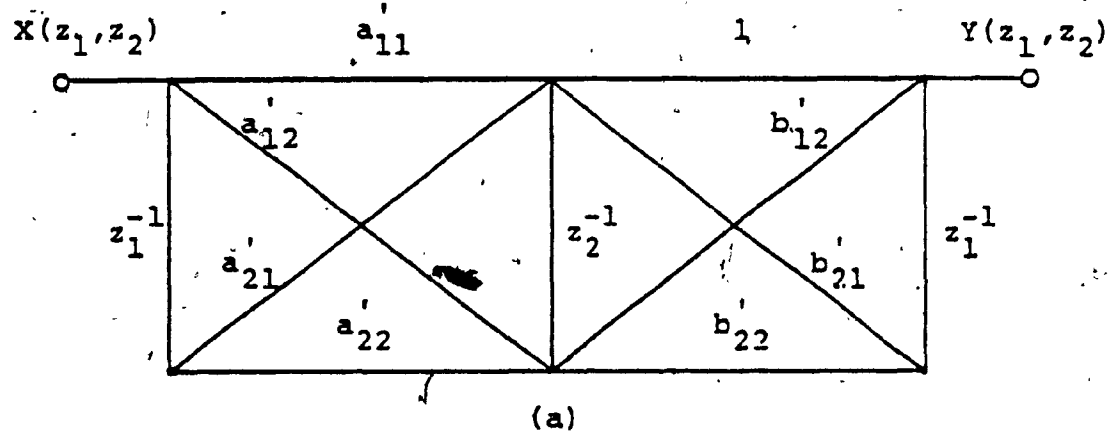


Figure 5.3 (a) Flowgraph Representation of a First-Order Section for Scanning the Input Data Row by Row, (b) The Transpose Flowgraph.

Wave digital filters based on the transformation of Shanks et al [18] have been realized on a minicomputer by Lennarz and Höfmann [48]. The approach used here is similar. However, since the transformation used to obtain pseudo-rotated filters is not the same, different realizations are obtained. The advantages gained are the advantages associated with the transformation of Eqn. 2.8. For example, stable realizations are always obtained which are free of non-essential singularities of the second kind, and the need of guard filters is usually eliminated.

5.3.1 Impedance transformation

Given an LC structure which represents an analog 1-D filter, the corresponding 2-D pseudo-rotated wave digital filter can be obtained by transforming impedances in the s domain to impedances in the (s_1, s_2) domain. We can write

$$Z_{2D}(s_1, s_2) = Z_{1D}(s) \Big|_{s = f(s_1, s_2)} \quad (5.12)$$

where

$$f(s_1, s_2) = \frac{s_1 \cos(\beta) + s_2 \sin(\beta)}{1 + c s_1 s_2} \quad (5.13)$$

For a capacitor

$$z_{1D}(s) = \frac{R_x}{s} \quad (5.14)$$

where R_x is a positive constant and from Eqn. 5.13 we obtain

$$\begin{aligned} z_{2D}(s_1, s_2) &= \frac{R_x}{\frac{s_1 \cos(\beta) + s_2 \sin(\beta)}{1 + c s_1 s_2}} \\ &= \frac{R_x (1 + c s_1 s_2)}{s_1 \cos(\beta) + s_2 \sin(\beta)} \end{aligned} \quad (5.15)$$

$$z_{2D}(s_1, s_2) = \left\{ \begin{aligned} &\frac{R_x}{\frac{1}{\frac{s_1 \cos(\beta)}{s_1 \cos(\beta)} + \frac{s_2 \sin(\beta)}{s_2 \sin(\beta)}}} + \\ &\frac{R_x c}{\sin(\beta) \cos(\beta)} \frac{s_1 \cos(\beta) s_2 \sin(\beta)}{s_1 \cos(\beta) + s_2 \sin(\beta)} \end{aligned} \right. \quad (5.16)$$

In effect, $z_{2D}(s_1, s_2)$ is the impedance of two capacitors in parallel in series with two inductors in parallel, as illustrated in Fig. 5.4(a)

where

$$C_1 = C \cos(\beta)$$

$$C_2 = C \sin(\beta)$$

(5.17)

$$L_1 = \frac{c}{C \sin(\beta)}$$

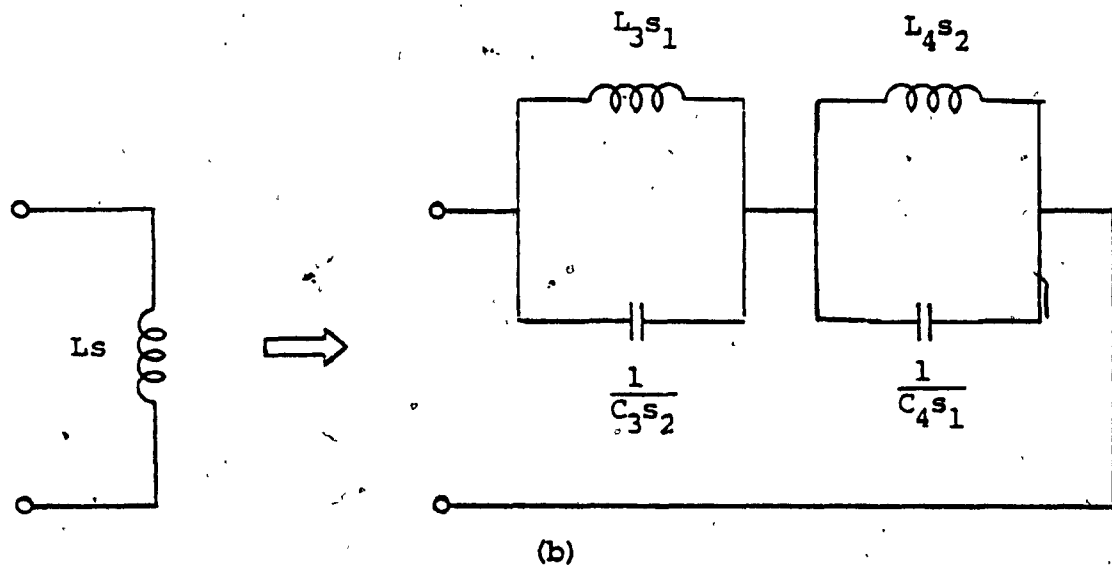
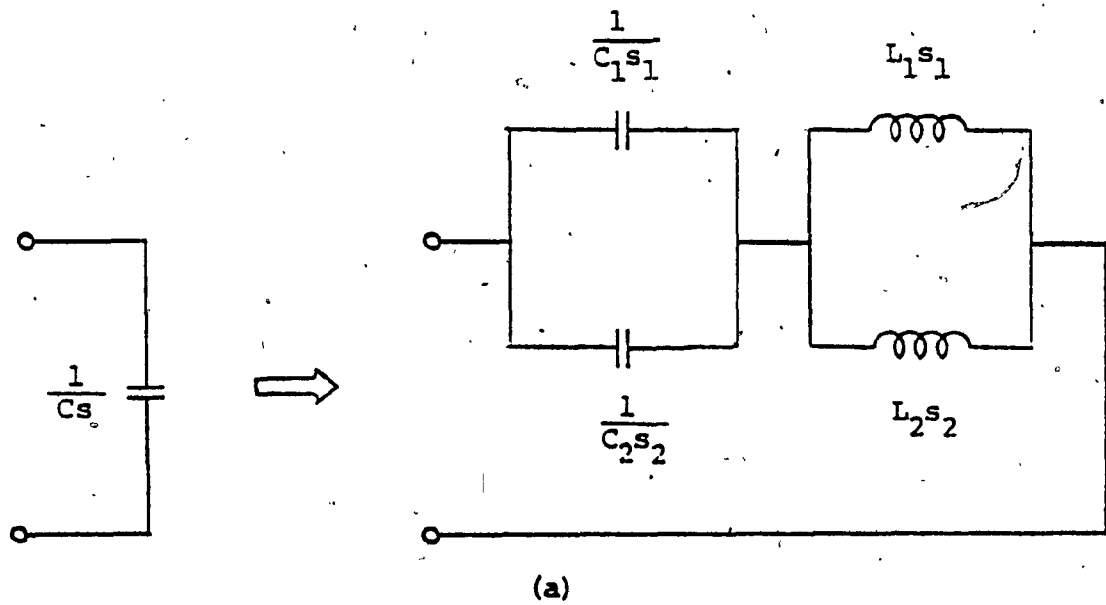


Figure 5.4 Impedance Transformations, (a) Capacitor, (b) Inductor

$$L_2 = \frac{c}{C \cos(\beta)}$$

For an inductor

$$Z_{1D}(s) = R_x s \quad (5.18)$$

where R_x is a positive constant and from Eqn. 5.13, we obtain

$$\begin{aligned} Z_{2D}(s_1, s_2) &= \frac{R_x (s_1 \cos(\beta) + s_2 \sin(\beta))}{1 + c s_1 s_2} \\ &= R_x \cos(\beta) \frac{s_1}{1 + c s_1 s_2} + R_x \sin(\beta) \frac{s_2}{1 + c s_1 s_2} \end{aligned} \quad (5.19)$$

or

$$Z_{2D}(s_1, s_2) = \frac{R_x \cos(\beta)}{c} \frac{c s_1 \frac{1}{s_2}}{c s_1 + \frac{1}{s_2}} + \frac{R_x \sin(\beta)}{c} \frac{\frac{1}{s_1} c s_2}{\frac{1}{s_1} + c s_2} \quad (5.20)$$

In effect, $Z_{2D}(s_1, s_2)$ is the impedance of a capacitor and an inductor in parallel, in series with an inductor and a

capacitor in parallel, as illustrated in Fig. 5.4(b)

where

$$L_3 = L \cos(\beta)$$

$$C_3 = \frac{C}{L \cos(\beta)}$$

(5.21)

$$L_4 = L \sin(\beta)$$

$$C_4 = \frac{C}{L \sin(\beta)}$$

The above impedance transformations will convert a 1-D LC analog filter into a 2-D LC analog filter. Then any one of the approaches due to Fettweis [36], Constantinides [3], and Swamy and Thyagarajan [37], [38] can readily be applied to deduce a wave realization for a pseudo-rotated digital filter. The digital realization of capacitors and inductors is illustrated in Fig. 5.5.

5.4 Comparison between direct and wave realizations

Let us consider the realization of a 2-D circularly symmetric pseudo-rotated lowpass digital filter by means of the direct realization and the wave realization. Consider the 2-D specifications

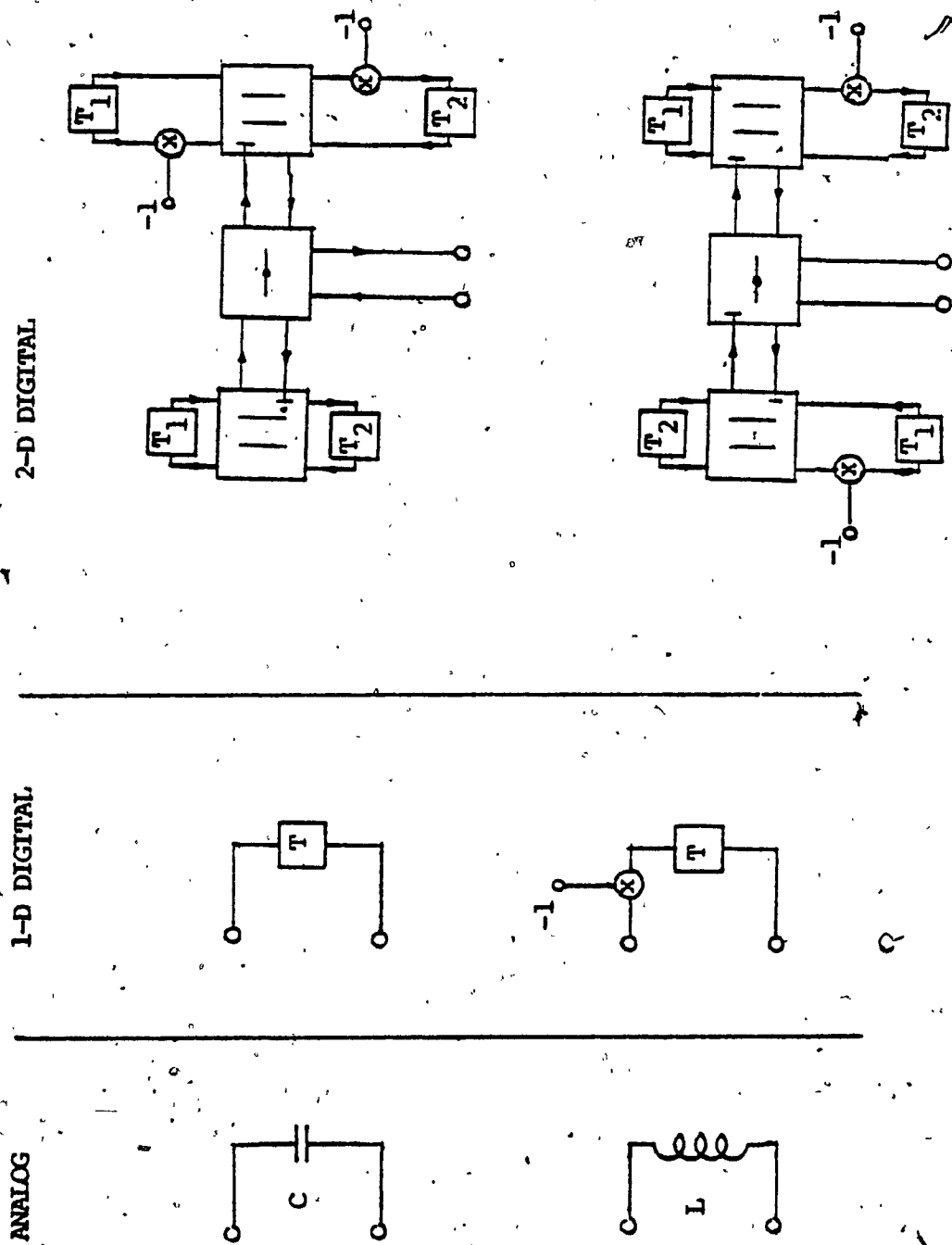


Figure 5.5 Digital Realizations of Capacitors and Inductors

$$A_p^{2D} = 0.39 \text{ dB}$$

$$A_a^{2D} = 28.0 \text{ dB}$$

$$W_p^{2D} = 0.927 \text{ rad/s}$$

$$W_a^{2D} = 1.48 \text{ rad/s}$$

$$W_s = 2\pi \text{ rad/s}$$

and assume that the rotation angles are $\pm 30^\circ$ and $\pm 60^\circ$.

According to Chapter 3, the corresponding 1-D digital-filter specifications are

$$A_p^{1D} = 0.098 \text{ dB}$$

$$A_a^{1D} = 14.0 \text{ dB}$$

$$W_p^{1D} = 0.927 \text{ rad/s}$$

$$W_a^{1D} = 1.282 \text{ rad/s}$$

and the corresponding 1-D analog-filter specifications can be obtained as [42]

$$A_p = 0.098 \text{ dB}$$

$$A_a = 14.0 \text{ dB}$$

$$W_p = 1.0 \text{ rad/s}$$

$$W_a = 1.494 \text{ rad/s}$$

where the warping effect has been taken into account in the calculation of W_p and W_a .

By using filter-design tables like those found in [49], we obtain the equally-terminated LC elliptic lowpass filter shown in Fig. 5.6. The filter order is 3 and the component values are :

$$R = 1\Omega \quad C_1 = C_2 = 0.7652 \text{ F} \quad C_3 = 0.4847 \text{ F} \quad L_4 = 0.7411 \text{ H}$$

The 1-D analog transfer function is given by

$$H(s) = \frac{(s-z)(s-z^*)}{(s-p_1)(s-p_1^*)(s-p_2)} \quad (5.22)$$

where

$$z = +j \frac{1}{\sqrt{L_4 C_3}}$$

$$p_1 = \frac{-L_4 + j \sqrt{8L_4 R^2 (C_1 + 2C_3)} - L_4}{2L_4 R (C_1 + 2C_3)} \quad (5.23)$$

$$p_2 = -\frac{1}{R C_2}$$

This transfer function can also be obtained by using the above 1-D digital-filter specifications in conjunction with the design procedures given in [42].

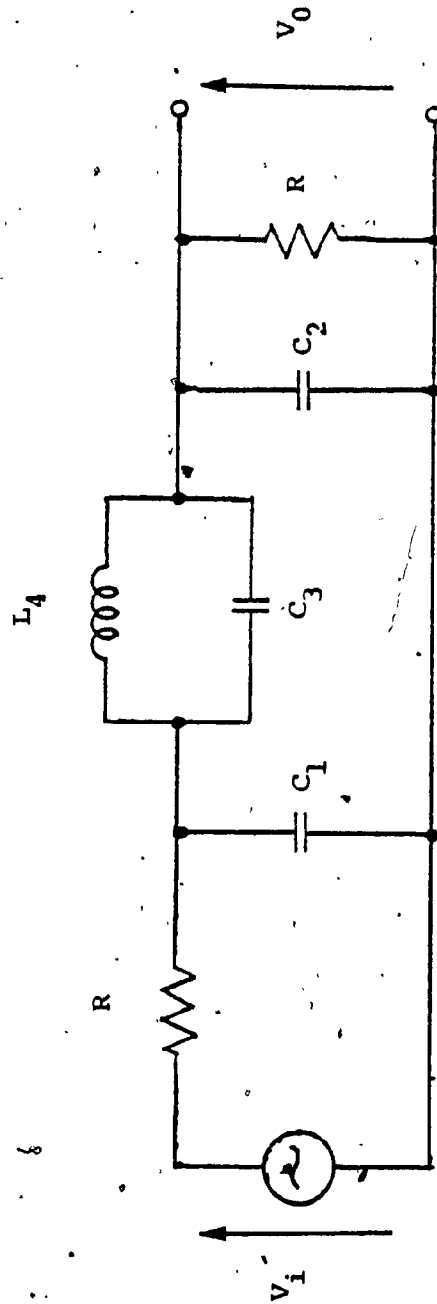


Figure 5.6 Equally-Terminated LC Elliptic Filter.

5.4.1 Direct realization

On applying the technique of pseudo-rotation to the analog-filter transfer function in Eqn. 5.22, the 2-D discrete transfer function in Eqn. 5.3 is obtained which has real coefficients. The amplitude response as computed by using the CDC Cyber 552/552 computer ($L = \infty$) is illustrated in Fig. 5.7. In order to assess to some extent the effect of coefficient quantization, the effective wordlength L was reduced to 14, 12, 10, and 8 bits, and the corresponding amplitude responses were obtained. Fixed-point arithmetic was assumed and the quantization was carried out by truncation. The 3-D and contour plots obtained for $L = 10$ and 8 are illustrated in Figs. 5.8-5.9.

5.4.2 Wave realization

Here a realization is obtained by using the approach due to Fettweis [50] - [53]. By using Eqns. 5.17 and 5.21, the 2-D wave digital filter can be obtained from the corresponding analog LC filter shown in Fig. 5.6. The 2-D pseudo-rotated wave digital filter is shown in Fig. 5.10.

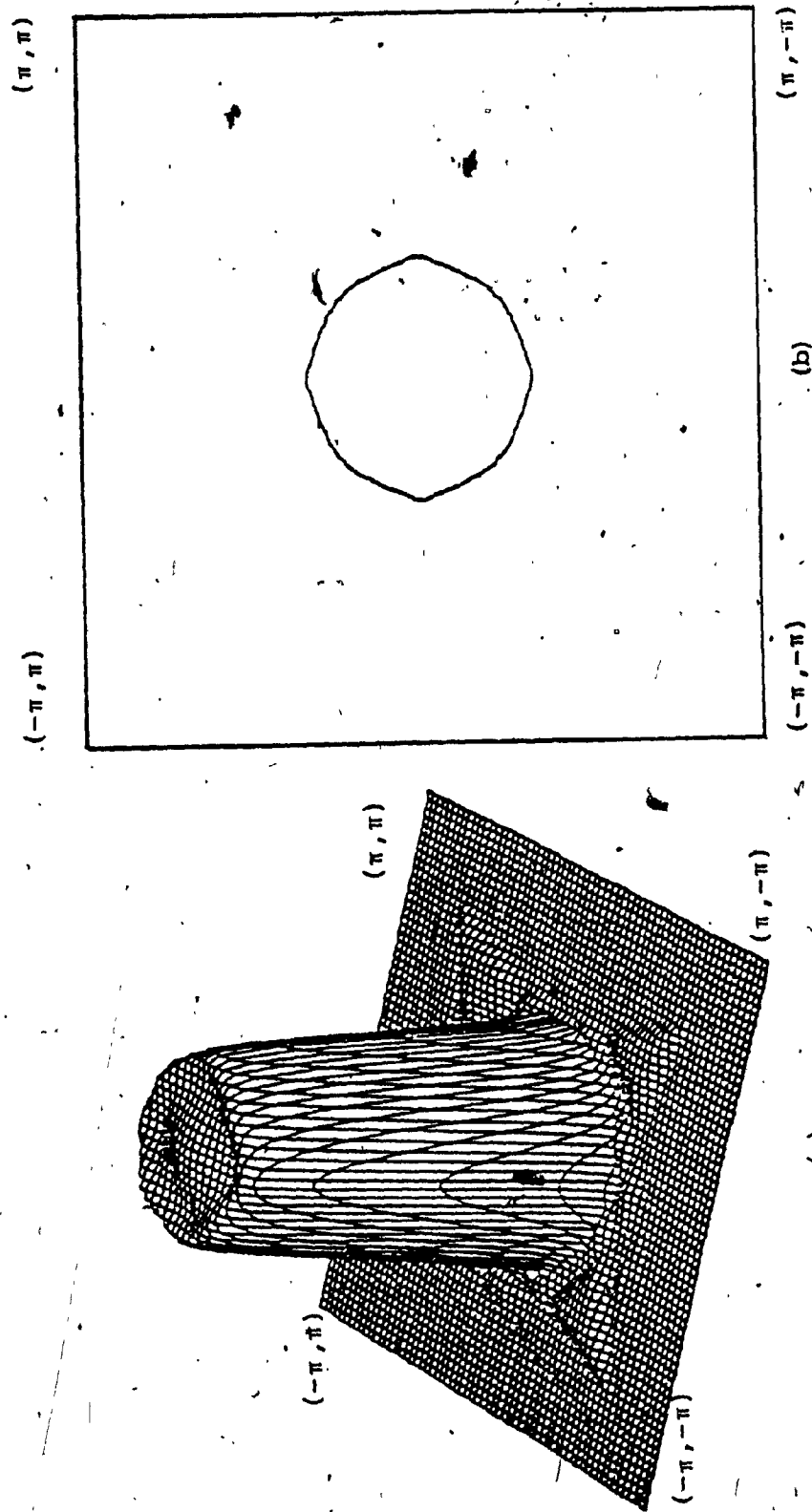


Figure 5.7 Direct Realization of Pseudo-Rotated Filter ($L = \infty$), (a) 3-D Plot, (b) Contour Plot for Attenuation of 0.4 dB.

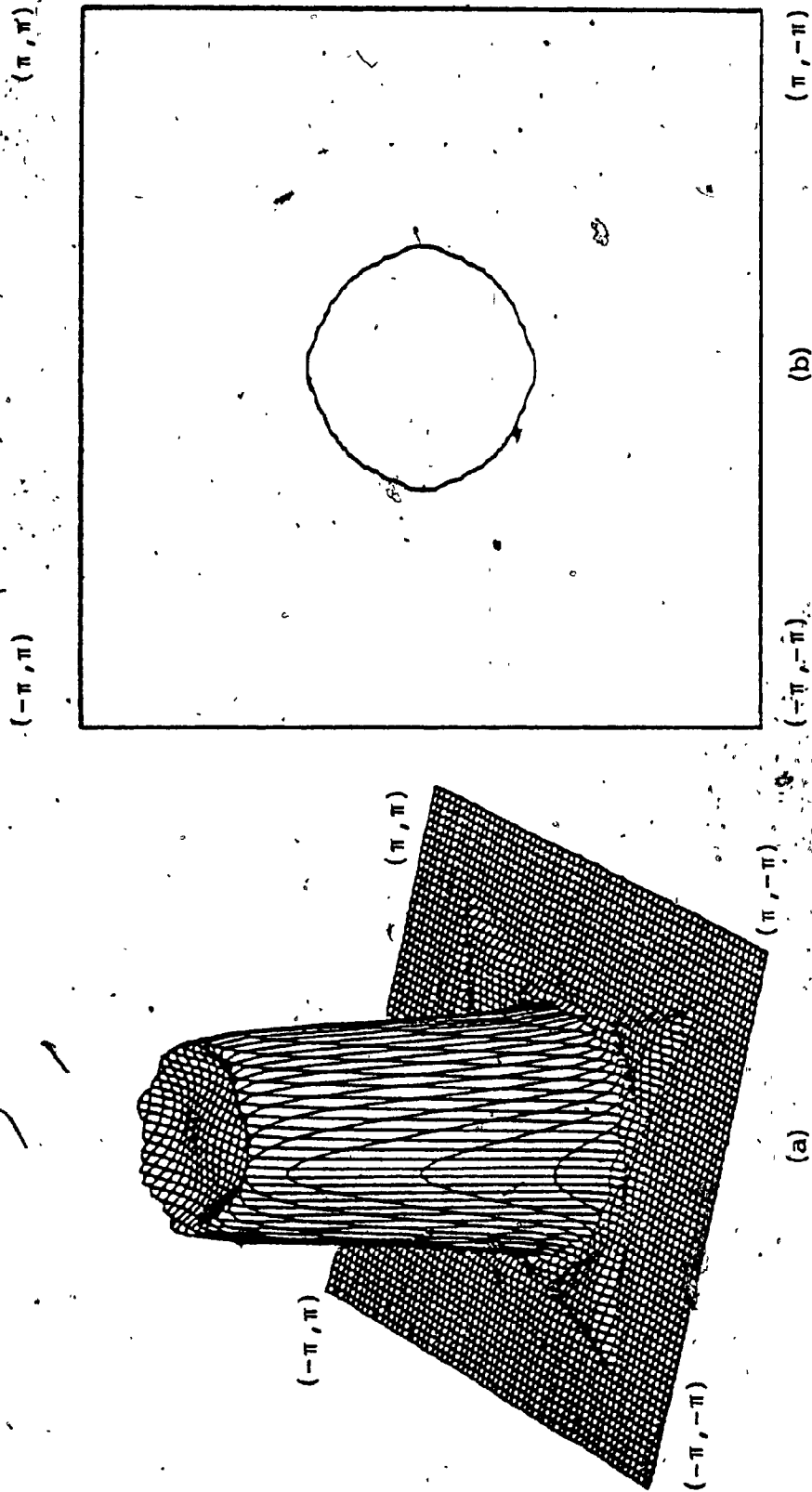


Figure 5.8 Direct Realization of Pseudo-Rotated Filter ($E = 10$), (a) 3-D Plot
(b) Contour Plot for Attenuation of 0.4 dB.

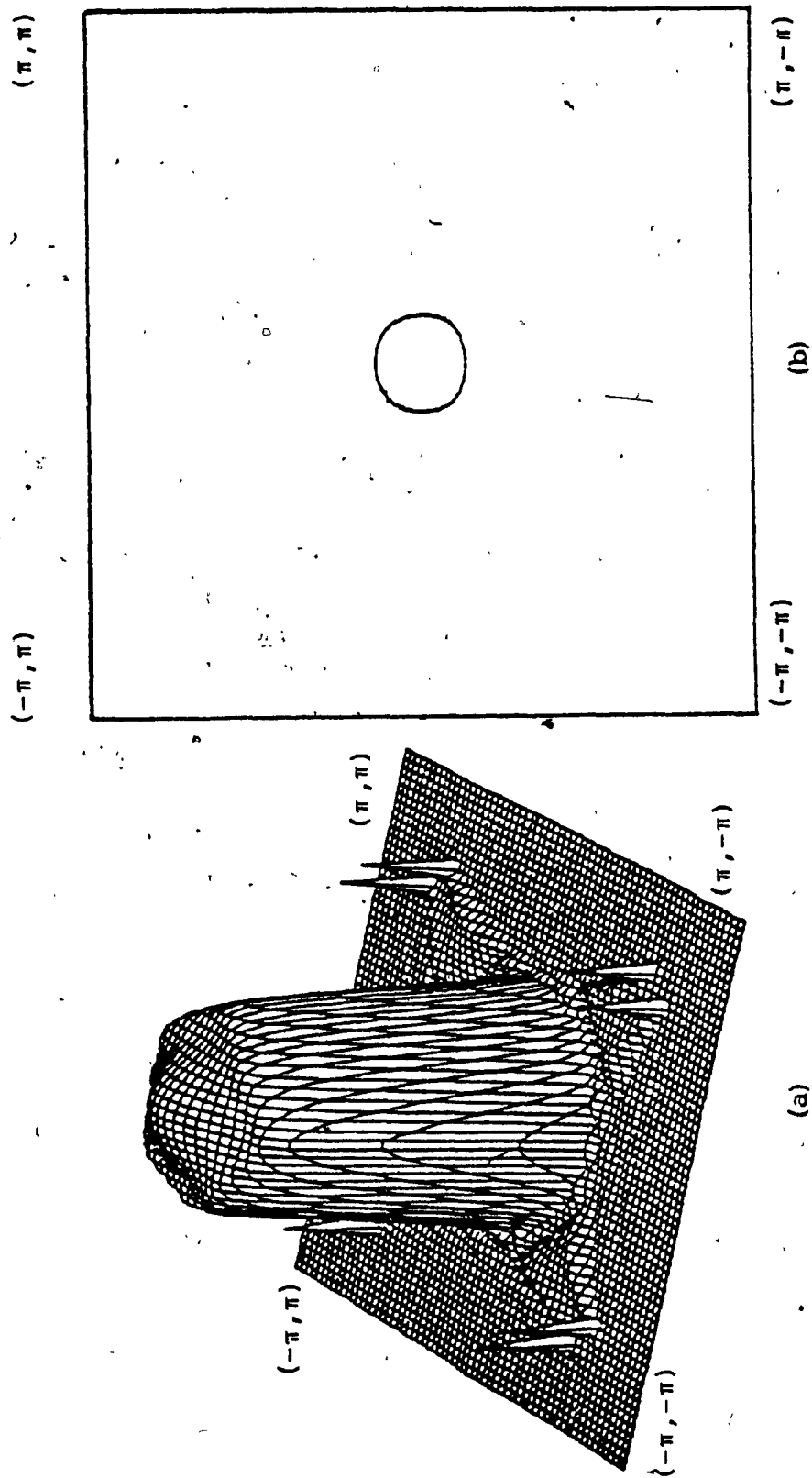


Figure 5.9 Direct Realization of Pseudo-Rotated Filter ($L = 8$), (a) 3-D Plot
(b) Contour Plot for Attenuation of 0.4 dB.

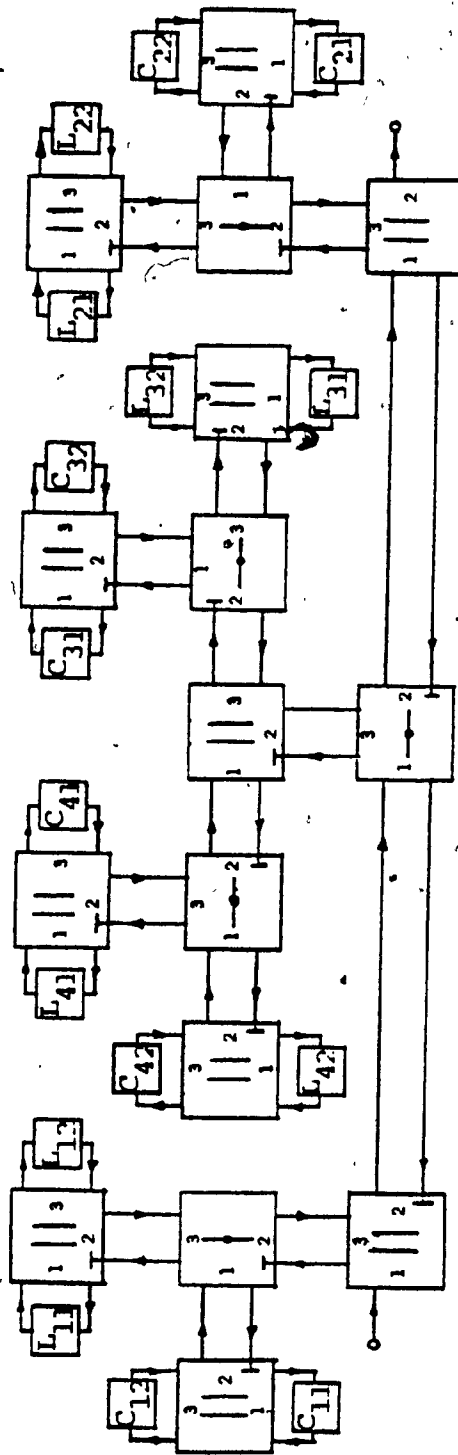


Figure 5.10 2-D Wave Realization Derived from Fig. 5.6.

Frequency domain analysis can be carried out by applying the same technique as in 1-D digital filters [42].

The filter obtained was analysed assuming fixed-point arithmetic and quantization was by truncation. The amplitude responses for $L = \infty$, $L = 10$ and $L = 8$ are shown in Figs. 5.11(a) to 5.13(a). The contour plots at the passband edge for $L = \infty$, $L = 10$ and $L = 8$ are shown in Figs. 5.11(b) to 5.13(b).

5.4.3 Comparison of direct and wave realizations

Table 5.1 shows the actual maximum passband ripple and the minimum stopband attenuation for the direct and wave realizations for wordlengths equal to $L = \infty$, 14, 12, 10 and 8. We can see from this table that for this specific example, both realizations are satisfying the specifications for wordlengths larger than 8 bits. For a wordlength of 8 bits, both realizations violate the specified maximum passband ripple. However, the amplitude response in the direct realization is more seriously affected by coefficient quantization than that in the wave realization. This can also be seen by comparing the 3-D plots in Figs. 5.9 and 5.13. In effect, the wave realization is less sensitive to coefficient quantization than the direct realization, as would be expected.

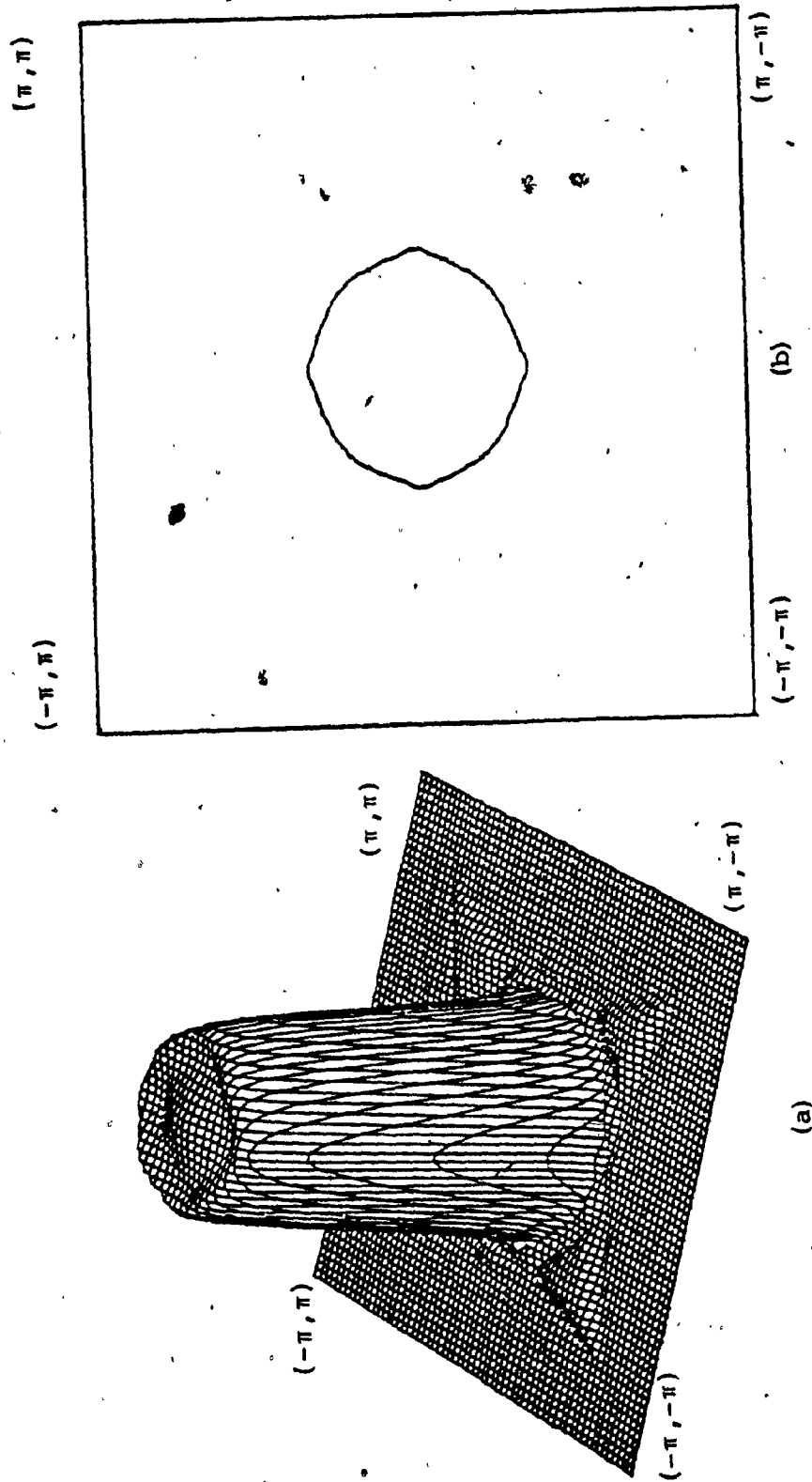


Figure 5.11 Wave Realization of Pseudo-Rotated Filter ($L = \infty$), (a) 3-D Plot
(b) Contour plot for Attenuation of 0.4 dB.

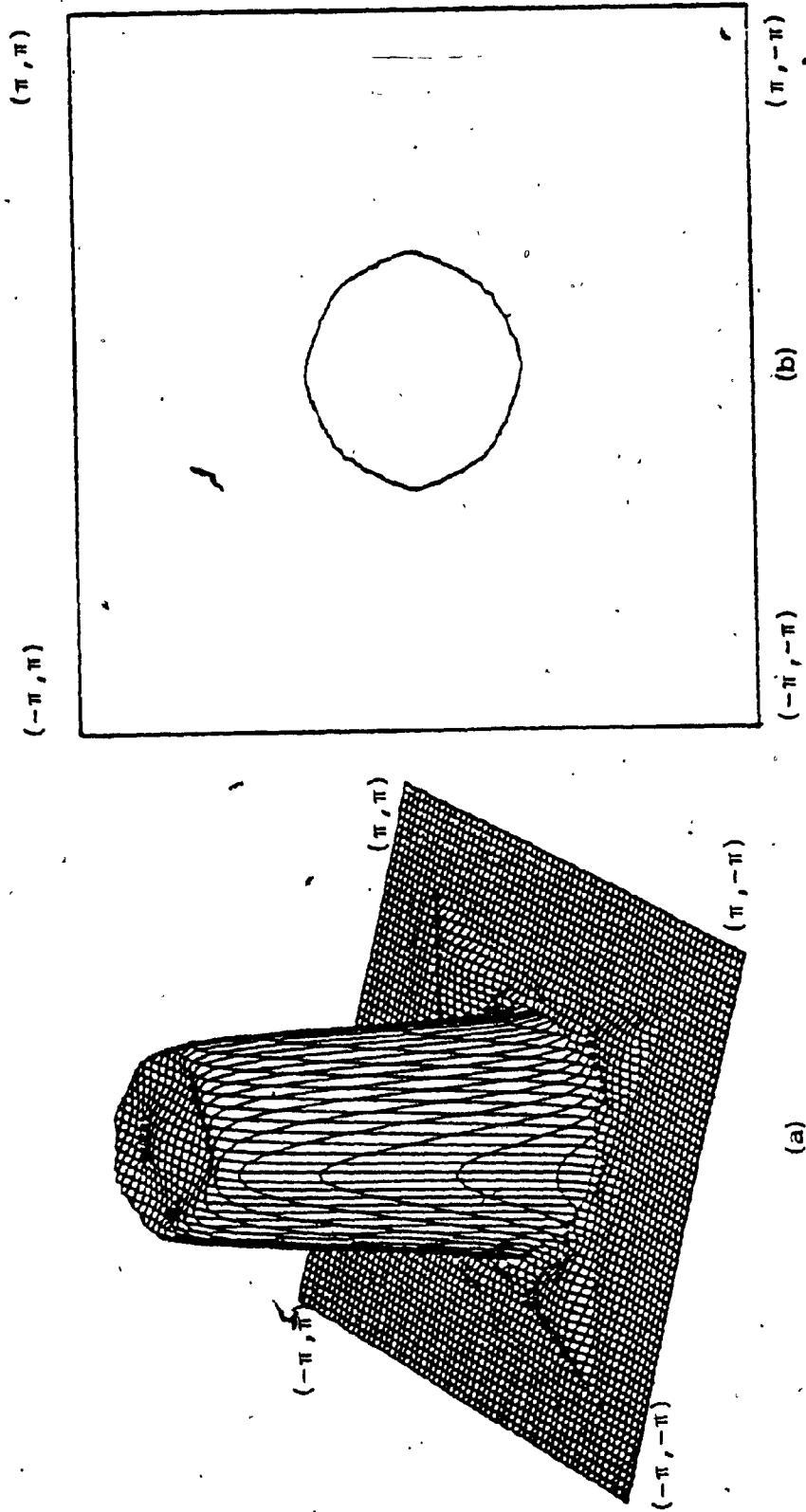


Figure 5.12 Wave Realization of Pseudo-Rotated Filter ($L = 10$), (a) 3-D Plot
(b) Contour Plot for Attenuation of 0.4 dB.

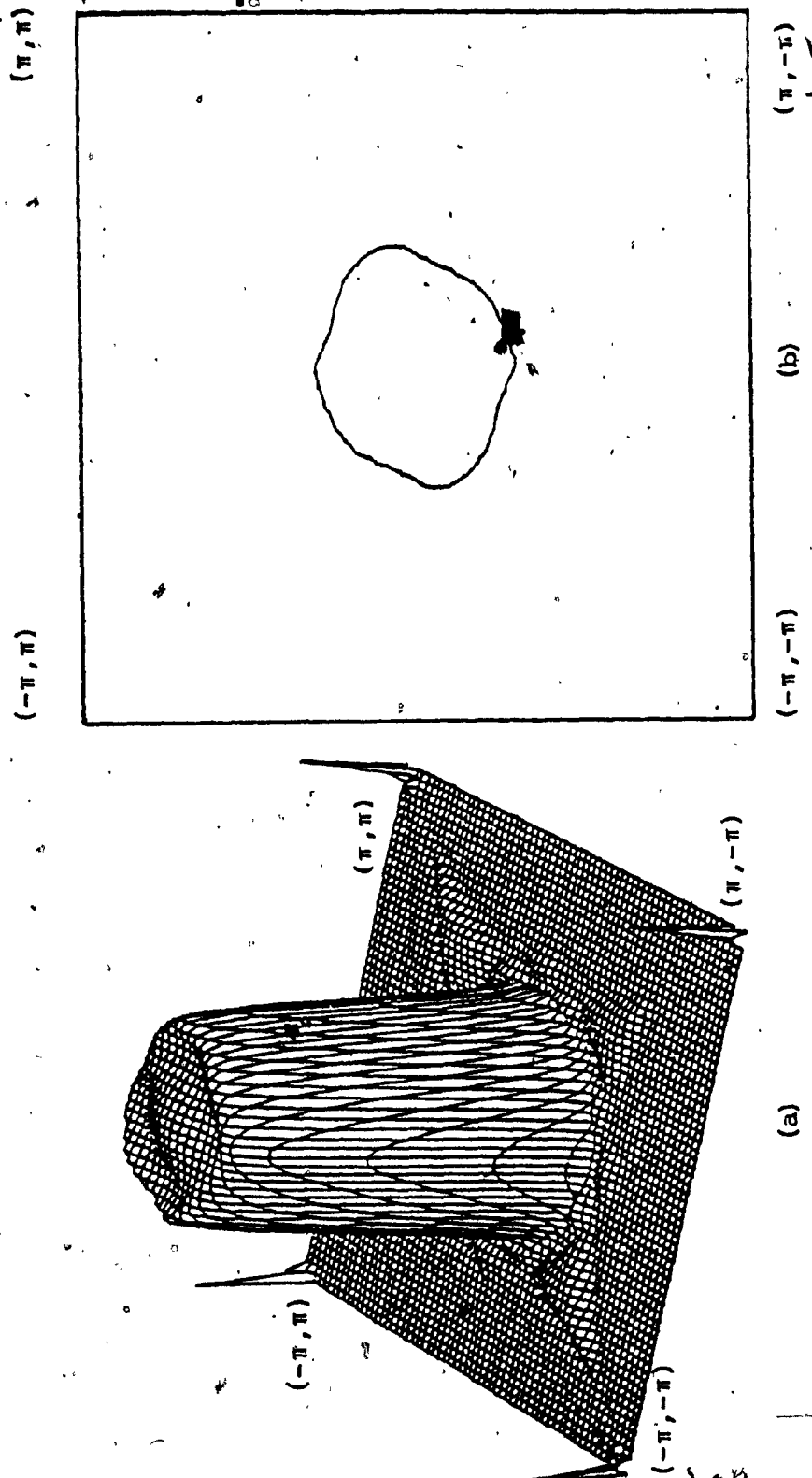


Figure 5.13 Wave Realization of Pseudo-Rotated Filter ($L = 8$), (a) 3-D Plot, (b) Contour Plot for Attenuation of 0.4 dB.

Table 5.1 Actual Maximum Passband Ripple and Minimum Stopband Attenuation for Direct and Wave Realizations

Word Length	Direct Form		Wave Digital Filter	
	A_p^{2D} (dB)	A_a^{2D} (dB)	A_p^{2D} (dB)	A_a^{2D} (dB)
$L = \infty$	0.298	31.71	0.296	31.71
$L = 14$	0.291	31.75	0.299	31.31
$L = 12$	0.221	31.52	0.288	31.40
$L = 10$	0.213	29.96	0.395	31.72
$L = 8$	1.063	28.32	0.773	30.68

5.5 Software implementation of pseudo-rotated filters

The software implementation of a 2-D pseudo-rotated filter can be obtained by programming the difference equations of the filter. From Eqn. 5.3 the difference equation for a second-order section can be written as

$$y(m,n) = \sum_{k=0}^2 \sum_{l=0}^2 A_{kl} x(m-k,n-l) - \sum_{\substack{i=0 \\ i+j \neq 0}}^2 \sum_{j=0}^2 B_{ij} y(m-i,n-j) \quad (5.24)$$

or for a first-order section as

$$y(m,n) = \sum_{k=0}^1 \sum_{l=0}^1 a_{kl} x(m-k,n-l) - \sum_{\substack{i=0 \\ i+l \neq 0}}^1 \sum_{l=0}^1 b_{il} y(m-i,n-l) \quad (5.25)$$

Eqns. 5.24 and 5.25 provide us with a means for computing sample output $y(m,n)$. The process of filtering and the operations involved in the calculation of each output data point are illustrated in Fig. 5.14. In this figure, output $y(6,7)$ is being calculated. The calculation requires the input values $x(6,7)$, $x(5,7)$, $x(4,7)$, $x(6,6)$, $x(5,6)$, $x(4,6)$, $x(6,5)$, $x(5,5)$, $x(4,5)$ and the output values $y(5,7)$, $y(4,7)$, $y(6,6)$, $y(5,6)$, $y(4,6)$, $y(6,5)$, $y(5,5)$, $y(4,5)$. The squares around the input and output values represent the input and the output masks, respectively.

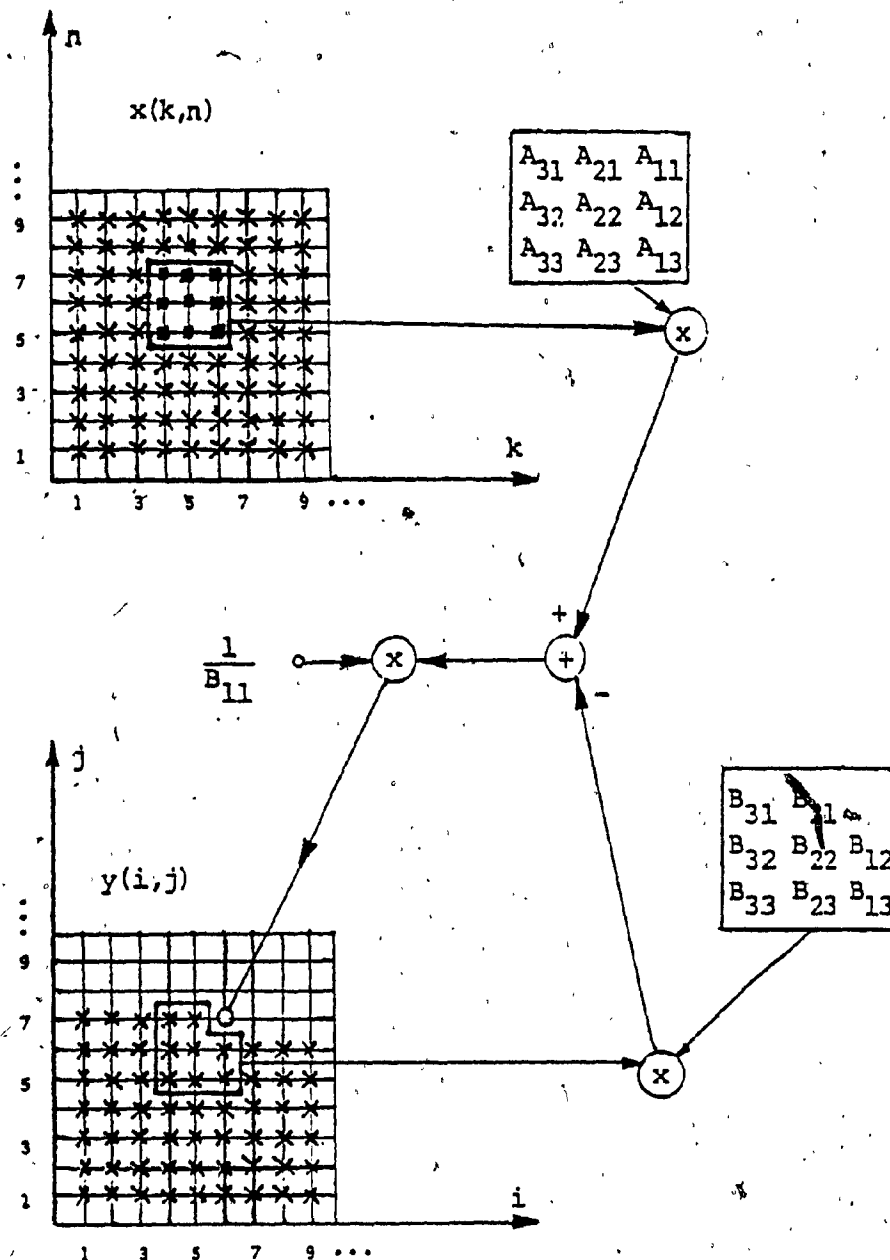


Figure 5.14 Filtering Process and Operations Involved in Software Implementation.

- - Subset of Input Values being Used
- x - Computed Output Values
- o - Output Value being Computed

5.5.1 Implementation of lowpass filters

A lowpass filter is very simple to implement by means of pseudo-rotated filters. To obtain circular symmetry and zero-phase, rotation angles in all four quadrants must be used. For maximum efficiency, the filter sections should be grouped accordingly to the recursion direction, namely, $(+,+)$, $(+,-)$, $(-,+)$, and $(-,-)$. With such an arrangement only four data manipulations are needed and each is carried out after the data has passed through each group of filters. The details of this procedure follow.

Consider the i th filter section, and let $X_i(z_1, z_2)$ and $Y_i(z_1, z_2)$ be the 2-D $z_1 z_2$ transforms of the input and output arrays, respectively. Also let $H_i(z_1, z_2)$ be the transfer function of the section. We can write

$$Y_i(z_1, z_2) = H_i(z_1, z_2) X_i(z_1, z_2)$$

where $X_{i+1}(z_1, z_2)$ is obtained from $Y_i(z_1, z_2)$ by applying an appropriate transformation of the data elements.

The necessary data transformations for the input data of the various groups of filters are illustrated in Fig. 5.15, where only four data elements are used for the sake of illustration.

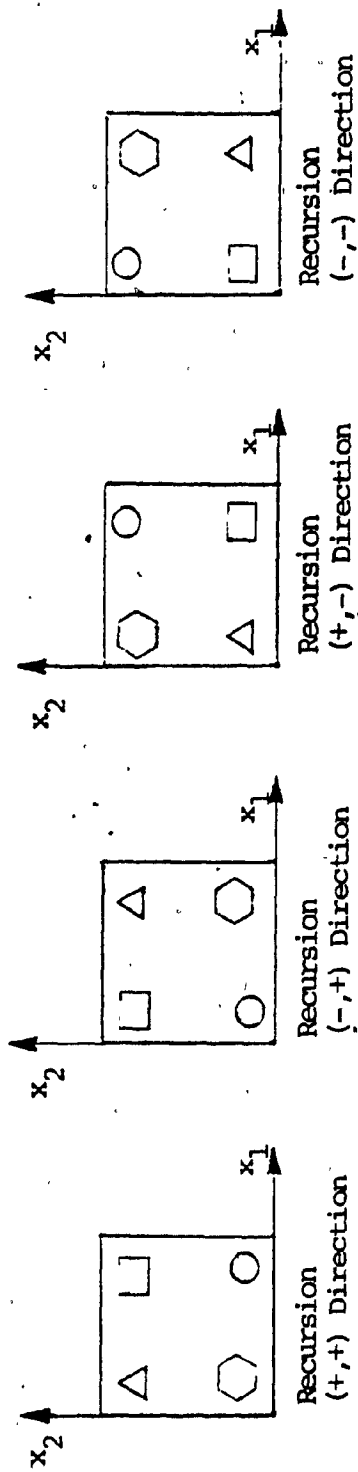


Figure 5.15 Data Transformations for Different Recursion Direction

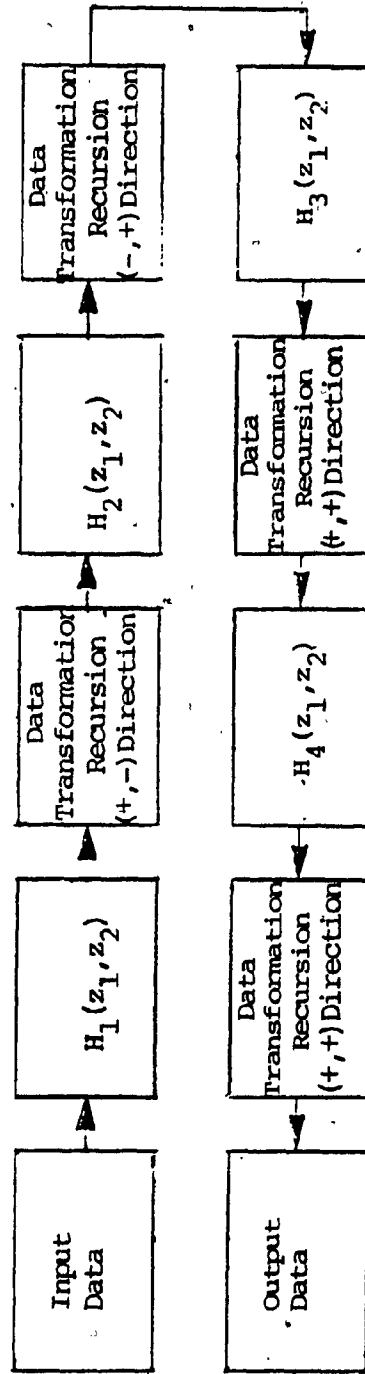


Figure 5.16 Block Diagram for Implementing Pseudo-Rotated Filters

Figure 5.16 shows the block diagram for the implementation of a 2-D circularly symmetric zero-phase filter and incorporates the necessary data transformations. In this figure, $H_1(z_1, z_2)$, $H_2(z_1, z_2)$, $H_3(z_1, z_2)$ and $H_4(z_1, z_2)$ correspond to the groups of filters recursing in the directions $(+, +)$, $(+, -)$, $(-, +)$, and $(-, -)$ respectively.

In Sec. 3.4 the rotation angles were chosen such that the 2-D transfer functions $H_1(z_1, z_2)$, $H_2(z_1, z_2)$, $H_3(z_1, z_2)$ and $H_4(z_1, z_2)$ of Fig. 5.16 can all be implemented by using transfer function $H_1(z_1, z_2)$ in conjunction with appropriate data transformations. Hence it is sufficient to design only the pseudo-rotated filters which are recursing in the $(+, +)$ direction. A corresponding implementation is illustrated in Fig. 5.16 [54]-[55].

The implementation shown in Fig. 5.16 is not necessarily the most desirable one. If the computer being used does not have sufficient high-speed storage to hold all the data at once, then the data must be stored on a disc. The transformations depicted in Fig. 5.15 require matrix transposition and can be time consuming if data are to be stored on a disc. Discussions of high-speed matrix transposition can be found in [56] and [57].

5.5.2 - Implementation of highpass filters

In the implementation of highpass filters, each pseudo-rotated filter has to be interconnected as shown in the block diagram of Fig. 2.7. Here it is not possible to group all filter sections recursing in the same direction. Hence, a large number of filter sections is undesirable since the filtering process would be slow.

As in case of lowpass filters only the coefficients of the filters recursing in the $(+,+)$ direction need to be stored in the computer memory if data manipulations are to be performed.

In a software or hardware implementation, numbers are ultimately stored in finite wordlength registers. As a result, the coefficients of the transfer functions as well as signal values must be quantized by rounding or truncation before they can be stored. Since $H^{++} H^{--}$ and $H^{+-} H^{-+}$ in Fig. 2.7 represent zero-phase filters the coefficients obtained by using Eqn. 2.21 must be quantized before the real coefficients in Eqns. 5.5 and 5.6 are obtained. Otherwise, a zero-phase filter might not be obtained.

For highpass filters, the filtering process becomes more efficient if the filter sections recurse in just one direction.

It should be pointed out here that data transformations can be avoided if necessary. Instead the processing can be carried out by scanning the data array in different directions. This possibility is illustrated in Figs. 5.17 and 5.18. However, if data is to be stored on a disc, this approach is far more time consuming than the approach based on data transformations.

5.6 Conclusions

In this chapter the realization of 2-D pseudo-rotated filters has been considered. First, by expressing the overall transfer function as a product of first- and second-order transfer functions which have real coefficients, a direct cascade realization of 2-D pseudo-rotated filters has been obtained. Second, by transforming a 1-D analog filter into a 2-D analog filter and then applying the wave characterization, a wave realization of 2-D pseudo-rotated filters has been obtained.

The two types of realizations were applied to a specific lowpass filter, and the effect of coefficient quantization was examined to some extent. As would be expected, the wave realization was found to be less sensitive to coefficient quantization.

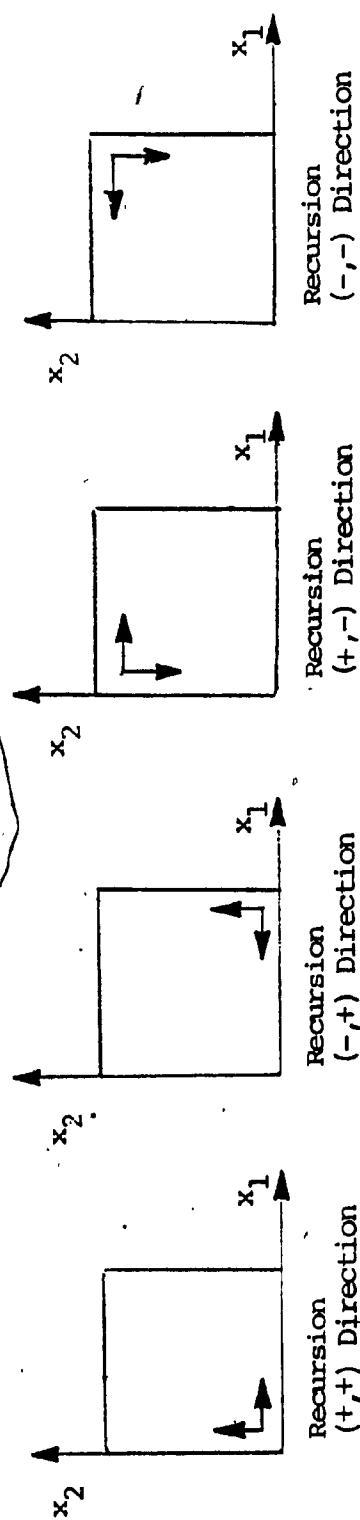


Figure 5.17 Recursion in Different Directions.

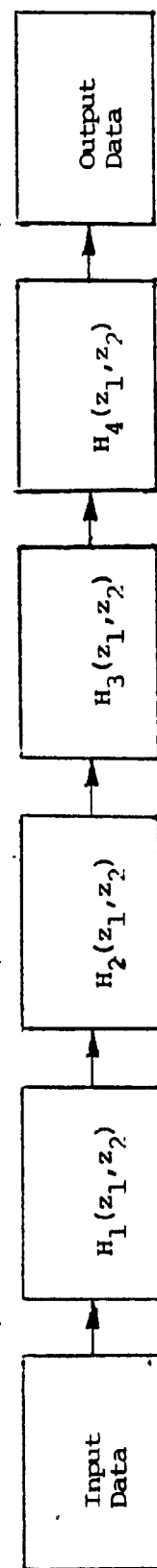


Figure 5.18 Implementation of Pseudo-Rotated Filters Using Different Recursion Directions.

The advantage of pseudo-rotated structures over structures based on true rotation is that they are always stable and are free of non-essential singularities of the second kind. This property is inherent in the transformation used.

In addition, the software implementation of 2-D pseudo-rotated lowpass and highpass filters was considered to some extent and some problems related to the implementation of these filters were examined.

CHAPTER 6SUMMARY AND CONCLUSIONS6.1 Conclusions

In this thesis the design, realization, and implementation of 2-D circularly symmetric pseudo-rotated digital filters have been investigated.

In Chapter 2, a transformation has been obtained by combining two known transformations. The new transformation performs pseudo-rotation of the s_1 and s_2 axes which can be made to approach true rotation as closely as desired. The transformation leads to stable 2-D digital filters which are free of non-essential singularities of the second kind.

Two methods for the design of 2-D circularly symmetric pseudo-rotated lowpass filters have been described. In the first method the design starts with a 1-D analog or a 1-D IIR filter while in the second method the design starts with a 1-D FIR filter. In the first method, the pseudo-rotation of the axes is forced to approach true rotation closely and, consequently, the amplitude response of the prototype filter, is preserved in the 2-D digital filter. Therefore, no guard filters were found to be necessary. On the other hand, in the second method the pseudo-rotation is not

allowed to approach true rotation too closely, and the transformation does not preserve the amplitude response of the prototype filter at points in the neighborhoods of the Nyquist points. Therefore, guard filters are necessary in this case. The first method leads to lower-order transfer functions but two additional manipulations of the input data are necessary in the implementation.

A new configuration comprising series and parallel pseudo-rotated (or rotated) filters has been proposed which can be used for the design of 2-D circularly symmetric highpass digital filters. In the design, four spurious transmission zeros appear at the Nyquist points which may cause difficulties in certain applications. A method for designing 2-D highpass digital filters which are recursing in just one direction has also been introduced. Further, the design of 2-D circularly symmetric bandpass and bandstop digital filters using combinations of 2-D lowpass and highpass digital filters ~~in~~ in cascade or in parallel has been considered.

In Chapter 3, the design of 2-D pseudo-rotated, circularly symmetric, digital filters satisfying prescribed amplitude specifications has been investigated. The required specifications were defined in terms of the passband and stopband edges, the maximum passband ripple, and the minimum stopband loss. In addition, a circularity measure was defined and used for the prediction of the minimum number of

pseudo-rotated filters to obtain 2-D filters with prescribed degree of circularity. Then prediction formulas were deduced which give the specifications of the 1-D digital filter so as to satisfy the required specifications in the 2-D circularly symmetric digital filter. With the 1-D digital-filter specifications known, those of the 1-D analog prototype filter can readily be derived, and the design of the 2-D filter can be carried out. Several procedures have been developed which can be used to design lowpass, highpass, bandpass and bandstop filters. These procedures have been used to design several digital filters of different types. The results obtained have shown that prescribed specifications can easily be obtained in the design of Butterworth, Chebyshev and elliptic filters. These procedures can be used to construct a computer-aided filter-design package which can be used by filter designers.

In Chapter 4, an attempt has been made to check if improvements can be obtained in pseudo-rotated filters through the use of an optimization method. The improvements of interest were reduction in the number of cascade sections, reduction in the maximum passband ripple, increase in the minimum stopband loss, and increase in the degree of circularity of the filter. The optimization method used was SUMT and a least-squares error function was assumed. The starting values for the variables of the optimization problem were assumed to be the coefficients of the 2-D

pseudo-rotated filter as designed by the methods of Chapter 3. The approach was applied to design several elliptic lowpass filters. Then several configurations of the pseudo-rotated filters, each with a reduced number of sections, were optimized. The results have shown that generally the maximum passband ripple is increased, and/or the minimum stopband loss is reduced. Nevertheless, the degree of circularity is usually improved. In effect, the method of Chapter 3 appears to yield near-optimal approximations for the required specifications. This is to be expected, however, since the predictions of Chapter 3 lead to the lowest-order elliptic (or optimal) analog filter which, when used as prototype, will lead to the 2-D digital filter that will just satisfy the required specifications.

Unlike optimization methods, the method of pseudo-rotated filters entails an insignificant amount of computation by comparison, and since it readily yields filters that satisfy the required specifications, it is to be preferred in practice.

In Chapter 5, direct and wave realizations of pseudo-rotated filters have been considered. In a direct realization, the transfer function is realized by connecting first- and second-order filter sections which have transfer functions with real coefficients. In a wave digital realization, on the other hand, the 2-D digital structure is deduced from a corresponding 1-D analog filter by applying

impedance transformations. The direct and wave realizations have been applied to a specific lowpass filter, and the effect of coefficient quantization has been examined. The wave realization was found to be less sensitive to coefficient quantization.

Finally, the software implementation of 2-D circularly symmetric pseudo-rotated lowpass and highpass filters has been considered to some extent and several features of the implementation have been examined.

6.2 Scope for further work

As was stated earlier, two methods are possible for the design of pseudo-rotated filters : a method starting with 1-D analog or 1-D IIR filter, and a method starting with a 1-D FIR filter. The first method leads to a lower-order transfer function but more manipulations of the input data are needed in the implementation. Therefore, it would be useful to apply both methods to image processing and to compare the computational efficiency inherent in the two types of implementation. This investigation should be carried out on a dedicated computer.

A disadvantage of the design method based on the use of a 1-D FIR filter is that guard filters are needed, as was

pointed out earlier. However, mechanisms probably exist for the elimination of these filters, and this possibility should be explored.

An inherent problem in the design of 2-D circularly symmetric highpass filters is the presence of spurious transmission zeros at the Nyquist points. Although these need not cause serious difficulties if the frequency spectrum of the image is bandlimited, trouble can be expected in certain other applications. Therefore, a way must be found to circumvent this problem.

The prediction formulas of Chapter 3 were found to be quite satisfactory for the limited range of filters considered in this thesis. In certain demanding applications, however, where very selective narrow-band filters are necessary, the 2-D filters obtained may violate the prescribed specifications. This problem can be prevented by refining the prediction formulas further, although this would necessitate much more computation.

The design of 2-D pseudo-rotated filters is carried out through step-by-step procedures in a deterministic manner, even though the formulas used are empirical. Consequently, the design process can easily be automated and an appropriate computer-aided filter-design package can be constructed. This would be of great value to engineers and filter designers.

The method of pseudo-rotated filters based on 1-D analog or 1-D IIR filters appears to yield near-optimal lowpass designs for the given specifications. However, further work would be needed to determine whether near-optimal highpass, bandpass, and bandstop designs can be obtained through the methods described. Specifically, it may be possible to identify other configurations for these filters, in particular for highpass filters, which lead to more efficient designs.

An attempt was made in this thesis to investigate to some extent the effect of coefficient quantization in 2-D pseudo-rotated filters but the results obtained are barely conclusive. Much more effort is needed in this area to investigate not only the effect of coefficient quantization under fixed-point and floating point arithmetic, but also to investigate the effects of product quantization on the output roundoff noise and the extent to which small scale (granularity) or large scale (overflow) parasitic oscillations can be eliminated. All this would require a considerable amount of work, particularly if wave realizations are also considered.

REFERENCES

- [1] J.K. Aggarwal (editor), "Digital Signal Processing," Western Periodicals Co., 1979.
- [2] A.V. Oppenheim (editor), "Applications of Digital Signal Processing," Prentice Hall, 1980.
- [3] V. Cappellini, A.G. Constantinides, P.L. Emiliani, "Digital Filters and their Applications," Academic Press, 1975.
- [4] J.M. Tribolet, "Seismic Applications of Homomorphic Signal Processing," Prentice Hall, 1982.
- [5] T.S. Huang (editor), "Picture Processing and Digital Filtering," Springer Verlag, 1979.
- [6] L.R. Rabiner and B. Gold, "Theory and Applications of Digital Signal Processing," Prentice Hall, 1975.
- [7] D.E. Dudgeon and R.M. Mersereau, "Multidimensional Digital Signal Processing," Prentice Hall, 1984.
- [8] R.E. Crochiere and L.R. Rabiner, "Multirate Digital Signal Processing," Prentice Hall, 1983.
- [9] T.S. Huang, W.F. Schreiber, and O. Tretiak, "Image Processing," Proc. IEEE, vol. 59, pp. 1586-1609, Nov. 1971.

- [10] R.E. Crochiere and A.V. Oppenheim, "Analysis of Linear Digital Networks," Proc. IEEE, vol. 63, pp. 581-595, April 1975.
- [11] B. Ramān, "Approximation and Realization of a Class of Multivariable Analog and Digital Transfer Function," Ph.D. Thesis, Concordia University, Montreal, March 1981.
- [12] T.S. Huang, "Stability of Two-Dimensional Recursive Filters," IEEE Trans. Audio Electroacoustics, vol. AU-20, pp. 158-163, June 1972.
- [13] D.M. Goodman, "Some Stability Properties of Two-dimensional Linear Shift-invariant Digital Filters," IEEE Trans. Circuits and Systems vol. CAS-24, pp. 201-208, April 1977.
- [14] A. Antoniou, M. Ahmadi, and C. Charalambous, "Design of Factorable Lowpass 2-Dimensional Digital Filters Satisfying Prescribed Specifications," IEE Proc., vol. 128, pt. G, no. 2, April 1981.
- [15] M.T. Manry and J.K. Aggarwal, "Picture Processing Using One-Dimensional Implementations of Discrete Planar Filters," IEEE Trans. Acoustics, Speech, and Signal Processing, vol. ASSP-22, pp. 164-173, June 1974.
- [16] V. Ramachandran and A.S. Rao, "A Multivariable

Array and its Application to Ladder Networks," IEEE Trans. Circuit Theory, vol. CT-20, no. 5, pp. 511-518, Sept. 1973.

- [17] M.O. Ahmad, C.H. Reddy, V. Ramachandran, and M.N.S. Swamy, "Ladder Realizations of Multivariable Positive Real Functions," Journal of the Franklin Inst., vol. 307, no. 2, pp. 71-81, Feb. 1979.
- [18] J.L. Shanks, S. Treitel, and J.H. Justice, "Stability and Synthesis of Two-dimensional Recursive Filters," IEEE Trans. Audio and Electroacoustics, vol. AU-20, pp. 115-128, June 1972.
- [19] J.M. Costa and A.N. Venetsanopoulos, "Design of Circularly Symmetric Two-dimensional Recursive Filters," IEEE Trans. Acoustic, Speech, and Signal Processing, vol. ASSP-22, pp. 432-443, Dec. 1974.
- [20] H. Chang and J.K. Aggarwal, "Design of Two-Dimensional Recursive Filters by Interpolation," IEEE Trans. Circuit and Systems, vol. CAS-24, pp. 281-291, June 1977.
- [21] M. Ahmadi, A.G. Constantinides, and R.A. King, "Design Technique For a Class of Stable Two-dimensional Recursive Digital Filters," Proc. of 1976 IEEE International Conference on Acoustics, Speech, and Signal Processing, pp. 145-147.

- [22] N.A. Pendergrass, E.I. Jury, and S.K. Mitra, "Spectral Transformations for Two-dimensional Digital Filters," IEEE Trans. Circuits and Systems, vol. CAS-23, pp. 26-35, Jan. 1976.
- [23] S. Chakrabarti, B.B. Bhattacharyya, and M.N. Swamy, "Approximation of Two-variable Filter Specifications in Analog Domain," IEEE Trans. Circuits and Systems, vol. CAS-24, no. 7, pp. 378-388, July 1978.
- [24] S. Chakrabarti and S.K. Mitra, "Design of Two-dimensional Digital Filters via Spectral Transformation," Proc. IEEE, no. 6, pp. 905-914, June 1977.
- [25] G.A. Maria and M.M. Fahmy, "An Lp Design Technique for Two-dimensional Digital Recursive Filters," IEEE Trans. Acoustics, Speech, and Signal Processing, vol. ASSP-22, pp. 15-21, Feb. 1974.
- [26] P. Karivaratharajan and M.N.S. Swamy, "Quadrantal Symmetry Associated with Two-Dimensional Digital Transfer Functions," IEEE Trans. Circuits and Systems, vol. CAS-25, no. 6, pp. 340-343, June 1978.
- [27] P. Karivaratharajan and M.N.S. Swamy, "Design of Separable Denominator 2-Dimensional Digital Filters

- Possessing Real Circularly Symmetric Frequency Responses," IEE Proc. vol. 129, pt. G, no. 5, pp. 235-240, Oct. 1982.
- [28] C. Charalambous, "Design of 2-Dimensional Circularly Symmetric Digital Filters," IEE Proc., vol. 129, pt. G, no. 2, pp. 47-54, April 1982.
- [29] G. Crebbin and J. Attikiouzel, "The General Purpose Design of 2-Dimensional Recursive Digital Filters," IEE Proc., vol. 130, pt. G, no. 5, Oct. 1983.
- [30] P.A. Ramamoorthy and L.T. Bruton, "Design of Stable Two-dimensional Analog and Digital Filters with Applications in Image Processing," Intl. J. Circuits Theory and Applications, vol. 7, pp. 229-246, April 1979.
- [31] M. Ahmadi and V. Ramachandran, "A Method for the Design of Stable (N-D) Analog and Digital Filters," Proc. 1981 IEEE International Conference on Acoustics, Speech, and Signal Processing, pp. 704-707.
- [32] P. Karivaratharajan, H.C. Reddy, M.N.S. Swamy, and V. Ramachandran, "Generation of Two-dimensional Digital Functions without Nonessential Singularities of Second Kind," IEEE Trans. Acoustics, Speech, and Signal Processing, vol. ASSP-28 no. 2, pp. 216-223,

April 1980.

- [33] V. Ramachandran and M. Ahmadi, "Design of 2-D Stable Analog and Recursive Digital Filters Using Properties of Derivative of Even or Odd Parts of Hurwitz Polynomials," Journal of the Franklin Institute, vol. 315, no. 4, pp. 259-267, April 1983.
- [34] Y. Kamp, "Realization of Multivariable Functions by Cascade of Lossless Two-port Separable by Non-commensurate Stubs," Philips Res. Rep., vol. 26, no. 6, pp. 443-452, Dec. 1971.
- [35] M.O. Ahmad, C.H. Reddy, V. Ramachandran, and M.N.S. Swamy, "A Class of Multivariable Positive Real Functions Realizable by Resistively-terminated Lossless Ladder Networks," IEEE Trans. Circuits and Systems, vol. CAS-26, no. 8, pp. 659-662, Aug. 1971.
- [36] A. Fettweis, "Principles of Multidimensional Wave Digital Filtering" in Digital Signal Processing, J.K. Aggarwal, editor, Western Periodicals, 1979.
- [37] M.N.S. Swamy and K.S. Thyagarajan, "A New Type of Wave Digital Filter," Journal of the Franklin Institute, 300, pp. 41-58, July 1975.
- [38] M.N.S. Swamy, K.S. Thyagarajan, and V.

Ramachandran, "Two-dimensional Wave Digital Filters Using Doubly-terminated Two-variable LC-ladder Configurations," Journal of the Franklin Institute, vol., 304, pp. 201-216, Nov. 1977.

- [39] D.M. Goodman, "A Design Technique for Circularly Symmetric Lowpass Filters," IEEE Trans. Acoustics, Speech, and Signal Processing, vol. ASSP-26, no. 4, pp. 290-304, Aug. 1978.
- [40] A. Antoniou, "Accelerated Procedure for the Design of Equiripple Nonrecursive Digital Filters," IEE Proc., vol., 129, pt. G, no. 1, Feb. 1982.
- [41] A. Aliphas, S.S. Narayan, A.M. Peterson, "Finding the Zeros of Linear Phase FIR Frequency Sampling Digital Filters," IEEE Trans. Acoustics, Speech, and Signal Processing, vol. ASSP-28, no. 3, pp. 729-734, June 1983.
- [42] A. Antoniou, "Digital Filters : Analysis and Design," McGraw-Hill, 1979.
- [43] A.V. Fiacco and G.P. McCormick, "Nonlinear Programming : Sequential Unconstrained Minimization Techniques," John Wiley, 1968.
- [44] D.M. Himmelblau, "Applied Nonlinear Programming," McGraw-Hill, 1972.

- [45] J.L. Kuester and J.H. Mize, "Optimization Techniques with Fortran," McGraw-Hill, pp. 412-453, 1973.
- [46] R. Fletcher, "Practical Methods of Optimization," John Wiley, 1980.
- [47] J.B. Knowles and E.M. Olcayto, "Coefficient Accuracy and Digital Filter Response," IEEE Trans. Circuit Theory, vol. CT-14, pp. 31-41, March 1968.
- [48] P.Lennarz and L. Hofmann, "Computer Realization of Two-Dimensional Wave Digital Filters," Proc. European Conf. on Circuit Theory and Design," pp. 360-364, 1978.
- [49] A.I. Zverev, "Handbook of Filter Synthesis," John Wiley, 1967.
- [50] A. Fettweis, "Digital Filter Structures Related to Classical Filter Networks," AEU, vol. 25, pp. 79-89, Feb. 1971.
- [51] A. Fettweis, "Some Principles of Designing Digital Filters Imitating Classical Filter Structures," IEEE Trans. Circuit Theory, vol. CT-18, pp. 314-316, March 1971.
- [52] A. Sedlmeyer and A. Fettweis, "Digital Filters with True Ladder Configuration," Int. J. Circuit Theory

Applications, vol. 1, pp. 5-10, March 1973.

- [53] A. Fettweis and K. Meerkoter, "On Adaptors for Wave Digital Filters," IEEE Trans. Acoustics, Speech, and Signal Processing, vol. ASSP-23, pp. 516-525, Dec. 1975.
- [54] J.M. Costa and A.N. Venetsanopoulos, "A Group of Linear Spectral Transformations for Two-Dimensional Digital Filters," IEEE Trans. Acoustics, Speech, and Signal Processing, vol. ASSP-24, pp. 424-425, Oct. 1976.
- [55] K.P. Prasad, A. Antoniou, and B.B. Bhattacharyya, "On the Properties of Linear Spectral Transformation for 2-Dimensional Digital Filters," Circuits Systems Signal Process., vol. 2, no. 2, pp. 203-211, 1983.
- [56] J.O. Eklundh, "A Fast Computer Method for Matrix Transposing," IEEE Trans. Computer, vol. C-21, pp. 801-803, July 1972.
- [57] R.E. Twogood and M.P. Ekstrom, "An Extension of Eklundh's Matrix Transposition Algorithm and its Applications in Digital Image Processing," IEEE Trans. Computer, vol. C-25, pp. 950-952, Sept. 1976.